

---

# Bosonization of dimerized spinless-fermion and Hubbard chains

---

Zur Erlangung des akademischen Grades eines  
Doktors der Naturwissenschaften  
der Mathematisch-Naturwissenschaftlichen Fakultät  
der Universität Augsburg

angenommene

Dissertation

von

**M. Sc. Carmen Mocanu**

Erstgutachter: Prof. Dr. Ulrich Eckern  
Zweitgutachter: Prof. Dr. Gert-Ludwig Ingold  
Tag der mündlichen Prüfung: 11 Februar 2005



# Contents

<b>1</b>	<b>Introduction</b>	<b>5</b>
<b>2</b>	<b>Bosonization</b>	<b>7</b>
2.1	Bosonization prerequisite . . . . .	7
2.2	Klein factors . . . . .	13
2.3	Luttinger model . . . . .	15
<b>3</b>	<b>Spinless fermions</b>	<b>19</b>
3.1	Model and formalism . . . . .	19
3.2	Phase diagram . . . . .	23
3.3	Self-consistent harmonic approximation . . . . .	23
3.4	Finite systems . . . . .	26
3.5	Drude weight . . . . .	28
3.5.1	Drude weight within bosonization . . . . .	28
3.5.2	Drude weight for free spinless fermions . . . . .	30
<b>4</b>	<b>Hubbard model</b>	<b>33</b>
4.1	Hubbard model . . . . .	33
4.2	Peierls-Hubbard model . . . . .	36
4.2.1	Self-consistent harmonic approximation . . . . .	38
4.2.2	Finite systems . . . . .	44
4.3	Ionic Hubbard model . . . . .	47
4.3.1	Self-consistent harmonic approximation . . . . .	49
4.3.2	Finite systems . . . . .	56
4.4	Conclusions . . . . .	64
<b>5</b>	<b>Screening in low-dimensional electron systems</b>	<b>65</b>
5.1	Phase transition in $\text{VO}_2$ . . . . .	65
5.2	The model . . . . .	67
5.3	Charge and spin susceptibility . . . . .	68
5.3.1	Luttinger model . . . . .	68
5.3.2	Luttinger model coupled to $3d$ electrons . . . . .	69

5.3.3	Dispersion of the charge excitations . . . . .	70
5.4	Discussion . . . . .	73
<b>6</b>	<b>Summary and outlook</b>	<b>75</b>
<b>A</b>	<b>Derivation of the gap equations</b>	<b>79</b>
<b>B</b>	<b>The trial Hamiltonian in terms of bosonic operators</b>	<b>83</b>
<b>C</b>	<b>Quantum theory of Josephson junctions</b>	<b>85</b>
<b>D</b>	<b>Mathieu equation</b>	<b>87</b>
<b>E</b>	<b>The Klein Hamiltonian as a <math>2d</math> tight binding model</b>	<b>89</b>
<b>F</b>	<b>Analytical solution of the gap equations</b>	<b>91</b>

# Chapter 1

## Introduction

The interplay between electron-electron interaction and electron-phonon coupling in strongly correlated fermionic systems has been intensively studied in the past and is still a major challenge for a realistic description and a better understanding of many materials.

In the last decades, particular attention has been paid to one-dimensional fermionic systems, from both the theoretical and the experimental point of view. Starting from the features of one-dimensional electron systems, the initial goal was to understand correlation effects in higher dimensions, too. Furthermore, one-dimensional models are attractive from a theoretical point of view: there exists, in fact, a variety of methods that work exclusively in one dimension, sometimes even allowing for an exact solution. As a special feature of one dimension, the Fermi liquid theory breaks down and a new paradigm has to be introduced, namely the Luttinger liquid [1, 2]. The first version of the generic model was proposed by Tomonaga, who showed that the excitations of a one-dimensional electron gas with linear dispersion are bosons, even though the elementary constituents are fermions. The excitations involve two particles, and the wave function of the two fermion states has bosonic properties. This model proved to be of fundamental importance for purely one- or quasi one-dimensional systems, e.g. quasi one-dimensional organic conductors [3, 4, 5, 6, 7] or spin-Peierls compounds [8, 9] where correlations are known to play an important role. In the last years, evidence for Luttinger liquid behavior has been found in semiconductor quantum wires [10] and carbon nanotubes [11].

The concept of a Luttinger liquid is intimately connected with the bosonization technique whose origins date back to the seminal paper by Tomonaga [1] in 1950. During the following decades the method was worked out and successfully applied to one-dimensional electron and spin systems [12, 13, 14, 15]. Despite its long history there are still some subtle points in the bosonization formalism which are not taken into consideration in the majority of the literature. One of these issues is the proper treatment of the so-called Klein factors which have to be introduced in order to preserve the anti-commutation property of the fermionic fields during the bosonization

procedure. Often, the existence of Klein factors has been ignored in the literature: this may be justified for infinite systems [15], but in general they have to be treated carefully as pointed out, for example, in the context of impurity models and two-leg ladders [14, 25, 26, 27, 28]. The importance of Klein factors has also been emphasized by Schönhammer [26, 27], who noted that the common practice of neglecting them may lead to erroneous results when nonlinear terms are considered. Such nonlinear terms arise in the presence of perturbations like impurity scattering or a modulation of the hopping. For the system with a perturbation an exact solution is known only in some special cases [16]. In general one has to resort to approximative methods like renormalization group calculations [17]. Another more intuitive method is the self-consistent harmonic approximation (SCHA) where the nonlinear terms are replaced by a harmonic potential with parameters to be determined self-consistently according to a variational principle for the energy or the free energy. The SCHA has been successfully applied to various nonlinear models [18, 19, 20, 21, 22, 23, 24].

In this work we handle the Klein factors in a systematic way, both in the thermodynamic limit and for finite systems. We develop an extension of the SCHA which treats the bosonic fields and the Klein factors on equal footing. As prototypical models we consider one-dimensional dimerized spinless fermions and Hubbard models with periodic modulation of the hopping (Peierls-Hubbard model) and of the chemical potential (ionic Hubbard model), respectively. Note that, throughout this work, we consider exclusively ground-state properties, i.e. the zero-temperature limit.

We start with a short presentation of the bosonization method in chapter 2, where we focus in particular on the properties of the Klein factors. The chapter ends with a description of the Luttinger model, which, in certain cases, can be solved exactly. In the next two chapters we present a method for treating the Klein factors in bosonized Hamiltonians with nonlinear terms, and apply this method to spinless fermions in chapter 3, and to the Hubbard model in chapter 4.

In chapter 5 we consider a model of one-dimensional interacting electrons coupled to a three-dimensional weakly correlated conduction band through a Coulomb interaction. This model is motivated by materials like  $\text{VO}_2$ , where at the Fermi energy one encounters both a band with one-dimensional dispersion and bands with three-dimensional character. We calculate the spin and the charge susceptibility in order to arrive at a description in terms of coupled one-dimensional chains with intra- and inter chain coupling in the spin and charge channel mediated through the  $3d$  environment.

In chapter 6 we summarize our results and give an outlook to some still open problems. Some technical details are described in six appendices.

# Chapter 2

## Bosonization

### 2.1 Bosonization prerequisite

Fermion systems in one dimension have features quite distinct from those in higher dimensions. In the early work of Mattis and Lieb [29] and Bychkov et al. [30] it has been shown that Landau type quasi-particles do not exist and the Fermi liquid theory breaks down in these systems. As a consequence a new concept has to be introduced to describe one-dimensional interacting electrons, known as the Tomonaga-Luttinger liquid. Corresponding models were first introduced by Tomonaga [1] and Luttinger [2] and have been continuously improved in order to obtain an accurate characterization of real systems [29, 3, 17, 12, 13, 14, 15, 26]. The theory of the Luttinger liquid is closely related to the bosonization technique, which has been successfully applied to strongly correlated one-dimensional models. The basic idea behind bosonization is that particle-hole excitations have a bosonic character and are well defined quasi-particles at low energies. It consists essentially in a systematic mapping of a fermionic system (states, operators, Hamiltonians) into a bosonic one. It turns out that the bosonic language is often more suited for the understanding of the physics of the system, sometimes even allowing for an exact solution.

A feature specific to one dimension and central to the whole development is the reduction of the Fermi sphere to two disconnected Fermi points  $\pm k_F$ . For energies close to the Fermi level, the dispersion relation can be linearized around the Fermi points. Following closely the notation of von Delft and Schoeller [14], we consider a Hamiltonian with linear dispersion

$$H_0 = \sum_{k < 0, \sigma} [\epsilon_F - v_F(k + k_F)] c_{k\sigma}^+ c_{k\sigma} + \sum_{k > 0, \sigma} [\epsilon_F + v_F(k - k_F)] c_{k\sigma}^+ c_{k\sigma}, \quad (2.1)$$

where  $\epsilon_F$  is the Fermi energy and  $c_{k\sigma}^+$  ( $c_{k\sigma}$ ) creates (annihilates) an electron with momentum  $k$  and spin direction  $\sigma = \uparrow, \downarrow$ ; we take  $\hbar = 1$  here and in the following. Since we are interested in low energy excitations, but not in the total ground state energy, we

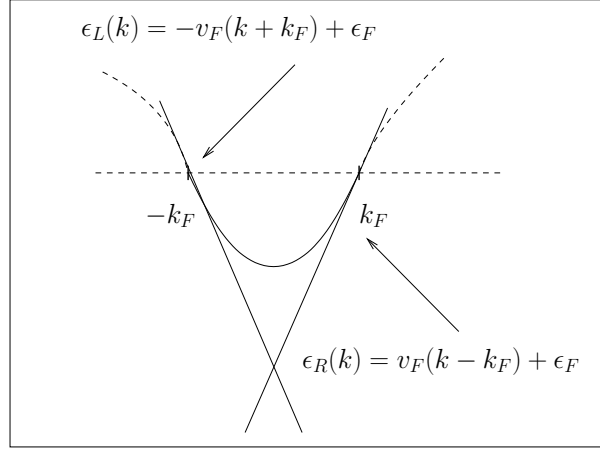


Figure 2.1: Linearization of the spectrum around the Fermi points  $\pm k_F$ . The momentum domain of the left branch  $k \in (-\infty, 0)$  and of the right branch  $k \in (0, \infty)$  was extended to  $k \in (-\infty, \infty)$ .

can extend the momentum domain of the first sum from  $k \in (-\infty, 0)$  to  $k \in (-\infty, \infty)$ , and the momentum domain of the second sum from  $k \in (0, \infty)$  to  $k \in (-\infty, \infty)$ . In the following we will refer to these sums as left and right branches and we introduce the notion of left and right movers. As a result of the extension of the spectrum to minus infinity, the Hilbert space of the model is not the usual electron Hilbert space, but has been expanded to include a sea of unphysical states as well. This second, unphysical set of fermions requires high energies for their excitation and will not affect the low energy properties. In order to avoid the divergences associated with them, the normal ordering

$$: A : = A - {}_0\langle 0|A|0\rangle_0 \quad (2.2)$$

is introduced, where the reference state  $|0\rangle_0$  is the filled non-interacting Fermi sea.

The physical fermion fields, defined as

$$\psi_{phys}(x) = \frac{1}{\sqrt{L}} \sum_{\sigma} \sum_{k=-\infty}^{\infty} e^{ikx} c_{k\sigma}, \quad (2.3)$$

are separated in left and right movers with respect to the  $\pm k_F$  points as follows:

$$\begin{aligned} \psi_{phys}(x) &\approx \frac{1}{\sqrt{L}} \sum_{\sigma} \sum_{k>0} [e^{ikx} c_{k\sigma} + e^{-ikx} c_{-k\sigma}] \\ &= \frac{1}{\sqrt{L}} \sum_{\sigma} \sum_{k>-k_F} [e^{-ik_F x} e^{-ikx} c_{-k-k_F\sigma} + e^{ik_F x} e^{ikx} c_{k+k_F\sigma}]. \end{aligned} \quad (2.4)$$



For an interacting model, the separation into left and right moving fermions allows the sorting of various scattering processes according to their initial and final states [17] (“g-ology”). Using the notation  $\psi_{kL\sigma} = c_{-k-k_F\sigma}$  for the left movers and  $\psi_{kR\sigma} = c_{k+k_F\sigma}$  for the right movers, the corresponding left and right fermion fields are defined by

$$\psi_{L\sigma}(x) = \frac{1}{\sqrt{L}} \sum_{k=-\infty}^{\infty} e^{-ikx} \psi_{kL\sigma}, \quad (2.5)$$

$$\psi_{R\sigma}(x) = \frac{1}{\sqrt{L}} \sum_{k=-\infty}^{\infty} e^{ikx} \psi_{kR\sigma}, \quad (2.6)$$

where again we extended the domain of momentum  $k \in (-k_F, \infty)$  of each branch to  $k \in (-\infty, \infty)$ . These fermion fields satisfy the usual anti-commutation relations

$$\{\psi_{\gamma}(x), \psi_{\gamma'}^+(x')\} = \delta(x - x') \delta_{\gamma\gamma'}, \quad (2.7)$$

where  $\gamma, \gamma' \in \{R \uparrow, R \downarrow, L \uparrow, L \downarrow\}$ .

The density operator for particles with spin  $\sigma$  is generally

$$\rho_{\sigma}(q) = \sum_k c_{k+q\sigma}^+ c_{k\sigma}. \quad (2.8)$$

When the momentum  $q$  is small, it may be written as a sum of left and right movers

$$\begin{aligned} \rho_{\sigma}(q) &\approx \sum_{k>0} c_{k+q\sigma}^+ c_{k\sigma} + \sum_{k<0} c_{k+q\sigma}^+ c_{k\sigma} \\ &= \sum_k \psi_{k+qR\sigma}^+ \psi_{kR\sigma} + \sum_k \psi_{k-qL\sigma}^+ \psi_{kL\sigma} = \rho_{R\sigma}(q) + \rho_{L\sigma}(q). \end{aligned} \quad (2.9)$$

The left and right density operators  $\rho_{R\sigma}(q)$  and  $\rho_{L\sigma}(q)$  obey the following commutation relations:

$$[\rho_{R\sigma}(q), \rho_{R\sigma'}(-q')] = -\frac{qL}{2\pi} \delta_{\sigma\sigma'} \delta_{qq'}, \quad (2.10)$$

$$[\rho_{L\sigma}(q), \rho_{L\sigma'}(-q')] = \frac{qL}{2\pi} \delta_{\sigma\sigma'} \delta_{qq'}, \quad (2.11)$$

$$[\rho_{L\sigma}(q), \rho_{R\sigma'}(q')] = 0. \quad (2.12)$$

In evaluating the commutators (2.10)-(2.12) we use Eq. (2.2) for the density operators  $\rho_\gamma(q) = : \rho_\gamma(q) : - {}_0\langle 0 | \rho_\gamma(q) | 0 \rangle_0$ . The left and right charge and spin density operators are defined as

$$\rho_{L/R}(q) = \rho_{L/R\uparrow}(q) + \rho_{L/R\downarrow}(q), \quad (2.13)$$

$$\sigma_{L/R}(q) = \rho_{L/R\uparrow}(q) - \rho_{L/R\downarrow}(q). \quad (2.14)$$

In terms of left and right movers, the kinetic energy part of the Hamiltonian reads

$$\begin{aligned} H_0 &= \sum_{\sigma} \sum_{k=-\infty}^{\infty} [\epsilon_F + kv_F] (\psi_{kR\sigma}^+ \psi_{kR\sigma} + \psi_{kL\sigma}^+ \psi_{kL\sigma}) \\ &= \sum_{\sigma} \int_0^L dx [ : \psi_{R\sigma}^+(x) i \partial_x \psi_{R\sigma}(x) : + : \psi_{L\sigma}^+(x) i \partial_x \psi_{L\sigma}(x) : ]. \end{aligned} \quad (2.15)$$

As a consequence of the linear dispersion,  $H_0$  and the density operators obey the following commutation relations:

$$[H_0, \rho_{R\sigma}(q)] = v_F q \rho_{R\sigma}(q), \quad [H_0, \rho_{L\sigma}(q)] = -v_F q \rho_{L\sigma}(q), \quad (2.16)$$

which allows expressing the kinetic energy part of the Hamiltonian as a quadratic form of charge and spin density operators.

Using the density operators, one defines the following operators:

$$b_{qL\sigma} = \frac{i}{\sqrt{n_q}} \rho_{L\sigma}(q), \quad b_{qL\sigma}^+ = -\frac{i}{\sqrt{n_q}} \rho_{L\sigma}(-q), \quad (2.17)$$

$$b_{qR\sigma} = \frac{i}{\sqrt{n_q}} \rho_{R\sigma}(-q), \quad b_{qR\sigma}^+ = -\frac{i}{\sqrt{n_q}} \rho_{R\sigma}(q), \quad (2.18)$$

where  $n_q = qL/2\pi$ , and  $q > 0$ . These operators fulfill the bosonic commutation rules

$$[b_{q\gamma}, b_{q'\gamma'}^+] = \delta_{qq'} \delta_{\gamma\gamma'}, \quad (2.19)$$

where  $\gamma, \gamma' \in \{R\uparrow, R\downarrow, L\uparrow, L\downarrow\}$ .

Returning to real space, bosonic fields are defined as

$$\varphi_{L\sigma}(x) = \sum_{q>0} \frac{1}{\sqrt{n_q}} e^{-iqx - aq/2} b_{qL\sigma}, \quad (2.20)$$

$$\varphi_{R\sigma}(x) = - \sum_{q>0} \frac{1}{\sqrt{n_q}} e^{iqx - aq/2} b_{qR\sigma}, \quad (2.21)$$

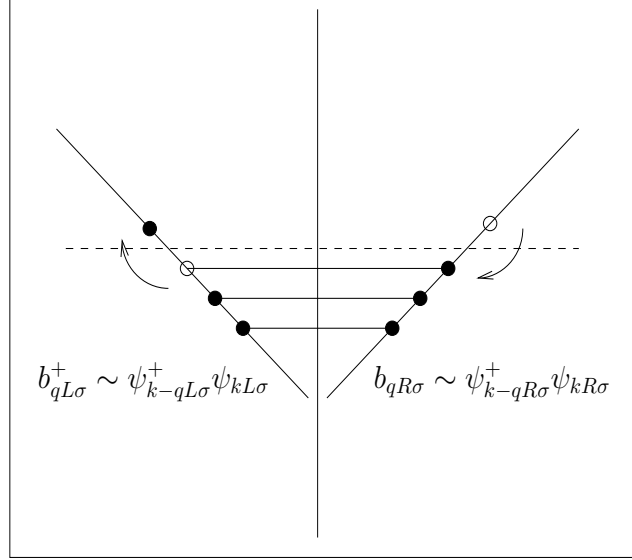


Figure 2.2:  $b_{qL\sigma}^+$  creates a particle-hole excitation on the left side, while  $b_{qR\sigma}$  annihilates a particle-hole excitation on the right side.

where  $a \rightarrow 0$  is assumed. Formally,  $a^{-1}$  is a cutoff for the  $q$ -summation; physically,  $a$  corresponds to the lattice constant. It has been shown that the fermionic field operators are related to the bosonic fields via the following bosonization identity [12, 14]:

$$\Psi_{L\sigma}(x) = \frac{1}{\sqrt{L}} F_{L\sigma} e^{-i\varphi_{L\sigma}^+(x)} e^{-i\varphi_{L\sigma}(x)} e^{-2\pi i N_{L\sigma} x/L} \quad (2.22)$$

$$= \frac{1}{\sqrt{2\pi a}} F_{L\sigma} e^{-i(\varphi_{L\sigma}^+(x) + \varphi_{L\sigma}(x))} e^{-2\pi i N_{L\sigma} x/L}, \quad (2.23)$$

$$\Psi_{R\sigma}(x) = \frac{1}{\sqrt{2\pi a}} F_{R\sigma} e^{i(\varphi_{R\sigma}^+(x) + \varphi_{R\sigma}(x))} e^{2\pi i N_{R\sigma} x/L}. \quad (2.24)$$

The factor  $\sqrt{L/2\pi a}$  in Eq. (2.23) comes from the commutator

$$[\varphi_{\gamma}^+(x), \varphi_{\gamma}(x)]/2 = -\ln \sqrt{L/2\pi a}.$$

The  $N_{\gamma}$  operators introduced in the bosonization identity count the number of  $\gamma$ -electrons relative to the reference state  $|0\rangle_0$ :

$$N_{\gamma} \equiv \sum_{k=-\infty}^{\infty} : \psi_{k\gamma}^+ \psi_{k\gamma} : = \sum_{k=-\infty}^{\infty} [\psi_{k\gamma}^+ \psi_{k\gamma} - {}_0\langle 0 | \psi_{k\gamma}^+ \psi_{k\gamma} | 0 \rangle_0]. \quad (2.25)$$

The  $F_{\gamma}^+, F_{\gamma}$  operators, known as Klein factors or ladder operators, raise or lower the fermion numbers and assure that fermions of different species anti-commute. A detailed discussion of their properties is given in section 2.2.

Later it will be convenient to introduce new charge and spin fields,  $\phi_{c,s}$  and  $\theta_{c,s}$ , which are linear combinations of left and right movers

$$\phi_{c,s} = \frac{1}{2\sqrt{2}}(\varphi_{L\uparrow} \pm \varphi_{L\downarrow} + \varphi_{R\uparrow} \pm \varphi_{R\downarrow} + \text{h.c.}), \quad (2.26)$$

$$\theta_{c,s} = \frac{1}{2\sqrt{2}}(\varphi_{L\uparrow} \pm \varphi_{L\downarrow} - \varphi_{R\uparrow} \mp \varphi_{R\downarrow} + \text{h.c.}), \quad (2.27)$$

where the index  $c$  stands for charge and the index  $s$  stands for spin. They satisfy the commutation relations

$$[\phi_\beta(x), \phi_{\beta'}(y)] = [\theta_\beta(x), \theta_{\beta'}(y)] = 0, \quad (2.28)$$

$$[\phi_\beta(x), \theta_{\beta'}(y)] = -i\pi\Theta(x-y)\delta_{\beta\beta'} + \frac{i\pi}{2}\delta_{\beta\beta'} + \frac{i\pi}{L}(x-y)\delta_{\beta\beta'}, \quad a \rightarrow 0, \quad (2.29)$$

$$[\phi_\beta(x), \partial_y\theta_{\beta'}(y)] = i\pi\delta(x-y)\delta_{\beta\beta'} - \frac{i\pi}{L}\delta_{\beta\beta'}, \quad a \rightarrow 0, \quad (2.30)$$

where  $\beta, \beta' \in \{c, s\}$ . In the thermodynamic limit, i.e. when the term  $\frac{1}{L}\delta_{\beta\beta'}$  can be neglected, the fields  $\phi_\beta(x)$  and  $\partial_x\theta_\beta(x)$  are conjugate variables.

We express now the electron density using the bosonization formalism. In real space, the density operator reads

$$\rho_\sigma(x) = \sum_q e^{iqx} \rho_\sigma(q) \approx \sum_{|q| \ll 2k_F} e^{iqx} \rho_\sigma(q) + \sum_{\pm} \sum_{|q| \ll 2k_F} e^{i(\pm 2k_F + q)x} \rho_\sigma(\pm 2k_F + q), \quad (2.31)$$

which in terms of bosonic fields is

$$\begin{aligned} \rho_\sigma(x) &\approx \frac{N_{R\sigma} + N_{L\sigma}}{L} + \frac{1}{2\pi} \partial_x [\phi_{L\sigma}(x) + \phi_{R\sigma}(x)] \\ &+ \frac{1}{2\pi a} F_{L\sigma}^+ F_{R\sigma} e^{-2ik_F x} e^{2\pi i(N_{R\sigma} + N_{L\sigma} + 1)x/L} e^{i(\phi_{L\sigma} + \phi_{R\sigma})} e^{-ix(G - 4k_F)} \\ &+ \frac{1}{2\pi a} F_{R\sigma}^+ F_{L\sigma} e^{-2ik_F x} e^{-2\pi i(N_{R\sigma} + N_{L\sigma} + 1)x/L} e^{-i(\phi_{L\sigma} + \phi_{R\sigma})} + \text{h.c.} \end{aligned} \quad (2.32)$$

Here, the term in the second line is important for commensurate band filling, when the reciprocal lattice vector is  $G \approx 4k_F$ . In the literature [20], ignoring both the Klein factors and the term in the second line, the density operator is simply given as

$$\rho_\sigma(x) = \frac{1}{2\pi} \partial_x [\phi_{L\sigma}(x) + \phi_{R\sigma}(x)] + \frac{1}{\pi a} \cos[-2k_F x + \phi_{L\sigma}(x) + \phi_{R\sigma}(x)]. \quad (2.33)$$

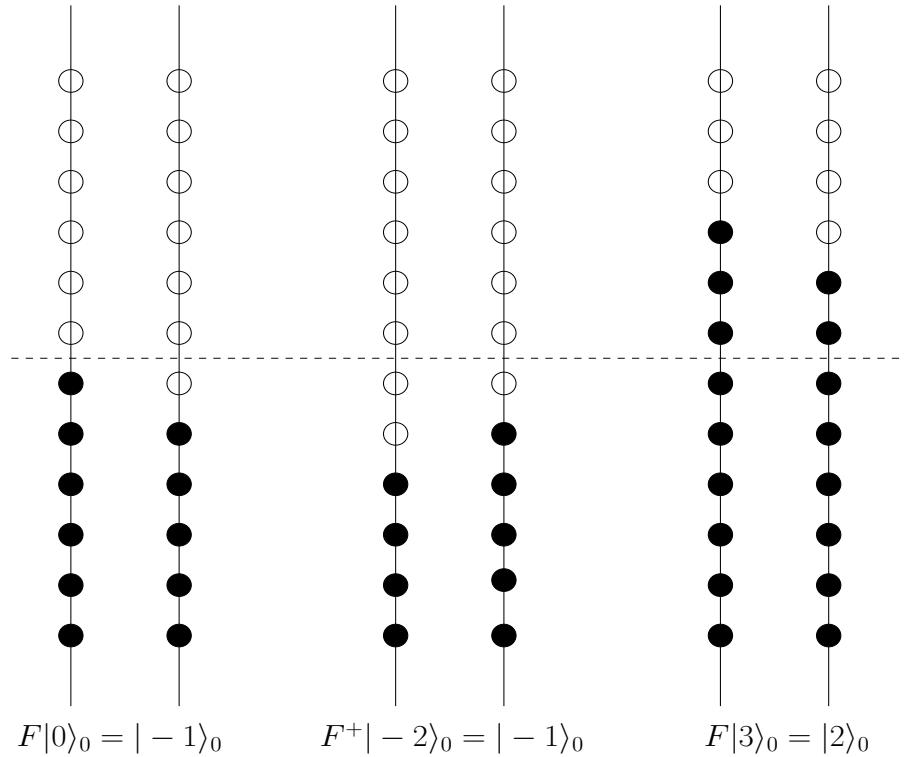


Figure 2.3: The action of  $F$  on the states  $|0\rangle_0$  and  $|3\rangle_0$ , and the action of  $F^+$  on the state  $|-2\rangle_0$ .

## 2.2 Klein factors

The Klein operators  $F_\gamma$  and  $F_\gamma^+$  lower or raise the total fermion number by one, which no combination of bosonic operators can ever do, and they assure also that fermions of different species anti-commute. In the thermodynamic limit and for gapless systems, for most practical purpose, e.g. the computation of correlation functions, there is no difference between states containing  $N_\gamma$  and  $N_\gamma \pm 1$  particles. However, when gaps open up, giving rise to finite correlation lengths, one must be careful when dealing with these operators [26, 27, 31].

For systems with only one type of fermions the Klein factors  $F_\gamma, F_\gamma^+$  simply modify the number of particles corresponding to the ground state on which the boson excitations are created, as depicted in Fig. 2.3. The Klein factors commute with the bosonic operators  $b_{q\gamma}, b_{q\gamma}^+$ , but not with the particle number operator  $N_\gamma$ :

$$[F_\gamma, N_\gamma] = F_\gamma, \quad [F_\gamma^+, N_\gamma] = -F_\gamma^+. \quad (2.34)$$

If more than one species of fermions is considered, e.g. two in the case of spinless

fermions, the corresponding  $(N_L, N_R)$ -particle ground states are tensor products of left and right movers:

$$|N_L, N_R\rangle_0 = |N_L\rangle_0 \otimes |N_R\rangle_0. \quad (2.35)$$

In order to preserve the fermionic character of the annihilation/creation operators, the  $F_R/F_R^+$  operators are defined such that they pick up a minus sign when they pass the left fermionic operators:

$$F_R|N_L, N_R\rangle_0 \equiv (-1)^{N_L}|N_L\rangle_0 \otimes |N_R - 1\rangle_0, \quad (2.36)$$

$$F_R^+|N_L, N_R\rangle_0 \equiv (-1)^{N_L}|N_L\rangle_0 \otimes |N_R + 1\rangle_0. \quad (2.37)$$

In general, for fermionic systems consisting of  $M$  species, one has to define a particular order for the species  $(N_1, \dots, N_M)$ , such that

$$|N_1, N_2, \dots, N_M\rangle_0 \equiv |N_1\rangle_0 \otimes |N_2\rangle_0 \otimes \dots \otimes |N_M\rangle_0 \quad (2.38)$$

and the Klein factors pick up the total sign change from the preceding fermionic operators:

$$F_\gamma|N_1, N_2, \dots, N_M\rangle_0 \equiv (-1)^{\sum_{\alpha=1}^{\gamma-1} N_\alpha} |N_1, N_2, \dots, N_\gamma - 1, \dots, N_M\rangle_0, \quad (2.39)$$

$$F_\gamma^+|N_1, N_2, \dots, N_M\rangle_0 \equiv (-1)^{\sum_{\alpha=1}^{\gamma-1} N_\alpha} |N_1, N_2, \dots, N_\gamma + 1, \dots, N_M\rangle_0. \quad (2.40)$$

For fermions with spin 1/2 (i.e.  $M = 4$ ), the following order is defined:

$$|N_{L\uparrow}, N_{L\downarrow}, N_{R\uparrow}, N_{R\downarrow}\rangle_0. \quad (2.41)$$

According to their definition, the Klein factors of different kind anti-commute. The commutation relations fulfilled by the Klein factors are

$$[b_{q\gamma}, F_{\gamma'}] = [b_{q\gamma}^+, F_{\gamma'}] = [b_{q\gamma}, F_{\gamma'}^+] = [b_{q\gamma}^+, F_{\gamma'}^+] = 0, \quad (2.42)$$

$$\{F_\gamma^+, F_{\gamma'}\} = 2\delta_{\gamma\gamma'}, \quad (2.43)$$

$$\{F_\gamma, F_{\gamma'}\} = \{F_\gamma^+, F_{\gamma'}^+\} = 0 \quad (\text{if } \gamma \neq \gamma'), \quad (2.44)$$

$$[F_\gamma, N_{\gamma'}] = \delta_{\gamma\gamma'} F_\gamma, \quad (2.45)$$

$$[F_\gamma^+, N_{\gamma'}] = -\delta_{\gamma\gamma'} F_\gamma^+. \quad (2.46)$$

## 2.3 Luttinger model

As a result of the approximations made, namely the spectrum linearization around the Fermi points and the introduction of a filled Fermi sea, some one-dimensional models become exactly solvable in certain cases, within the bosonization method. The Hamiltonian under consideration is

$$H = H_0 + H(g_1) + H(g_2) + H(g_3) + H(g_4), \quad (2.47)$$

where  $H_0$  is the kinetic energy given in Eq. (2.15) and  $H(g_1), \dots, H(g_4)$  are interaction terms, given by

$$\begin{aligned} H(g_1) &= \frac{1}{L} \sum_{kpq\sigma\sigma'} (g_{1\parallel} \delta_{\sigma\sigma'} + g_{1\perp} \delta_{-\sigma\sigma'}) \psi_{kR\sigma}^+ \psi_{pL\sigma'}^+ \psi_{-p+qR\sigma'} \psi_{-k+qL\sigma}, \\ H(g_2) &= \frac{1}{L} \sum_{kpq\sigma\sigma'} (g_{2\parallel} \delta_{\sigma\sigma'} + g_{2\perp} \delta_{-\sigma\sigma'}) \psi_{kR\sigma}^+ \psi_{pL\sigma'}^+ \psi_{p-qL\sigma'} \psi_{k-qR\sigma}, \\ H(g_3) &= \frac{1}{2L} \sum_{kpq\sigma\sigma'} (g_{3\parallel} \delta_{\sigma\sigma'} + g_{3\perp} \delta_{-\sigma\sigma'}) \\ &\quad \times (\psi_{kL\sigma}^+ \psi_{pL\sigma'}^+ \psi_{q-pR\sigma'} \psi_{-k-q-(G-4k_F)R\sigma} \\ &\quad \quad \quad + \psi_{kR\sigma}^+ \psi_{pR\sigma'}^+ \psi_{-p-q-(G-4k_F)L\sigma'} \psi_{-k+qL\sigma}), \\ H(g_4) &= \frac{1}{2L} \sum_{kpq\sigma\sigma'} (g_{4\parallel} \delta_{\sigma\sigma'} + g_{4\perp} \delta_{-\sigma\sigma'}) \\ &\quad \times (\psi_{kR\sigma}^+ \psi_{pR\sigma'}^+ \psi_{p+qR\sigma'} \psi_{k-qR\sigma} + \psi_{kL\sigma}^+ \psi_{pL\sigma'}^+ \psi_{p-qL\sigma'} \psi_{k+qL\sigma}). \end{aligned} \quad (2.48)$$

For a graphical representation see Fig. 2.4.

The nomenclature in terms of  $g_i$  is standard in the literature and is called ‘‘g-ology’’ [17]. The  $g_2$  and  $g_4$  interactions are scattering processes with small momentum transfer, i.e.  $\ll 2k_F$ , while the  $g_1$  interaction is a scattering process with a large momentum transfer  $\approx 2k_F$ . Umklapp scattering is relevant only for  $G \approx 4k_F, 6k_F, \dots$ , where  $G$  is a reciprocal lattice vector, i.e. for commensurate filling. If the interactions are assumed to be instantaneous and local, the Pauli principle forbids the processes corresponding to  $g_{3\parallel}$  and  $g_{4\parallel}$ . In the absence of the  $g_{1\perp}$  and  $g_{3\perp}$  processes the bosonization of the

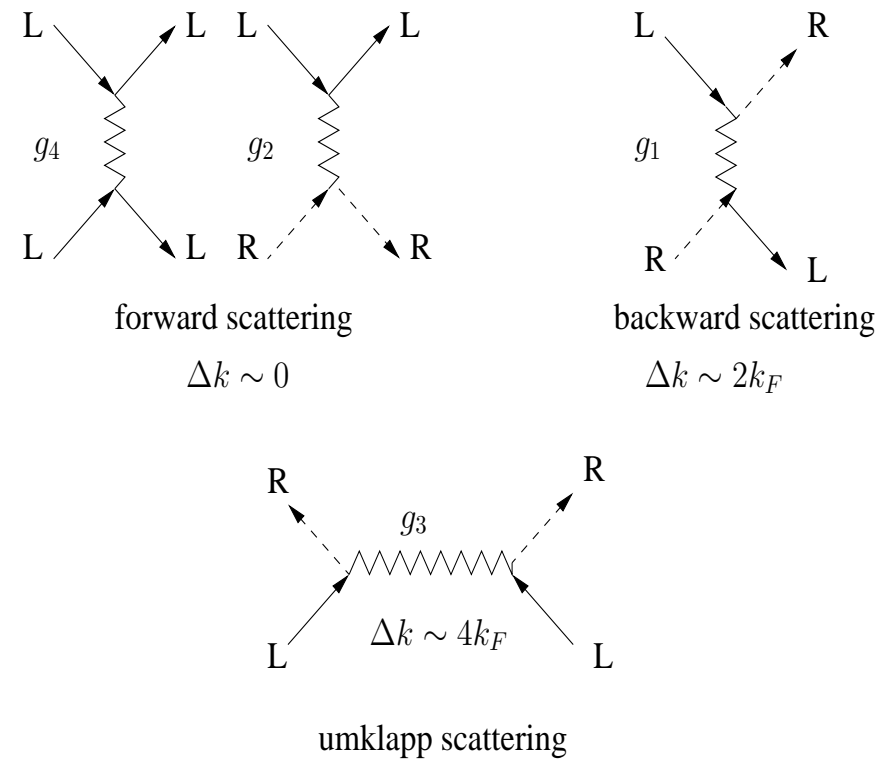


Figure 2.4: Graphic representation of the scattering processes. The solid and the dashed lines correspond to electrons belonging to the branches containing  $-k_F$  and  $+k_F$ , respectively.



terms (2.15) and (2.48) leads to the exactly solvable quadratic Hamiltonian

$$\begin{aligned}
H_{\text{Luttinger}} &= \sum_{q>0} \left( \frac{\pi v_F}{L} + \frac{g_{4\parallel} + g_{4\perp}}{2L} \right) (\rho_L(q)\rho_L(-q) + \rho_R(q)\rho_R(-q)) \\
&+ \sum_{q>0} \frac{-g_{1\parallel} + g_{2\parallel} + g_{2\perp}}{2L} (\rho_L(q)\rho_R(-q) + \rho_R(q)\rho_L(-q)) \\
&+ \sum_{q>0} \left( \frac{\pi v_F}{L} + \frac{g_{4\parallel} - g_{4\perp}}{2L} \right) (\sigma_L(q)\sigma_L(-q) + \sigma_R(q)\sigma_R(-q)) \\
&+ \sum_{q>0} \frac{-g_{1\parallel} + g_{2\parallel} - g_{2\perp}}{2L} (\sigma_L(q)\sigma_R(-q) + \sigma_R(q)\sigma_L(-q)) \\
&+ \text{“zero modes” } (q = 0),
\end{aligned} \tag{2.49}$$

which in terms of dual charge and spin fields, Eqs. (2.26)-(2.27), is known as Luttinger Hamiltonian

$$\begin{aligned}
H_{\text{Luttinger}} &= \sum_{\alpha=c,s} \int_0^L \frac{dx}{2\pi} \left[ \frac{v_\alpha}{g_\alpha} (\partial_x \phi_\alpha)^2 + v_\alpha g_\alpha (\partial_x \theta_\alpha)^2 \right] \\
&+ \frac{\pi}{4L} \sum_{\alpha=c,s} \left[ \frac{v_\alpha}{g_\alpha} N_\alpha^2 + v_\alpha g_\alpha J_\alpha^2 \right].
\end{aligned} \tag{2.50}$$

The coefficients  $v_\alpha$  and  $g_\alpha$  are called Luttinger parameters, and they are related to the  $g$ 's via [13]

$$v_s = v_F \sqrt{\left(1 + \frac{g_{4\parallel}}{2\pi v_F} - \frac{g_{4\perp}}{2\pi v_F}\right)^2 - \left(\frac{g_{2\parallel} - g_{1\parallel} - g_{2\perp}}{2\pi v_F}\right)^2}, \tag{2.51}$$

$$v_c = v_F \sqrt{\left(1 + \frac{g_{4\parallel}}{2\pi v_F} + \frac{g_{4\perp}}{2\pi v_F}\right)^2 - \left(\frac{g_{2\parallel} - g_{1\parallel} + g_{2\perp}}{2\pi v_F}\right)^2}, \tag{2.52}$$

$$g_s = \sqrt{\frac{2\pi v_F + g_{4\parallel} - g_{4\perp} - g_{2\parallel} + g_{1\parallel} + g_{2\perp}}{2\pi v_F + g_{4\parallel} - g_{4\perp} + g_{2\parallel} - g_{1\parallel} - g_{2\perp}}}, \tag{2.53}$$

$$g_c = \sqrt{\frac{2\pi v_F + g_{4\parallel} + g_{4\perp} - g_{2\parallel} + g_{1\parallel} - g_{2\perp}}{2\pi v_F + g_{4\parallel} + g_{4\perp} + g_{2\parallel} - g_{1\parallel} + g_{2\perp}}}. \tag{2.54}$$

The Luttinger Hamiltonian has the same type of low energy excitations as the harmonic chain, i.e. it corresponds to a free boson model (see appendix B). It contains two decoupled sectors corresponding to charge and spin excitations. The phenomenon of spin-charge separation is an important feature of fermionic systems in one dimension. For example, a “real” electron which is injected into an interacting system will decay

into its constituent elementary excitations which are charge and spin density modes that propagate at different velocities ( $v_c$  and  $v_s$ ).

Besides the bosonic part, the Hamiltonian contains also a second part (given in the second line of (2.50)) which is a combination of  $N_\eta$  operators, defined as follows:

$$\text{total charge:} \quad N_c = N_{L,\uparrow} + N_{L,\downarrow} + N_{R,\uparrow} + N_{R,\downarrow}, \quad (2.55)$$

$$\text{charge current:} \quad J_c = N_{L,\uparrow} + N_{L,\downarrow} - N_{R,\uparrow} - N_{R,\downarrow}, \quad (2.56)$$

$$\text{total spin:} \quad N_s = N_{L,\uparrow} - N_{L,\downarrow} + N_{R,\uparrow} - N_{R,\downarrow}, \quad (2.57)$$

$$\text{spin current:} \quad J_s = N_{L,\uparrow} - N_{L,\downarrow} - N_{R,\uparrow} + N_{R,\downarrow}; \quad (2.58)$$

the fermionic ground state  $|N_{L,\uparrow}, N_{L,\downarrow}, N_{R,\uparrow}, N_{R,\downarrow}\rangle_0$  can be redefined in terms of these new operators as

$$|N_{L\uparrow}, N_{L\downarrow}, N_{R\uparrow}, N_{R\downarrow}\rangle_0 \equiv |N_c, J_c, N_s, J_s\rangle_0. \quad (2.59)$$

# Chapter 3

## Spinless fermions

In the Luttinger Hamiltonian, the Klein factors appear only in the combination  $F_\eta^+ F_\eta = 1$  and hence they can be ignored. The Klein factors become important when nonlinear terms appear. In order to study their role in more detail, we consider in the following a system of interacting spinless fermions with nearest-neighbor interaction on a one-dimensional lattice with static dimerization. The static dimerization is introduced as a periodic lattice distortion, which leads to a modulation of the hopping amplitude. Both the nearest-neighbor interaction and the static dimerization introduce nonlinearities in the bosonized Hamiltonian, with non-trivial combinations of Klein factors  $F_L^+ F_R$ , which require a careful and rigorous treatment [32]. Using a variational ansatz in which the bosonic fields and the Klein factors are treated on equal footing, we calculate the energy gap and the Drude weight. To verify the accuracy of the method we compare our results with numerical and exact results which are available for certain values of the model parameters.

### 3.1 Model and formalism

The system of interacting spinless fermions with static dimerization is described by the following Hamiltonian:

$$\begin{aligned} H = & -t \sum_j (1 + (-1)^j u) (c_j^+ c_{j+1} + c_{j+1}^+ c_j) \\ & + V \sum_j n_j n_{j+1}, \end{aligned} \quad (3.1)$$

where  $u$  is the dimerization parameter that leads to a periodic modulation of the hopping amplitude, and  $V$  is the strength of the nearest-neighbor interaction. In momentum space fermion operators are defined by

$$c_j = \frac{1}{\sqrt{L/a}} \sum_k e^{ikR_j} c_k, \quad \text{with } R_j = ja, \quad (3.2)$$

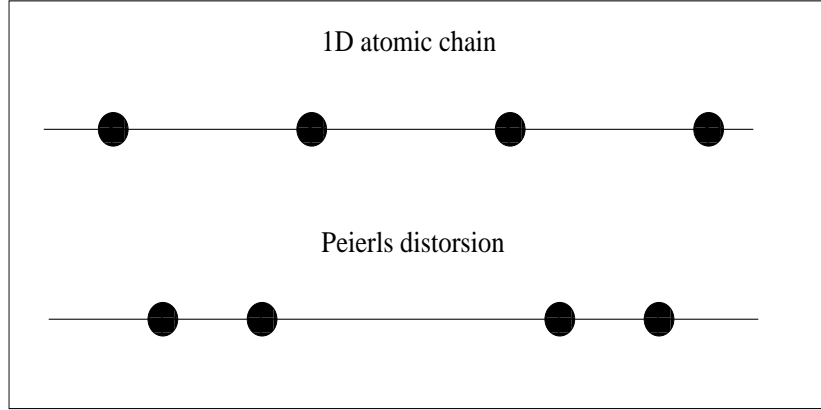


Figure 3.1: Modulation of the hopping amplitude

and correspondingly the Hamiltonian (3.1) reads

$$\begin{aligned}
 H = & \sum_k \epsilon(k) c_k^\dagger c_k + 2itv \sum_k \sin(ka) c_k^\dagger c_{k+\pi/a} \\
 & + \frac{a}{L} \sum_q V(q) \sum_{kp} c_k^\dagger c_p^\dagger c_{p-q} c_{k+q},
 \end{aligned} \tag{3.3}$$

where  $V(q) = V e^{-iqa}$ ,  $\epsilon(k) = -2t \cos(ka)$ , and  $a$  is the lattice spacing.

In order to have a non-degenerate ground state we consider a half-filled system with an odd number of particles. Note that in this case,  $k_F = \pi/2a - \pi/L$ . Before bosonizing the Hamiltonian we have to choose a reference state with respect to which the boson excitations are created; we choose the Fermi sea of the half-filled system as this reference state, as illustrated in Fig. 3.2. In order to bosonize the Hamiltonian (3.3) we follow the notation introduced in chapter 2. The left and right spinless boson fields, and the bosonization identities are given by Eqs. (2.20)-(2.23), where the spin index has to be dropped. Correspondingly, the charge and spin fields introduced as linear combinations of the left and right movers, given by Eqs. (2.26)-(2.27), are replaced for spinless fermions by

$$\phi(x) = \frac{1}{2}(\varphi_L + \varphi_R + \varphi_L^+ + \varphi_R^+), \tag{3.4}$$

$$\theta(x) = \frac{1}{2}(\varphi_L - \varphi_R + \varphi_L^+ - \varphi_R^+). \tag{3.5}$$

The bosonized Hamiltonian of this model reads

$$H = H_0 + H_{\text{Peierls}} + H_{\text{Umklapp}}. \tag{3.6}$$

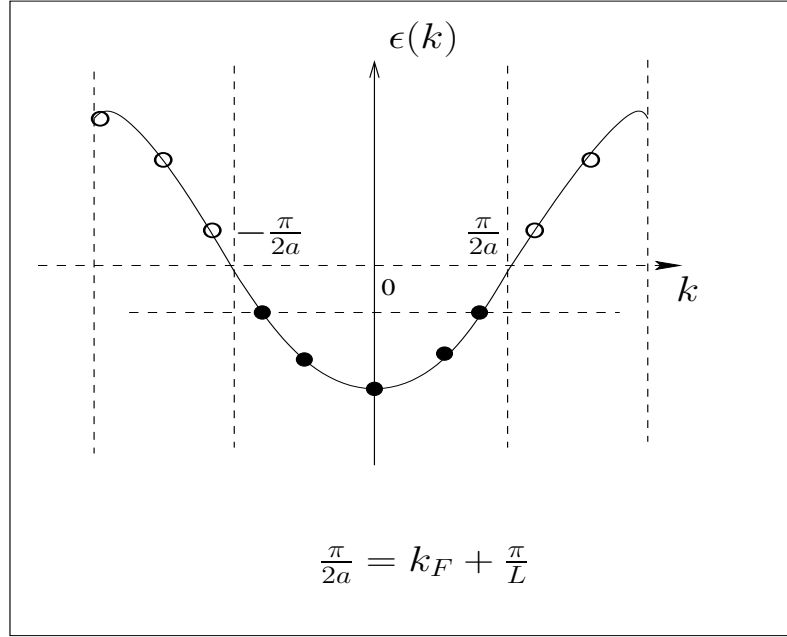


Figure 3.2: Reference state for a system with 10 lattice sites, chosen as the filled Fermi sea for 5 particles.

$$H_0 = \int_0^L \frac{dx}{2\pi} \left\{ \frac{v}{g} : (\partial_x \phi)^2 : + vg : (\partial_x \theta)^2 : \right\} + \frac{\pi v}{2Lg} N^2 + \frac{\pi v g}{2L} J^2, \quad (3.7)$$

$$H_{\text{Peierls}} = -\tilde{u} \int_0^L dx i F_L^+ F_R e^{2i\phi(x)} e^{2i\pi x N/L} + \text{h.c.}, \quad (3.8)$$

$$H_{\text{Umklapp}} = +\tilde{V} \int_0^L dx F_R^+ F_R^+ F_L F_L e^{-4i\phi(x)} e^{-4i\pi x N/L} + \text{h.c.}, \quad (3.9)$$

where  $\tilde{u} = tu/(\pi a)$ ,  $\tilde{V} = V(2k_F)/(2\pi)^2 a$  and  $V(2k_F) = -V e^{2i\pi a/L} \approx -V$ .  $\phi$  and  $\theta$  are defined in Eqs. (3.4)-(3.5) and the cut-off parameter  $a$  is chosen equal to the lattice spacing.  $N$  and  $J$  are the charge and current operators defined as  $N = N_L + N_R$  and  $J = N_L - N_R = 0, \pm 2, \pm 4, \dots$ . The particle number  $N$  is a conserved quantity and is counted relative to the reference state, i.e.  $N = 0$  in the case of half filling. The  $g$  and  $v$  are the Luttinger liquid parameters, given in the weak coupling limit by

$$v = v_F \sqrt{\left(1 + \frac{g_4}{\pi v_F}\right)^2 - \left(\frac{g_2}{\pi v_F}\right)^2}, \quad g = \sqrt{\frac{1 + \frac{g_4}{\pi v_F} - \frac{g_2}{\pi v_F}}{1 + \frac{g_4}{\pi v_F} + \frac{g_2}{\pi v_F}}}, \quad (3.10)$$

where we have introduced the notation  $g_4 = V(0)$ ,  $g_2 = V(0) - V(2k_F)$ . At half filling, for the model of spinless fermions with only nearest neighbor interaction, the Luttinger parameters can be exactly determined by comparison with the Bethe ansatz solution

$V/t$	-2	$-\sqrt{2}$	-1	0	1	$\sqrt{2}$	2
$\eta$	0	$\pi/8$	$\pi/6$	$\pi/4$	$\pi/3$	$3\pi/8$	$\pi/2$
$g$	$\infty$	2	$3/2$	1	$3/4$	$2/3$	$1/2$
$v/ta$	0	0.94	1.29	2	2.59	2.82	$\pi$

Table 3.1: Numerical examples for the relation between standard parameters of the spinless-fermion model at half filling, on the basis of the Bethe ansatz results in the regime  $-2t \leq V \leq 2t$ :  $V = -2t \cos(2\eta)$ ,  $g = \pi/4\eta$ , and  $v = \pi ta \sin(2\eta)/(\pi - 2\eta)$ .

[48]. The renormalized Fermi velocity  $v = \pi ta \sin(2\eta)/(\pi - 2\eta)$  and the Luttinger parameter  $g = \pi/4\eta$  are related with the interaction according to  $V = -2t \cos(2\eta)$ .

The Klein factors and the term proportional to the current operator  $\pi v g J^2/(2L)$  do not commute. We define a new operator  $A = F_R^+ F_L$  and its hermitian conjugate  $A^+ = F_L^+ F_R$ . The four-fermion terms arising from Umklapp scattering are  $F_R^+ F_R^+ F_L F_L = -A^2$  and  $F_L^+ F_L^+ F_R F_R = -(A^+)^2$ . Since the Klein factors are unitary operators, it is easy to show that also the operator  $A$  is unitary and one concludes that its eigenvalues are pure phase factors, i.e.

$$A|k\rangle = e^{ik}|k\rangle, \quad A^+|k\rangle = e^{-ik}|k\rangle, \quad (3.11)$$

with  $0 \leq k < 2\pi$ .

In the thermodynamic limit,  $L \rightarrow \infty$ , the term  $\sim J^2$  can be neglected if we restrict the range of  $J$  values to a finite interval. We can choose a basis which diagonalizes the Klein factors and replace them by their eigenvalues. At the end one obtains

$$H_{\text{Peierls}} = -\tilde{u} \int_0^L dx i e^{ik} e^{-2i\phi(x)} e^{-2i\pi x N/L} + \text{h.c.}, \quad (3.12)$$

$$H_{\text{Umklapp}} = +\tilde{V} \int_0^L dx e^{2ik} e^{-4i\phi(x)} e^{-4i\pi x N/L} + \text{h.c.}. \quad (3.13)$$

As a result the Hamiltonian separates into different sectors of purely bosonic Hamiltonians, labeled by  $k$ .

As discussed e.g. by Schulz [13], in the thermodynamic limit the Klein factors may be replaced by the Majorana (“real”) fermion operators  $\eta_\alpha$ , which assure the proper anti-commutation between the different species of fermions, but do not change the particle numbers of the ground state. The Majorana fermions satisfy the anti-commutation relation

$$\{\eta_\alpha, \eta_\beta\} = 2\delta_{\alpha,\beta}, \quad (3.14)$$

where  $\alpha, \beta$  could be  $R, L$  and  $\sigma$  for fermions with spin. A typical fermion interaction term, involving Klein factors, looks like

$$\psi_\alpha^+ \psi_\beta^+ \psi_\gamma \psi_\delta = F_\alpha^+ F_\beta^+ F_\gamma F_\delta \times (\text{boson operators}). \quad (3.15)$$

Using Majorana operators a state with  $N$  particles is equivalent to a state with  $N \pm 1$  particles and a fermion interaction term looks like

$$\psi_\alpha^+ \psi_\beta^+ \psi_\gamma \psi_\delta = \eta_\alpha \eta_\beta \eta_\gamma \eta_\delta \times (\text{boson operators}), \quad (3.16)$$

with

$$(\eta_\alpha \eta_\beta \eta_\gamma \eta_\delta)^2 = 1 \quad \Rightarrow \quad \eta_\alpha \eta_\beta \eta_\gamma \eta_\delta = \pm 1. \quad (3.17)$$

Using Eqs. (3.14) and (3.17), one obtains only the eigenvalues  $\eta_R \eta_L = -\eta_L \eta_R = \pm i$ , instead of  $e^{\pm ik}$ , i.e. the continuity is lost. Within the approximate approach using Majorana fermions the Hamiltonian (3.6) can be written as

$$H = H_0 + 2\tilde{u} \int_0^L dx \cos 2\phi(x) - 2\tilde{V} \int_0^L dx \cos 4\phi(x). \quad (3.18)$$

## 3.2 Phase diagram

The zero-temperature phase diagram of spinless fermions with static dimerization has been investigated both numerically and analytically; numerically it is often more convenient to study a dimerized spin 1/2 chain, which however can be mapped onto the model of interacting one-dimensional spinless fermions by the Jordan-Wigner transformation [33]. In the  $V - u$  diagram one obtains different phases: a metallic one where the system behaves as a Luttinger liquid, and an insulating one where a charge gap exists. For  $u \rightarrow 0$  the critical point  $V/t = -\sqrt{2}$  that separates the two phases has been obtained in [34]. For  $V/t \in (-\sqrt{2}, 2)$  the Umklapp scattering process is irrelevant and it is renormalized to zero, while for  $V/t > 2$  this process becomes relevant and results in the opening of a correlation gap. For  $u \neq 0$ , according to perturbative renormalization group calculations [35] and confirmed numerically using the density matrix renormalization group (DMRG) [23], the phase boundary in the  $V - u$  plane shifts to more negative values of  $V$  with increasing  $u$ , as can be seen in Fig. 3.3.

## 3.3 Self-consistent harmonic approximation

In the following we consider the bosonized form of the model given in Eq. (3.6). To discuss the gap formation, we use the self-consistent harmonic approximation (SCHA) which has originally been introduced for the sine-Gordon model [18]. The idea is to

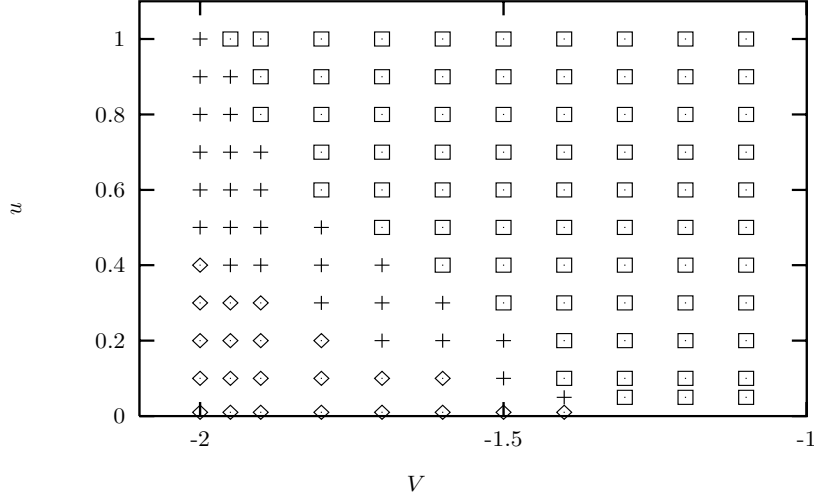


Figure 3.3: Phase diagram for dimerized spinless fermions as obtained using the DMRG [23]. The metallic phase of the system is denoted by  $\diamond$ . As demonstrated in [23] the metallic region increases when including not only a periodic modulation of the hopping parameter, but also in the interaction (+). The region with a gap in the excitation spectrum is marked by  $\square$ .

construct a trial Hamiltonian  $H_{\text{tr}}$  where the nonlinear terms  $\sim e^{\pm 2i\phi}$  in Eq. (3.8) are replaced by a quadratic form with a parameter  $\Delta$  to be determined self-consistently according to a variational principle for the energy.

As we discussed in the preceding section, in the thermodynamic limit we can replace the Klein factors by their eigenvalues Eq. (3.11), where we choose the phase factor  $k = \pi/2$ . The resulting Hamiltonian is equivalent to the Hamiltonian obtained within the Majorana fermion approach and is given in Eq. (3.18).

We introduce the trial Hamiltonian

$$H_{\text{tr}}^{\Delta} = \int_0^L \frac{dx}{2\pi} \left\{ \frac{v}{g} (\partial_x \phi)^2 + vg (\partial_x \theta)^2 + \frac{\Delta^2}{vg} \phi^2(x) \right\}. \quad (3.19)$$

Since we are only interested in properties at zero temperature we use the normalized ground state  $|\psi_0\rangle$  of  $H_{\text{tr}}$  as a variational wave function for the Hamiltonian (3.6). This provides us with an upper bound  $\tilde{E}$  for the ground state energy  $E$  of (3.6) due to the inequality

$$E \leq \tilde{E} = \langle \psi_0 | H | \psi_0 \rangle. \quad (3.20)$$

The variational energy is given by

$$\tilde{E} = \langle H_0 \rangle_{\text{tr}} + \langle H_{\text{Peierls}} \rangle_{\text{tr}}, \quad (3.21)$$

$$\frac{\tilde{E}}{L} = \frac{E_{\text{tr}}}{L} - \frac{\Delta^2}{2\pi vg} \langle \phi^2 \rangle_{\text{tr}} - 2\tilde{u} e^{-2\langle \phi^2 \rangle_{\text{tr}}}, \quad (3.22)$$



where  $E_{\text{tr}}$  is the ground state energy of  $H_{\text{tr}}^{\Delta}$ . Minimizing  $\tilde{E}$  with respect to the variational parameter  $\Delta$  yields the gap equation

$$\Delta^2 = 8\pi v g \tilde{u} e^{-2\langle\phi^2\rangle_{\text{tr}}}. \quad (3.23)$$

Since  $H_{\text{tr}}^{\Delta}$  is bilinear in the field operators it is straightforward to calculate the equal coordinate correlation function of the phase field  $\phi(x)$  entering Eq. (3.22)

$$\langle\phi^2\rangle_{\text{tr}} = \frac{\pi v g}{L} \sum_{k>0} \frac{e^{-ka}}{\sqrt{v^2 k^2 + \Delta^2}}, \quad (3.24)$$

where the  $k$ -values in the sum are multiples of  $2\pi/L$ . Replacing the sum in Eq. (3.24) by an integral we obtain (for  $\Delta \ll \Delta_0$ )

$$\langle\phi^2\rangle_{\text{tr}} = \frac{g}{2} \ln \frac{\Delta_0}{\Delta}, \quad (3.25)$$

where  $\Delta_0 = 2ve^{-\gamma}/a$  and  $\gamma = 0.5772$  is Euler's constant. Inserting Eq. (3.25) into Eq. (3.23) yields

$$\frac{\Delta}{\Delta_0} = \left(\frac{u}{u_0}\right)^{1/(2-g)}, \quad (3.26)$$

with  $u_0 = e^{-\gamma}\Delta_0/4gt$ . For  $g > 2$  the right hand side of Eq. (3.26) diverges as  $u \rightarrow 0$ , and the equation has only the trivial solution  $\Delta = 0$ , i.e. the line  $g = 2$  marks the transition from a gapless to a gapped phase in the  $g - u$  plane. In the spinless fermion model this corresponds to the line  $V/t = -\sqrt{2}$  in the  $V - u$  phase diagram. The value  $g_c = 2$  obtained within the variational approach is in accordance with the exact result [34]. However, according to renormalization group [35] and DMRG calculations [23], the phase boundary in the  $g - u$  plane shifts to larger values of  $g$  with increasing  $u$ , while the SCHA gives a vertical line. On the other hand, the exponent  $1/(2 - g)$  characterizing the opening of the gap is exact [19].

For non-interacting fermions  $V = 0$ , the Luttinger parameter is  $g = 1$  and correspondingly  $\Delta \propto u$ , in agreement with the exact energy gap. The prefactor however depends on the cut-off procedure used. From Eq. (3.26) we find  $\Delta = 4tue^{\gamma}$ , where the factor  $e^{\gamma}$  has its origins in the soft cut-off used in Eq. (3.24). If we replace in Eq. (3.24) the soft cut-off by a hard cut-off the result is  $\Delta = 4tu/\pi$ .

At  $V/t = 2$ ,  $g=1/2$ , where Umklapp scattering becomes relevant and leads to the opening of a correlation gap, Eq. (3.26) yields  $\Delta \propto u^{2/3}$  which agrees up to a logarithmic correction with the exact result  $\Delta_{ex} \propto u^{2/3}/\sqrt{|\ln u|}$  [36].

### 3.4 Finite systems

In the following we consider a finite system of length  $L$ . In this case it is not possible to replace the Klein factors by their eigenvalues, since the term proportional to the current operator  $J^2$  in the Luttinger Hamiltonian (3.7) does not commute with the  $F$ 's. The trial Hamiltonian is now chosen as a sum of two commuting parts  $H_{\text{tr}} = H_{\text{tr}}^{\Delta} + H_{\text{tr}}^B$ , with  $H_{\text{tr}}^{\Delta}$  given in Eq. (3.19) and the ‘‘Klein Hamiltonian’’

$$H_{\text{tr}}^B = -iB(F_L^+ F_R - F_R^+ F_L) + \frac{\pi v g}{2L} J^2, \quad (3.27)$$

where  $\Delta$  and  $B$  are variational parameters to be determined self-consistently.  $H_{\text{tr}}^B$  is of the form of a tight-binding Hamiltonian for a particle moving on a one-dimensional lattice in a harmonic potential. A class of similar Hamiltonians has been studied in [27]. In this case we decouple the Klein factors from the bosonic fields and the minimum condition for the variational energy is equivalent to the following substitution in the Peierls dimerization term

$$F_L^+ F_R e^{2i\phi(x)} \rightarrow \langle F_L^+ F_R \rangle e^{2i\phi(x)} + F_L^+ F_R \langle e^{2i\phi(x)} \rangle. \quad (3.28)$$

As a result, instead of replacing the products of Klein factors by their *eigenvalues* as in the thermodynamic limit we now have to replace them by their *expectation values* with respect to the ground state of  $H_{\text{tr}}^B$ . According to the Feynman-Hellmann theorem [37, 38], the expectation value  $\langle F_L^+ F_R \rangle$  can be expressed in terms of the derivative of the ground state energy  $E_0$  of the Klein Hamiltonian  $H_{\text{tr}}^B$

$$\langle F_L^+ F_R \rangle = i \frac{\partial E_0}{\partial B}. \quad (3.29)$$

The variational energy obtained from  $H_{\text{tr}}$  has to be minimized with respect to the parameters  $\Delta$  and  $B$  and we obtain the gap equations

$$\begin{aligned} \Delta^2 &= -4\pi v g \tilde{u} E_0'(B) e^{-2\langle \phi^2 \rangle_{\text{tr}}}, \\ B &= \tilde{u} L e^{-2\langle \phi^2 \rangle_{\text{tr}}}, \end{aligned} \quad (3.30)$$

where  $E_0(B)$  is the ground state energy of  $H_{\text{tr}}^B$  and  $E_0'(B) = \partial E_0(B)/\partial B$ . In order to calculate the ground state energy of  $H_{\text{tr}}^B$  it is convenient to switch to the momentum representation,  $J \rightarrow -id/dp_J$ , where the Hamiltonian reads

$$H_{\text{tr}}^B = -\frac{\pi v g}{2L} \frac{d^2}{dp_J^2} + 2B \cos(2p_J), \quad (3.31)$$

with periodic boundary conditions for the wave function,  $\Psi(p_J + \pi) = \Psi(p_J)$ . At this point, we note a close analogy with the quantum theory of Josephson junctions, see

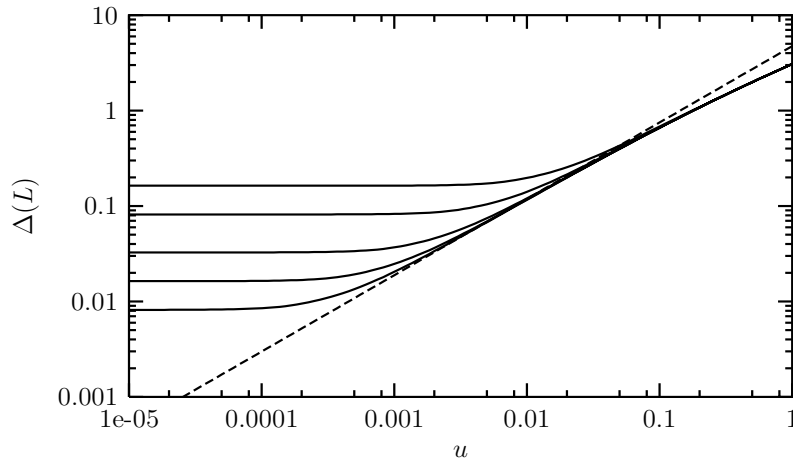


Figure 3.4: Energy gap  $\Delta(L)$  (in units of  $t$ ) as function of the dimerization parameter  $u$  for  $L = 100, 200, 500, 1000, 2000$  (from top to bottom). The dashed line is the analytic result of Eq. (3.26) valid for  $L \rightarrow \infty$  and  $\Delta \ll \Delta_0$ .

[39] and appendix C. The corresponding Schrödinger equation is the Mathieu equation. Accordingly, the ground state energy of  $H_{tr}^B$  has the following asymptotic behavior [40]:

$$E_0(B) \approx \begin{cases} -\frac{B^2 L}{\pi v g} & \text{for } LB \ll v, \\ -2B + \sqrt{\frac{2B\pi v g}{L}} & \text{for } LB \gg v. \end{cases} \quad (3.32)$$

Combining the two equations (3.30) one obtains

$$\Delta^2 L^2 = -4\pi v g E'_0(B) B L, \quad (3.33)$$

which can be used to relate the two limiting cases of Eq. (3.32) with two different physical situations: The condition of large system size  $L \gg v/B$  is equivalent with  $\Delta \gg v/L$  and therefore the results for  $\langle \phi^2 \rangle_{tr}$  and  $\Delta(u)$  are the same as for the infinite system. On the other hand, the condition of small systems,  $L \ll v/B$  implies that  $\Delta \ll v/L$ . In this case the size dependent energy gap  $\Delta(L)$  is purely due to the finite system size, i.e. it is of order  $v/L$ . Thus the crossover from a finite-size gap to a true dimerization gap coincides with the crossover between the regions where Klein factors are relevant or can be ignored.

In general, the set of equations (3.30) can only be solved numerically. Fig. 3.4 shows the size-dependent energy gap  $\Delta(L) = \sqrt{(2\pi v/L)^2 + \Delta^2}$  as function of  $u$  for several values of the system size  $L$ ; notice that periodic boundary conditions are imposed, where the smallest wave number is  $2\pi/L$ . The Luttinger parameter is  $g = 3/4$  which corresponds to  $V/t = 1$ .

### 3.5 Drude weight

The Drude weight or charge stiffness is a physical quantity used to characterize charge transport at zero frequency. At  $T = 0$  the real part of the electrical conductivity at frequency  $\omega$  is of the form  $\sigma(\omega) = 2\pi D\delta(\omega) + \sigma_{reg}(\omega)$  with  $\sigma_{reg}(\omega) \rightarrow 0$  for  $\omega \rightarrow 0$  in a system without impurities. Therefore  $D = 0$  characterizes an insulator while  $D > 0$  describes an (ideal) conductor [41]. The Drude weight is not a true order parameter related to a symmetry breaking, however, it can be used to distinguish the insulating from the metallic phase. The simplest way to calculate  $D$  is due to Kohn [41] who has shown that the Drude weight can be expressed as

$$D = \frac{L}{2} \left. \frac{\partial^2 E(\varphi)}{\partial \varphi^2} \right|_{\varphi=0} = \frac{L}{2} \left( \frac{\Phi_0}{2\pi} \right)^2 \left. \frac{\partial^2 E(\Phi)}{\partial \Phi^2} \right|_{\Phi=0}, \quad (3.34)$$

where  $E(\varphi)$  is the ground state energy of a ring of circumference  $L$  which is threaded by the magnetic flux  $\Phi$ , where  $\varphi = 2\pi\Phi/\Phi_0$  and  $\Phi_0 = h/e$ . In the fermionic model (3.1) the hopping parameter  $t$  picks up a phase factor  $\exp(\pm i\varphi/L)$  when a flux  $\Phi$  is applied. Alternatively, within a proper gauge transformation, the parameter  $\varphi$  can also be associated with a change of boundary conditions, i.e.  $\varphi = 0$  corresponds to periodic and  $\varphi = \pi$  to anti-periodic boundary conditions. The Drude weight is directly related to the persistent current  $I(\Phi)$  which flows in a ring that is penetrated by a magnetic flux [42, 43]

$$I(\Phi) = -\frac{\partial E(\Phi)}{\partial \Phi}.$$

#### 3.5.1 Drude weight within bosonization

We now turn to the calculation of the Drude weight  $D$  within the bosonization formalism. In the presence of the magnetic flux the only modification in the bosonized Hamiltonian of the Luttinger model appears in the current operator  $J$  which has to be replaced by  $J + \frac{\varphi}{\pi}$  [44] and the Drude weight is given by the product of Luttinger parameters  $D_0 = vg/2\pi$ . Correspondingly, for the system with dimerization, we modify the  $B$ -dependent part of the the trial Hamiltonian and write

$$H_{\text{tr}}^B(\varphi) = -iB(F_L^+ F_R - F_R^+ F_L) + \frac{\pi vg}{2L} \left( J + \frac{\varphi}{\pi} \right)^2. \quad (3.35)$$

Applying the same procedure as in the case  $\varphi = 0$  yields a variational estimate  $\tilde{E}$  for the ground state energy which now depends on the flux  $\varphi$ , i.e.  $\tilde{E} = \tilde{E}(\Delta, B, \varphi)$  where  $\Delta$  and  $B$ , obtained from the gap equations (3.30), are also functions of  $\varphi$ . On first sight it might seem impossible to calculate the Drude weight using Eq. (3.34) since there is no analytical solution of the gap equations (3.30) even for  $\varphi = 0$ . However, a

closer look reveals a great deal of simplification. From the second derivative

$$\begin{aligned} \frac{d^2 \tilde{E}}{d\varphi^2} &= \frac{\partial^2 \tilde{E}}{\partial \Delta^2} \left( \frac{\partial \Delta}{\partial \varphi} \right)^2 + \frac{\partial^2 \tilde{E}}{\partial B^2} \left( \frac{\partial B}{\partial \varphi} \right)^2 + \frac{\partial \tilde{E}}{\partial \Delta} \frac{\partial^2 \Delta}{\partial \varphi^2} \\ &\quad + \frac{\partial \tilde{E}}{\partial B} \frac{\partial^2 B}{\partial \varphi^2} + \frac{\partial^2 \tilde{E}}{\partial \varphi^2} + \text{mixed terms} \end{aligned} \quad (3.36)$$

one retains only

$$\left. \frac{d^2 \tilde{E}}{d\varphi^2} \right|_{\varphi=0} = \left. \frac{\partial^2 \tilde{E}(\Delta, B, \varphi)}{\partial \varphi^2} \right|_{\varphi=0} \quad (3.37)$$

since *i)*  $\frac{\partial \tilde{E}}{\partial \Delta} = \frac{\partial \tilde{E}}{\partial B} = 0$  due to the minimum condition of the energy and *ii)*  $\frac{\partial \Delta}{\partial \varphi} = \frac{\partial B}{\partial \varphi} = 0$  at  $\varphi = 0$  due to symmetry ( $\Delta$  and  $B$  are even functions of  $\varphi$ ). Since the trial Hamiltonian  $H_{\text{tr}} = H_{\text{tr}}^{\Delta} + H_{\text{tr}}^B(\varphi)$  consists of two commuting parts we may write  $\tilde{E}(\Delta, B, \varphi) = \tilde{E}(\Delta) + E_0(B, \varphi)$  where  $\tilde{E}(\Delta)$  depends only on  $\Delta$  and  $E_0(B, \varphi)$  is the ground state energy of  $H_{\text{tr}}^B(\varphi)$ , i.e. we obtain the simple result

$$D = \left. \frac{L}{2} \frac{\partial^2 E_0(B, \varphi)}{\partial \varphi^2} \right|_{\varphi=0}, \quad (3.38)$$

where  $B$  is given by Eq. (3.30).

To proceed we again represent  $H_{\text{tr}}^B(\varphi)$  in terms of the Mathieu equation (3.31) where now the boundary conditions are  $\Psi(p_J + \pi) = e^{i\varphi} \Psi(p_J)$ . It is now straightforward to calculate the Drude weight for a finite system of size  $L$  in the gapped phase  $g < 2$ . In the “finite size gap” region ( $L\Delta \ll v$ ), the confining potential of the trial Hamiltonian (3.35) is the dominant term and the hopping can be regarded as a small perturbation. In second order perturbation theory we obtain

$$D = D_0 \left( 1 - \frac{q^2}{2} + \dots \right), \quad (3.39)$$

where  $q = 2LB/\pi v g \propto uL^{2-g}$  and  $D_0 = vg/2\pi$  is the Drude weight of an unperturbed Luttinger liquid. In the limit  $q \rightarrow 0$  which is equivalent to  $uL^{2-g} \rightarrow 0$  the Drude weight is equal to the value  $D_0$ .

In the opposite limit ( $L\Delta \gg v$ ) which corresponds to a Mathieu equation with a large cosine potential the variation of the ground state energy with change of boundary conditions is exponentially small (as expected from the WKB approximation). A more careful treatment (see appendix D) yields the exponential dependence

$$D \approx D_0 \frac{4}{\pi} \left( \frac{L\Delta}{vg} \right)^{3/2} e^{-2L\Delta/\pi v g}, \quad (3.40)$$

where  $\Delta$  and  $u$  are related via Eq. (3.26).

For  $g > 2$  the system remains in the Luttinger liquid phase for small dimerization  $u$ , however with renormalized Luttinger parameters. These renormalizations are not obtained within the SCHA and consequently the Drude weight is not reduced in this region.

### 3.5.2 Drude weight for free spinless fermions

As a test case that can be solved exactly, we consider the Hamiltonian (3.1) in the limit  $V = 0$ . In this case we can calculate the ground state energy analytically. Our aim is to compare the exact result for the Drude weight with the result obtain within the SCHA in order to assess the accuracy of the method.

When a flux  $\Phi$  is applied, the system is described by the Hamiltonian

$$H = -t \sum_j (1 + u(-1)^j) (c_j^+ c_{j+1} e^{i\varphi/L} + \text{h.c.}), \quad (3.41)$$

which in momentum representation reads

$$H = -2t \sum_k' (c_k^+, c_{k+\pi}^+) \begin{pmatrix} \cos k & -iu \sin k \\ iu \sin k & -\cos k \end{pmatrix} \begin{pmatrix} c_k \\ c_{k+\pi} \end{pmatrix}. \quad (3.42)$$

The prime on the sum indicates the reduction of the Brillouin zone from  $[-\frac{\pi}{a}, \frac{\pi}{a}]$  to  $[-\frac{\pi}{2a}, \frac{\pi}{2a}]$ . The corresponding dispersion  $\epsilon_{1,2}(k) = \pm 2t \sqrt{\cos^2 k + u^2 \sin^2 k}$  is shown in Fig. 3.5. The ground state energy is

$$E(\varphi) = -2t \sum_k' \sqrt{\cos^2 k + u^2 \sin^2 k}, \quad (3.43)$$

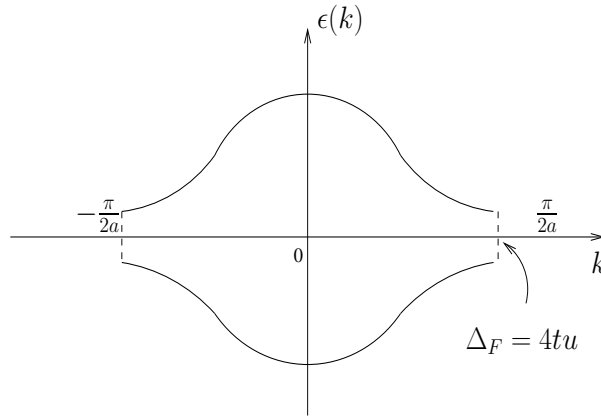
where for a system of length  $L$ ,  $k = (2\pi n + \varphi)/L$ , and the lattice constant is set to one. In the following we assume a dependence of the ground state energy on  $\varphi$  of the form [45]

$$E(\varphi) = E_0 + E_1 \cos(\varphi), \quad (3.44)$$

The second term, in general, is an infinite sum of harmonic terms, but for a ring with a Peierls distorsion, threatened by a magnetix flux, at  $T = 0$  the main contribution is given by the first harmonic term [45]. Under this assumption the Drude weight is given by

$$D = -\frac{LE_1}{2} = \frac{L}{4} [E(\pi) - E(0)]. \quad (3.45)$$

We calculate now the difference  $\Delta E = E(\pi) - E(0)$  which is needed in the Drude weight evaluation (3.45). We introduce  $z_m = e^{ik_m}$  and the function  $f(z) = 1/(z^L - e^{i\varphi})$

Figure 3.5: Dispersion of free fermions with dimerization  $u$ .

which has single poles at  $z_m$  with residues  $\text{Res}f(z)|_{z=z_m} = z_m e^{-i\varphi}/L$ . Expressing Eq. (3.43) in terms of  $z_m$  we may replace the sum by a contour integral and obtain

$$E(\varphi) = -\frac{tL e^{i\varphi} \sqrt{1-u^2}}{2} \oint_{\mathcal{C}} \frac{dz}{2\pi i} \frac{\sqrt{z^2 + z^{-2} + 2\gamma}}{z(z^L - e^{-i\varphi})}, \quad (3.46)$$

where  $\gamma = (1+u^2)/(1-u^2)$  and  $\mathcal{C}$  is a contour that encloses the singularities of  $f(z)$ . We choose  $\mathcal{C}$  to be composed of two circles with radii slightly larger or smaller than one, respectively. Substituting  $z \rightarrow 1/z$  the integral along the inner circle can be mapped onto the integral along the outer circle. The square root in the numerator has branch cuts along the imaginary axis in the interval  $[-y_1, y_1]$  and for  $|y| > y_0$  where  $\pm iy_0$  and  $\pm iy_1$  are the zeroes of the function under the square root. Now we deform the integration contour along the branch cut from  $\pm iy_0$  to  $\pm i\infty$ , as can be seen in Fig. 3.6 and obtain for the energy difference  $\Delta E = E(\pi) - E(0)$ :

$$\Delta E = \frac{4tL\sqrt{1-u^2}}{\pi} \int_{y_0}^{\infty} \frac{dy}{y} \frac{\sqrt{y^2 + y^{-2} - 2\gamma}}{y^L - y^{-L}}. \quad (3.47)$$

Substituting  $y = e^x$  yields

$$\Delta E = \frac{4tL\sqrt{1-u^2}}{\pi} \int_{x_0}^{\infty} dx \frac{\sqrt{2 \cosh(2x) - 2\gamma}}{e^{Lx} - e^{-Lx}}, \quad (3.48)$$

with  $2x_0 = \text{Arcosh}\gamma = \ln((1+u)/(1-u))$ . For  $Lx_0 \gg 1$  the integral is rapidly cut off by the exponential and we may expand the square root around  $x = x_0$ . The Drude weight is then

$$D = \frac{L\Delta E}{4} \approx t \sqrt{\frac{2uL}{\pi}} e^{-\frac{L}{2} \ln \frac{1+u}{1-u}} \left( 1 + \frac{3(1-u^2)}{8Lu} + \dots \right). \quad (3.49)$$

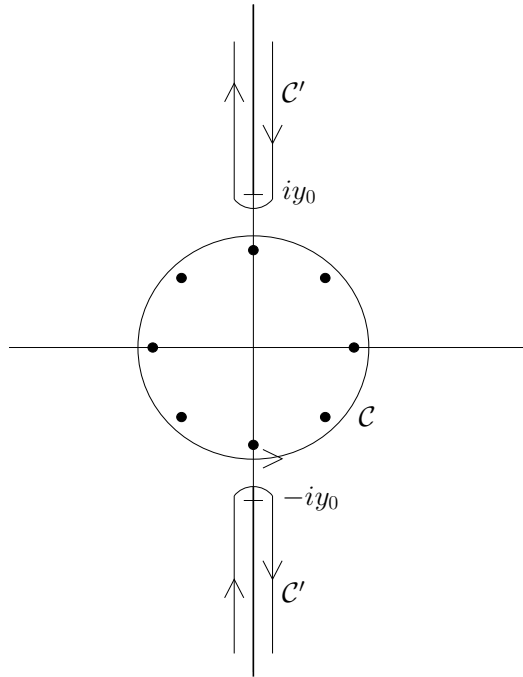


Figure 3.6: The contour  $\mathcal{C}$  is deformed into the contour  $\mathcal{C}'$  along the branch cuts between  $\pm iy_0$  and  $\pm i\infty$ .

Expanding the logarithm for  $u \ll 1$ , and inserting  $\Delta_{\text{ex}} = 4tu$  and  $v_F = 2t$  yields

$$D_{\text{ex}} \approx D_0 \left( \frac{\pi L \Delta_{\text{ex}}}{v_F} \right)^{1/2} e^{-L \Delta_{\text{ex}} / 2v_F}. \quad (3.50)$$

In the special case of free fermions, the Luttinger parameters are  $g = 1$  and  $v = v_F = 2t$ . If we insert these values in Eq. (3.40) we can compare the exact result, Eq. (3.50), with the Drude weight obtained within the SCHA, Eq. (3.40). We see that the exponential behavior  $D \sim \exp(-\text{const} \cdot L \Delta / v)$  is reproduced, however, with a different constant  $2/\pi$  instead of  $1/2$ . This slight difference is not surprising since the energy scale  $\Delta_0$ , see Eq. (3.26), is known to depend on the cutoff procedure within SCHA.



# Chapter 4

## Hubbard model

In order to analyze further the importance of Klein factors in bosonized Hamiltonians with several nonlinear perturbations, we consider in the following a system of interacting spin 1/2 fermions on a one-dimensional lattice. As in the case of spinless fermions, we demonstrate how to handle the Klein factors in a systematic way, both in the thermodynamic limit and for finite systems. Within the self-consistent harmonic approximation the decoupling of the Klein factors from the bosonic fields results in a two-dimensional tight binding Hamiltonian with a confining potential. While for spinless fermions, the Klein Hamiltonian can be mapped onto a Mathieu equation which can be solved analytically in certain limits, for fermions with spin the problem becomes more complicated. As an application we consider two different models, the Peierls-Hubbard model and the ionic Hubbard model. The first model contains a static alternating Peierls distortion  $u$  of the lattice, i.e. a modulation of the hopping amplitudes in the kinetic term. In the second model, an alternating on-site energy modulation is introduced, i.e. a staggered potential.

### 4.1 Hubbard model

The Hubbard model is described by the Hamiltonian

$$H = -t \sum_{i,\sigma} (c_{i\sigma}^+ c_{i+1\sigma} + \text{h.c.}) + U \sum_i n_{i\uparrow} n_{i\downarrow}, \quad (4.1)$$

where  $c_{i\sigma}^+$  creates an electron with spin direction  $\sigma = \uparrow, \downarrow$  and  $t$  is the hopping parameter.  $U$  is the interaction energy of two electrons at the same site, ( $U > 0$ ).

In momentum space the Hamiltonian reads

$$H = \sum_{k\sigma} \epsilon_k c_{k\sigma}^+ c_{k\sigma} + \frac{U}{N} \sum_{k,p,q} c_{k+q\uparrow}^+ c_{p-q\downarrow}^+ c_{p\downarrow} c_{k\uparrow} \quad (4.2)$$

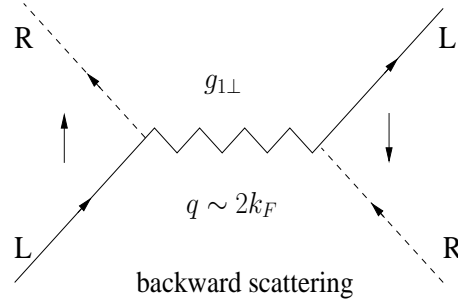


Figure 4.1: Schematic representation of backward scattering. Solid (dashed) lines refer to electrons close to the left (right) Fermi points.  $g_{1\perp}$  couples electrons with opposite spin.

where  $\epsilon_k = -2t \cos(ka)$  and  $N$  is the number of lattice sites. Applying the bosonization procedure, described in chapter 2 one obtains

$$H = H_0 + H_1 + H_2, \quad (4.3)$$

where  $H_0$  is the Luttinger Hamiltonian,

$$H_0 = \sum_{\alpha=c,s} \int_0^L dx \left\{ \frac{v_\alpha}{g_\alpha} (\partial_x \phi_\alpha)^2 + v_\alpha g_\alpha (\partial_x \theta_\alpha)^2 \right\} + \frac{\pi}{4L} \sum_{\alpha=c,s} \left\{ \frac{v_\alpha}{g_\alpha} N_\alpha^2 + v_\alpha g_\alpha J_\alpha^2 \right\}, \quad (4.4)$$

and  $H_1$  and  $H_2$  are the backscattering and Umklapp contribution, respectively. Backward and Umklapp scattering, which represent scatterings with large momentum transfer, introduce nonlinear terms in the spin and the charge sector, respectively. As a consequence the spin and the charge currents are no longer conserved.

The Hamiltonian resulting from the backward scattering corresponds to an interaction between left and right Fermi points with a momentum transfer  $q \sim 2k_F$ , see Fig. 4.1. In bosonized form the backward scattering term reads

$$H_1 = \tilde{U} \int_0^L dx \left[ F_{R\uparrow}^+ F_{L\downarrow}^+ F_{R\downarrow} F_{L\uparrow} e^{-i\frac{2\pi}{L} N_s x} e^{-i2\sqrt{2}\phi_s} + F_{L\uparrow}^+ F_{R\downarrow}^+ F_{L\downarrow} F_{R\uparrow} e^{i\frac{2\pi}{L} N_s x} e^{i2\sqrt{2}\phi_s} \right], \quad (4.5)$$

with  $\tilde{U} = UL/[(2\pi a)^2 N]$ .

The Umklapp term  $H_2$  is only important for commensurate band fillings. This process comes about because the state at  $k_F$  is equivalent to the state  $k_F + nG$ , where  $n$  is an integer and  $G$  is a reciprocal lattice vector,  $G = 2\pi/a$ , with  $a$  being the lattice spacing. For the half-filled band case,  $k_F = \pi/2a$ , and therefore the scatterings  $k_F \rightarrow k_F + 2k_F$  and  $k_F \rightarrow -k_F$  are equivalent. The Umklapp process is characterized by scattering of two particles in the same direction across the Fermi surface with a

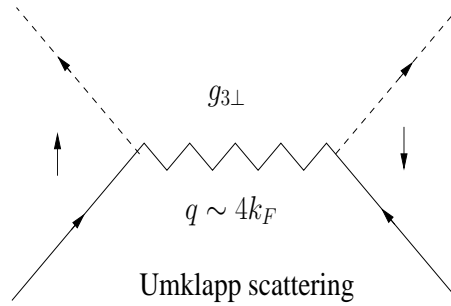


Figure 4.2: Schematic representation of Umklapp scattering. Solid (dashed) lines refer to electrons close to left (right) Fermi points.  $g_{3\perp}$  couples electrons with opposite spin.

momentum transfer  $q \sim 4k_F$ , see Fig. 4.2.

The bosonized form of the Umklapp term is

$$\begin{aligned}
 H_2 = & \tilde{U} \int_0^L dx \left[ F_{R\uparrow}^+ F_{R\downarrow}^+ F_{L\downarrow} F_{L\uparrow} e^{-i\frac{2\pi}{L} N_c x} e^{-i2\sqrt{2}\phi_c} \right. \\
 & \left. + F_{L\uparrow}^+ F_{L\downarrow}^+ F_{R\downarrow} F_{R\uparrow} e^{i\frac{2\pi}{L} N_c x} e^{i2\sqrt{2}\phi_c} \right]. \quad (4.6)
 \end{aligned}$$

The Hubbard model is a particular case of the “g-ology” model given by Eq. (2.4), for which the coupling parameters are  $g_{i\perp} = U$  and  $g_{i\parallel} = 0$ . From Eqs. (2.51)-(2.54) the corresponding Luttinger parameters are obtained as

$$\begin{aligned}
 v_s &= v_F \sqrt{1 - \frac{U}{\pi v_F}}, & v_c &= v_F \sqrt{1 + \frac{U}{\pi v_F}} \\
 g_s &= \frac{1}{\sqrt{1 - \frac{U}{\pi v_F}}}, & g_c &= \frac{1}{\sqrt{1 + \frac{U}{\pi v_F}}},
 \end{aligned}$$

where  $v_F = 2ta \sin(k_F a)$  is the Fermi velocity. The ground state phase diagram of the “g-ology” model has been investigated in detail using renormalization group techniques [17]. Schulz [13] noticed that in the small  $U$  perturbative regime, for all filling factors the backward scattering renormalizes to the weak-coupling fixed point  $g_{1\perp}^* = 0$  and the  $g_s$  parameter scales to  $g_s^* = 1$ . In lowest order of the renormalization group equations the charge parameter  $g_c$  remains unrenormalized and its perturbative value is  $g_c = 1 - U/2\pi v_F$ <sup>1</sup>. Schulz also pointed out that there is no phase transition in the Hubbard model between weak and strong coupling, and hence the small and large  $U$  limits belong to the same phase. As a consequence, the equality  $g_s = 1$  remains valid for all repulsive interactions.

<sup>1</sup>There is a misprint in [13], where the perturbative value of the charge parameter is given by  $g_c = 1 - U/\pi v_F$ .

In the strong coupling limit ( $U \gg t$ ), there are no low-energy charge excitations involving doubly occupied sites. In a restricted Hilbert space containing only singly occupied sites, in second order in  $t/U$  the Hubbard Hamiltonian can be mapped onto the  $t - J$  model, where the spins are coupled through an effective antiferromagnetic exchange integral  $J = 4t^2/U$  [49]

$$H_{t-J} = -t \sum_j [(1 - n_{j-\sigma})c_{j\sigma}^\dagger c_{j+1\sigma}(1 - n_{j+1-\sigma}) + \text{h.c.}] + J \sum_j \left[ \mathbf{S}_j \cdot \mathbf{S}_{j+1} - \frac{1}{4}n_j n_{j+1} \right]. \quad (4.7)$$

At half filling the  $t - J$  model reduces to the antiferromagnetic Heisenberg model

$$H = J \sum_j \mathbf{S}_j \cdot \mathbf{S}_{j+1}, \quad (4.8)$$

which can be transformed to the spinless-fermion Hamiltonian with nearest neighbor interaction using the Jordan-Wigner transformation [33], discussed in the previous chapter, for the special case  $V = 2t$ ,  $g = 1/2$ .

The exact solution of the one-dimensional Hubbard model via Bethe ansatz has been found by Lieb and Wu [48]. However, the Bethe ansatz wave function is in many cases too complicated for the evaluation of expectation values or correlation functions. Still, the Bethe ansatz is a convenient starting point to determine the Luttinger parameters for arbitrary band filling and interaction strength [13].

## 4.2 Peierls-Hubbard model

The coupling of a one-dimensional metal to an elastic lattice results in an instability towards a lattice distortion known as Peierls instability [50]. A lattice distortion decreases the electronic energy which overweights an increase in lattice energy. Due to an opening of a band gap at the Fermi energy the system becomes an insulator. This phenomenon has been observed in various quasi one-dimensional materials, e.g. conjugated polymers [7] like polyacetylene, charge-transfer salts [51] and more recently in the one-dimensional spin systems  $\text{CuGeO}_3$  [8] and  $\text{NaV}_2\text{O}_5$  [9].

From a theoretical point of view, a first step towards a quantitative description of the Peierls transition has been made by Su, Schrieffer and Heeger [52]. However, in their model no electron-electron interactions are taken into account.

The effects of electronic correlations on the Peierls transition have been studied using a variety of methods including variational wave functions [53, 54], Hartree Fock [55], quantum Monte Carlo [56], numerical diagonalization of small systems [57, 58, 59], bosonization [60, 61], and incremental expansion [62, 63].

In the following we neglect the lattice dynamics and consider a model with static lattice distortion given by the Hamiltonian

$$H = -t \sum_{j,\sigma} (1 + (-1)^j u) (c_{j\sigma}^+ c_{j+1\sigma} + c_{j+1\sigma}^+ c_{j\sigma}) + U \sum_j n_{j\uparrow} n_{j\downarrow}, \quad (4.9)$$

which is the usual Hubbard Hamiltonian with an additional periodic modulation of the hopping described by the dimerization parameter  $u$ . For the case of a half-filled band, which we consider here, the lattice modulation is alternating. In momentum space, the Peierls contribution reads

$$H_{\text{Peierls}} = tu \sum_{k,\sigma} (e^{ika} c_{k\sigma}^+ c_{k+\pi\sigma} + \text{h.c.}) \quad (4.10)$$

and in bosonized form

$$\begin{aligned} H_{\text{Peierls}} &= \frac{itu}{\pi a} \int_0^L dx F_{R\uparrow}^+ F_{L\uparrow} e^{-i\frac{\pi}{L}(N_c+N_s)x} e^{-i\sqrt{2}(\phi_c+\phi_s)} \\ &+ \frac{itu}{\pi a} \int_0^L dx F_{R\downarrow}^+ F_{L\downarrow} e^{-i\frac{\pi}{L}(N_c-N_s)x} e^{-i\sqrt{2}(\phi_c-\phi_s)} + \text{h.c.} \end{aligned} \quad (4.11)$$

At half filling,  $N_c = N_s = 0$ , and using the notation  $\tilde{u} = tu/\pi a$  we obtain

$$H_{\text{Peierls}} = \tilde{u} \int_0^L dx \{iF_{R\uparrow}^+ F_{L\uparrow} e^{-i\sqrt{2}(\phi_c+\phi_s)} + iF_{R\downarrow}^+ F_{L\downarrow} e^{-i\sqrt{2}(\phi_c-\phi_s)} + \text{h.c.}\}. \quad (4.12)$$

In the following we focus on the role of the Klein factors. Due to the conservation of charge and spin all combinations of Klein factors appearing in the Hamiltonian (4.12) can be expressed in terms of the operators  $A_\uparrow = F_{R\uparrow}^+ F_{L\uparrow}$  and  $A_\downarrow = F_{R\downarrow}^+ F_{L\downarrow}$  plus their hermitian conjugates. In particular, the four-fermion terms arising from Umklapp and backscattering read

$$F_{R\uparrow}^+ F_{R\downarrow}^+ F_{L\downarrow} F_{L\uparrow} = F_{R\uparrow}^+ F_{L\uparrow} F_{R\downarrow}^+ F_{L\downarrow} = A_\uparrow A_\downarrow, \quad (4.13)$$

$$F_{R\uparrow}^+ F_{L\downarrow}^+ F_{R\downarrow} F_{L\uparrow} = F_{R\uparrow}^+ F_{L\uparrow} F_{L\downarrow}^+ F_{R\downarrow} = A_\uparrow A_\downarrow^+. \quad (4.14)$$

Since the Klein factors are unitary,  $F_\alpha^+ F_\alpha = F_\alpha F_\alpha^+ = 1$ , it is easy to show that

$$[A_\uparrow, A_\uparrow^+] = [A_\downarrow, A_\downarrow^+] = 0, \quad (4.15)$$

and we may choose a basis where  $A_\sigma$  and  $A_\sigma^+$  are both diagonal. From  $A_\uparrow^+ A_\uparrow = A_\downarrow^+ A_\downarrow = 1$  one concludes that the eigenvalues of  $A_\sigma$  are pure phase factors, i.e.

$$A_\uparrow |k_\uparrow, k_\downarrow\rangle = e^{ik_\uparrow} |k_\uparrow, k_\downarrow\rangle, \quad A_\uparrow^+ |k_\uparrow, k_\downarrow\rangle = e^{-ik_\uparrow} |k_\uparrow, k_\downarrow\rangle, \quad (4.16)$$

$$A_\downarrow |k_\uparrow, k_\downarrow\rangle = e^{ik_\downarrow} |k_\uparrow, k_\downarrow\rangle, \quad A_\downarrow^+ |k_\uparrow, k_\downarrow\rangle = e^{-ik_\downarrow} |k_\uparrow, k_\downarrow\rangle, \quad (4.17)$$

with  $0 \leq k_\sigma < 2\pi$ . Although the terms  $\sim J_{c,s}^2$  appearing in (4.4) do not commute with the Klein factors it seems reasonable to neglect them in the thermodynamic limit  $L \rightarrow \infty$ . We may thus replace the Klein factors in  $H_1, H_2$  and  $H_{\text{Peierls}}$  by their eigenvalues, and obtain

$$H_1 = \tilde{U} \int_0^L dx \{e^{i(k_\uparrow - k_\downarrow)} e^{-i2\sqrt{2}\phi_s} + \text{h.c.}\}, \quad (4.18)$$

$$H_2 = \tilde{U} \int_0^L dx \{e^{i(k_\uparrow + k_\downarrow)} e^{-i2\sqrt{2}\phi_c} + \text{h.c.}\}, \quad (4.19)$$

$$H_{\text{Peierls}} = \tilde{u} \int_0^L dx \{ie^{ik_\uparrow} e^{-i\sqrt{2}(\phi_c + \phi_s)} + ie^{ik_\downarrow} e^{-i\sqrt{2}(\phi_c - \phi_s)} + \text{h.c.}\}. \quad (4.20)$$

As a result the Hamiltonian of the dimerized Hubbard model separates into different sectors of purely bosonic Hamiltonians which are labeled by  $k_\uparrow$  and  $k_\downarrow$ . In an approach where the Klein factors are replaced by Majorana fermions [15] one obtains only the eigenvalues  $\pm i$  for the two-fermion terms, and  $\pm 1$  for the four-fermion terms, i.e. the continuous symmetry is lost.

### 4.2.1 Self-consistent harmonic approximation

In order to study the opening of charge and spin gaps in the dimerized Hubbard model we use the self-consistent harmonic approximation (SCHA) in which the exponentials of field operators appearing in (4.19)-(4.20) are replaced by quadratic forms. In the thermodynamic limit we replace the Klein factors by their eigenvalues and introduce the trial Hamiltonian

$$H_{\text{tr}} = \sum_{\alpha=c,s} \int_0^L \frac{dx}{2\pi} \left\{ \frac{v_\alpha}{g_\alpha} (\partial_x \phi_\alpha)^2 + v_\alpha g_\alpha (\partial_x \theta_\alpha)^2 + \frac{\Delta_\alpha^2}{v_\alpha g_\alpha} \phi_\alpha^2 \right\}, \quad (4.21)$$

which provides us with a variational estimate for the ground state energy

$$\tilde{E} = \langle H_0 \rangle_{\text{tr}} + \langle H_1 \rangle_{\text{tr}} + \langle H_2 \rangle_{\text{tr}} + \langle H_{\text{Peierls}} \rangle_{\text{tr}}, \quad (4.22)$$

$$\frac{\tilde{E}}{L} = \frac{E_{\text{tr}}}{L} - \sum_{\alpha=c,s} \frac{\Delta_\alpha^2}{2\pi v_\alpha g_\alpha} \langle \phi_\alpha^2 \rangle_{\text{tr}} + e(k_\uparrow, k_\downarrow), \quad (4.23)$$

where  $E_{\text{tr}}$  is the ground state energy of  $H_{\text{tr}}$ , and

$$e(k_\uparrow, k_\downarrow) = 2B_c \cos(k_\uparrow + k_\downarrow) + 2B_s \cos(k_\uparrow - k_\downarrow) - 2B_{cs}(\sin k_\uparrow + \sin k_\downarrow), \quad (4.24)$$

range	$k_\uparrow$	$k_\downarrow$	$e_0(B_c, B_s, B_{cs})$
$0 < B_{cs} < 2B_s$	$\arcsin \frac{B_{cs}}{2B_s}$	$\pi - \arcsin \frac{B_{cs}}{2B_s}$	$-2B_c - 2B_s - \frac{B_{cs}^2}{B_s}$
$2B_s < B_{cs}$	$\frac{\pi}{2}$	$\frac{\pi}{2}$	$-4B_{cs} - 2B_c + 2B_s$

Table 4.1: Minimum  $e_0$  of  $e(k_\uparrow, k_\downarrow) = 2B_c \cos(k_\uparrow + k_\downarrow) + 2B_s \cos(k_\uparrow - k_\downarrow) - 2B_{cs}(\sin k_\uparrow + \sin k_\downarrow)$  which is used in the gap equations (4.28) and (4.29). The first line is only relevant for  $u = 0$  (Hubbard model without dimerization) whereas the second line is relevant for  $u > 0$ .

with

$$B_c = \tilde{U} e^{-4\langle\phi_c^2\rangle_{\text{tr}}}, \quad (4.25)$$

$$B_s = \tilde{U} e^{-4\langle\phi_s^2\rangle_{\text{tr}}}, \quad (4.26)$$

$$B_{cs} = \tilde{u} e^{-\langle\phi_c^2\rangle_{\text{tr}}} e^{-\langle\phi_s^2\rangle_{\text{tr}}}. \quad (4.27)$$

Minimizing the variational ground state energy with respect to  $\Delta_c$  and  $\Delta_s$  yields the gap equations

$$\frac{\Delta_c^2}{2\pi v_c g_c} = -4B_c \frac{\partial e_0}{\partial B_c} - B_{cs} \frac{\partial e_0}{\partial B_{cs}}, \quad (4.28)$$

$$\frac{\Delta_s^2}{2\pi v_s g_s} = -4B_s \frac{\partial e_0}{\partial B_s} - B_{cs} \frac{\partial e_0}{\partial B_{cs}}, \quad (4.29)$$

where  $e_0$  is the minimum of  $e(k_\uparrow, k_\downarrow)$  with respect to  $k_\uparrow$  and  $k_\downarrow$  (see Table 4.1).

The first minimum is only relevant for  $u = 0$  where  $B_{cs} = 0$ , i.e. the first line of Table 4.1 with  $\partial e_0 / \partial B_c = -2$ ,  $\partial e_0 / \partial B_s = -2$  corresponds to the Hubbard model without dimerization. In this case the equations for the charge and spin parameters are

$$\frac{\Delta_c^2}{2\pi v_c g_c} = 8B_c, \quad (4.30)$$

$$\frac{\Delta_s^2}{2\pi v_s g_s} = 8B_s. \quad (4.31)$$

The numerical solution of these equations is displayed in Fig. 4.3, where here and in all the following figures both  $\Delta_c$  and  $\Delta_s$  are given in units of  $t$ .

Since  $H_{\text{tr}}$  is quadratic in the bosonic fields it is straightforward to calculate  $\langle\phi_c^2\rangle_{\text{tr}}$  and  $\langle\phi_s^2\rangle_{\text{tr}}$  analytically. In the thermodynamic limit, where the sums are replaced by

integrals one obtains

$$\langle \phi_c^2 \rangle_{\text{tr}} = \frac{g_c}{2} \ln \frac{\Delta_{0c}}{\Delta_c}, \quad (4.32)$$

$$\langle \phi_s^2 \rangle_{\text{tr}} = \frac{g_s}{2} \ln \frac{\Delta_{0s}}{\Delta_s}, \quad (4.33)$$

where  $\Delta_{0c,0s}$  are cutoff-dependent energy scales of the order of the bandwidth, and  $\Delta_{c,s} < \Delta_{0c,0s}$  is assumed. The solution of the gap equations (4.30) and (4.31) is

$$\Delta_c = \Delta_{c0} \left( \frac{16\pi v_c g_c \tilde{U}}{\Delta_{c0}^2} \right)^{1/(2-2g_c)}, \quad (4.34)$$

$$\Delta_s = 0. \quad (4.35)$$

Using the perturbative result  $g_c = 1 - U/2\pi v_F$  and  $v_F = 2t$ , we obtain

$$\Delta_c \propto e^{-2\pi t \ln(t/U)/U} \quad (4.36)$$

in the small  $U$  limit. This should be compared with the exact solution from Bethe ansatz where for small  $U$  the charge gap is given by

$$\Delta_c^{\text{B.a.}} = \frac{8U}{\pi t} e^{-2\pi t/U}. \quad (4.37)$$

The SCHA result deviates from the exact solution by the factor  $\ln(t/U)$  in the exponent. We show the charge gap obtained within the SCHA in comparison with the exact solution from the Bethe ansatz in Fig. 4.4.

For non-zero dimerization  $u > 0$  a solution of the gap equations exists only for  $B_{cs} > 2B_s$ , i.e. the second line of Table 4.1 has to be used, with  $\partial e_0/\partial B_c = -2$ ,  $\partial e_0/\partial B_s = 2$  and  $\partial e_0/\partial B_{cs} = -4$ . The corresponding gap equations are

$$\frac{\Delta_c^2}{2\pi v_c g_c} = 4B_{cs} + 8B_c = 4\tilde{u} e^{-\langle \phi_c^2 \rangle_{\text{tr}} - \langle \phi_s^2 \rangle_{\text{tr}}} + 8\tilde{U} e^{-4\langle \phi_c^2 \rangle_{\text{tr}}}, \quad (4.38)$$

$$\frac{\Delta_s^2}{2\pi v_s g_s} = 4B_{cs} - 8B_s = 4\tilde{u} e^{-\langle \phi_c^2 \rangle_{\text{tr}} - \langle \phi_s^2 \rangle_{\text{tr}}} - 8\tilde{U} e^{-4\langle \phi_s^2 \rangle_{\text{tr}}}. \quad (4.39)$$

The numerical solution of these equations is represented in Fig. 4.5 for  $U/t = 1$ . For very small dimerization  $u$  the charge gap  $\Delta_c$  approaches a constant while the spin gap goes to zero, as expected for the Hubbard model without dimerization. On the other hand, for strong dimerization  $\Delta_c$  and  $\Delta_s$  approach each other as expected for a band insulator without correlations. The transition between the two regimes is smooth and continuous.



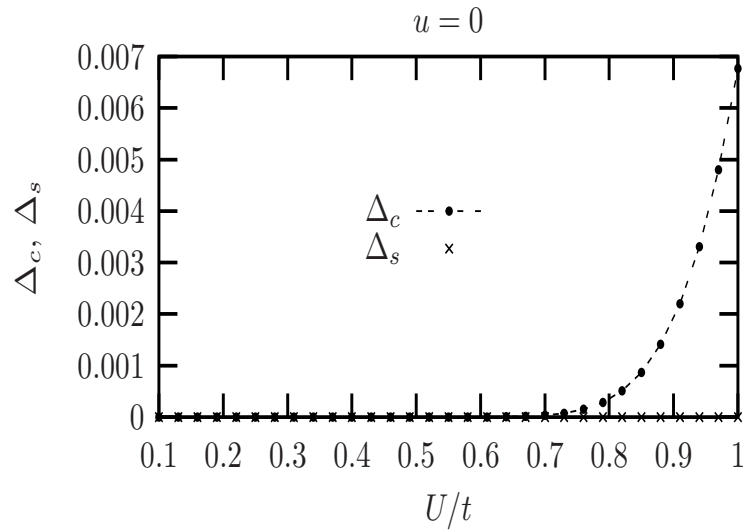


Figure 4.3: The charge gap  $\Delta_c$  (in units of  $t$ ), obtained within SCHA as function of the Hubbard  $U$  for  $u = 0$ . In this case  $\Delta_s = 0$ .

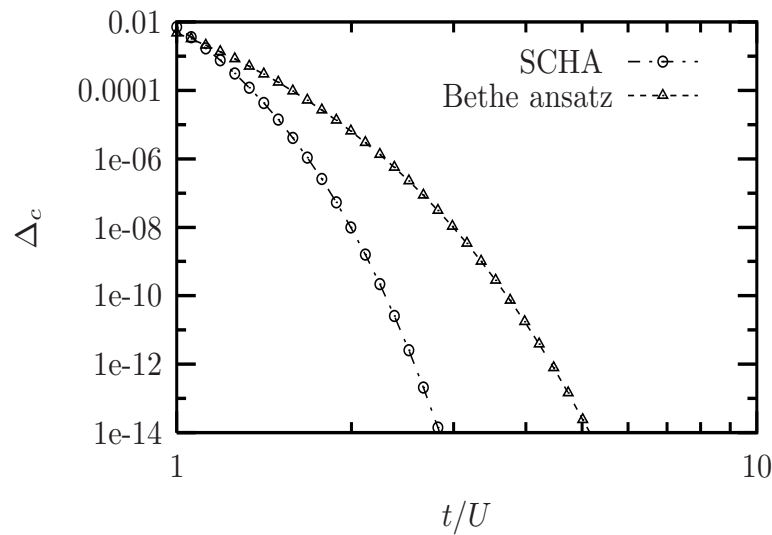


Figure 4.4: The gap parameter  $\Delta_c$  (in units of  $t$ ) as function of  $t/U$ : the SCHA solution  $\Delta_c^{\text{SCHA}} \sim e^{-2\pi t \ln(t/U)/U}$ , and the Bethe ansatz solution  $\Delta_c^{\text{B.a.}} \sim e^{-2\pi t/U}$ , both valid in the limit  $U/t \ll 1$ .

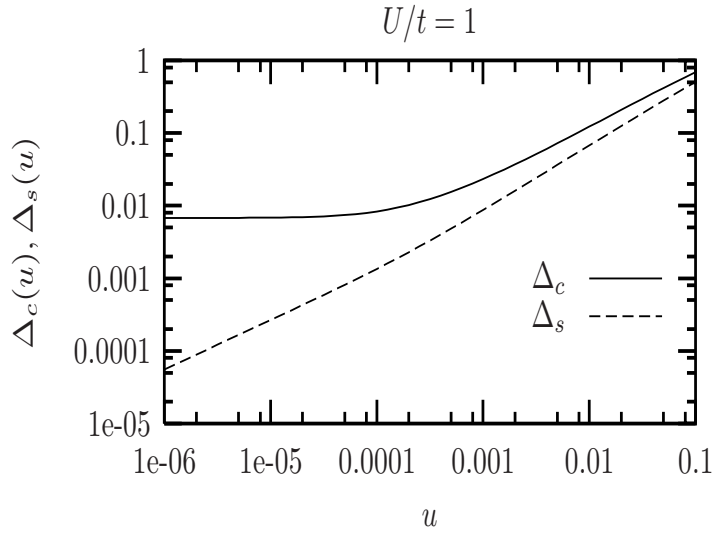


Figure 4.5: Charge gap  $\Delta_c$  and spin gap  $\Delta_s$  (in units of  $t$ ) of the dimerized Hubbard model for  $U/t = 1$  obtained within SCHA. We have used the value  $g_s = 1$  and the expressions  $g_c = 1/\sqrt{1 + U/(\pi v_F)}$ ,  $v_{c,s} = v_F \sqrt{1 \pm U/(\pi v_F)}$ .

For small  $U$  these results can be verified analytically. In order to solve the gap equations analytically we consider the case  $U > 0$  where  $g_s = 1$  and  $g_c < 1$ , and restrict ourselves to the limit of small dimerization  $u$ . Using the analytical results for  $\langle \phi_c^2 \rangle_{\text{tr}}$  and  $\langle \phi_s^2 \rangle_{\text{tr}}$ , given by Eqs. (4.32)-(4.33), one obtains that for  $u \rightarrow 0$  the spin gap vanishes while the charge gap approaches a constant according to

$$\Delta_c(u) - \Delta_c(0) \propto u^{4/3}, \quad (4.40)$$

$$\Delta_s(u) \propto u^{2/3}, \quad (4.41)$$

with cutoff-dependent prefactors (for details see appendix F). The exponent  $2/3$  that characterizes the opening of the spin gap is in accordance with the corresponding exponent of the dimerized antiferromagnetic Heisenberg chain up to a logarithmic correction in the prefactor [36]. Since the Heisenberg model corresponds to the  $U \rightarrow \infty$  limit of the half-filled Hubbard model, this indicates that the SCHA result (4.41) is exact and persists even in the strong-coupling regime  $U/t \gg 1$ . For  $u > u^*$  the behavior of the gap is changed to [64]

$$\Delta_c(u) \approx \Delta_s(u) \propto u^{2/(3-g_c)}, \quad (4.42)$$

where the crossover value  $u^*$  is defined by  $\Delta_s(u^*) = \Delta_c(0)$ . The  $u - U$  phase diagram is shown in Fig. 4.6. In Fig. 4.7 we show  $\Delta_c(u) - \Delta_c(0)$  and  $\Delta_s(u)$  as function of  $u$  for  $U/t = 1$  as obtained from the numerical solution of the gap equations. For comparison, the analytical results of Eqs. (4.40) and (4.41) are also shown.

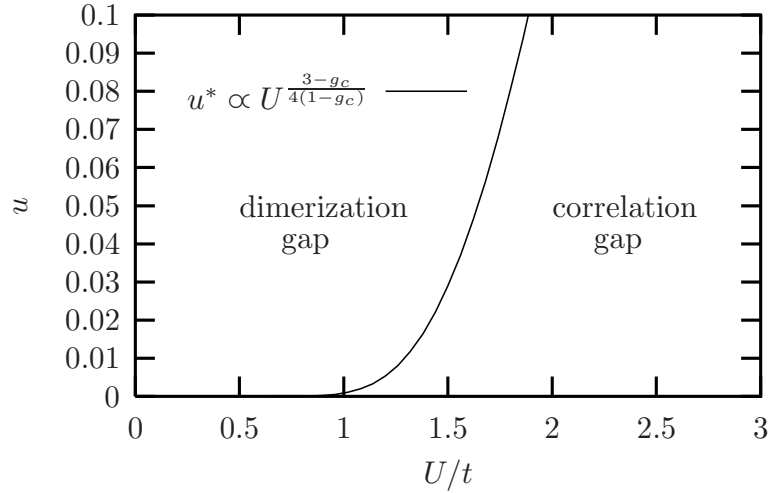


Figure 4.6: Phase diagram of the dimerized Hubbard model.  $u^*$  marks the crossover from a dimerization gap to a correlation gap.

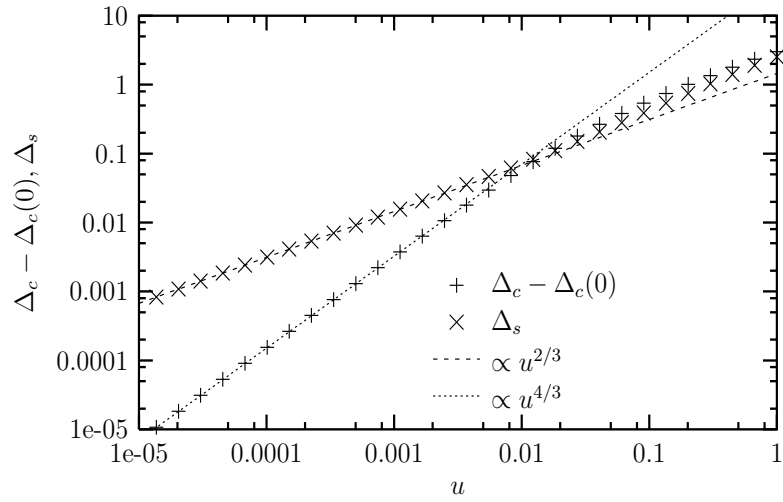


Figure 4.7: Charge gap  $\Delta_c(u) - \Delta_c(0)$  and spin gap  $\Delta_s(u)$  (in units of  $t$ ) of the dimerized Hubbard model for  $U/t = 1$  obtained within the SCHA. The straight lines are the analytic results of Eqs. (4.40) and (4.41) valid for  $u < u^*$ . Note that  $\Delta_c(0)$  is subtracted from the charge gap in order to highlight the power law behavior.

### 4.2.2 Finite systems

As in the case of spinless fermions, for a finite system it is not possible to simply replace the Klein factors by their eigenvalues since the terms proportional to the spin and charge current,  $J_c$  and  $J_s$ , in the Luttinger Hamiltonian (4.4) do not commute with the  $F$ 's. One may, however, decouple the Klein factors from the bosonic fields using a variational ansatz. We introduce the Klein Hamiltonian

$$\begin{aligned} H_{\text{tr}}^{B_{cs}B_cB_s} &= iB_{cs}L(F_{R\uparrow}^+F_{L\uparrow} + F_{R\downarrow}^+F_{L\downarrow}) + B_cLF_{R\uparrow}^+F_{R\downarrow}^+F_{L\downarrow}F_{L\uparrow} \\ &\quad + B_sLF_{R\uparrow}^+F_{L\downarrow}^+F_{R\downarrow}F_{L\uparrow} + \text{h.c.} \\ &\quad + \frac{\pi}{4L}(v_c g_c J_c^2 + v_s g_s J_s^2), \end{aligned} \quad (4.43)$$

where  $B_c$ ,  $B_s$  and  $B_{cs}$  are now variational parameters to be determined self-consistently.  $H_{\text{tr}}^{B_{cs}B_cB_s}$  is of the form of a tight-binding Hamiltonian for a particle moving on a  $2d$  lattice in a harmonic potential. The explicit representation of this Hamiltonian in the  $|J_c, J_s\rangle$  is given in appendix E. The minimum condition for the variational energy is equivalent to the following substitution in the backward and Umklapp terms

$$F_\alpha^+ F_\beta^+ F_\gamma F_\rho e^{\pm i k_a \phi_a} \rightarrow \langle F_\alpha^+ F_\beta^+ F_\gamma F_\rho \rangle e^{\pm i 2\sqrt{2}\phi_a} + F_\alpha^+ F_\beta^+ F_\gamma F_\rho \langle e^{\pm i 2\sqrt{2}\phi_a} \rangle \quad (4.44)$$

and to the substitution

$$F_\alpha^+ F_\beta e^{\pm i\sqrt{2}\phi_a \mp i\sqrt{2}\phi_b} \rightarrow \langle F_\alpha^+ F_\beta \rangle e^{\pm i\sqrt{2}\phi_a \mp i\sqrt{2}\phi_b} + F_\alpha^+ F_\beta \langle e^{\pm i\sqrt{2}\phi_a \mp i\sqrt{2}\phi_b} \rangle \quad (4.45)$$

in the Peierls term, where  $\alpha, \beta, \gamma, \rho \in \{R \uparrow, L \uparrow, R \downarrow, L \downarrow\}$  and  $a, b \in \{c, s\}$ . As a result, instead of replacing the products of Klein factors by their eigenvalues as in the thermodynamic limit we now have to replace them by their expectation values with respect to the ground state of  $H_{\text{tr}}^{B_{cs}B_cB_s}$  divided by the system size. The details of the calculations are given in appendix A. The Klein Hamiltonian (4.43) can only be diagonalized numerically. In the bosonic sector one ends up with a sine-Gordon type model like in the thermodynamic limit. In order to evaluate the mean field parameter, in the framework of the SCHA, the quantity  $e_0$  which enters the gap equations (and which is explicitly given in Table 4.1) is replaced by  $e_{\text{tr}}^0$ , the ground state energy of  $H_{\text{tr}}^{B_{cs}B_cB_s}$  divided by  $L$  (see appendix A). Apart from this modification Eqs. (4.28)-(4.29) remain unchanged.

We consider a system with both spin and charge gap, i.e.  $u \neq 0$ . For large systems the parameters  $B_{cs}$ ,  $B_c$  and  $B_s$  become size-independent, with the consequence that the kinetic energy in  $H_{\text{tr}}^{B_{cs}B_cB_s}$  dominates the confining potential. While approaching the thermodynamic limit, the  $e_{\text{tr}}^0$  is given by the minimum of  $e(k_\uparrow, k_\downarrow)$ , see Eq. (4.24), and the expectation values of the Klein factors converge to the corresponding eigenvalues as can be seen in Fig. 4.8.

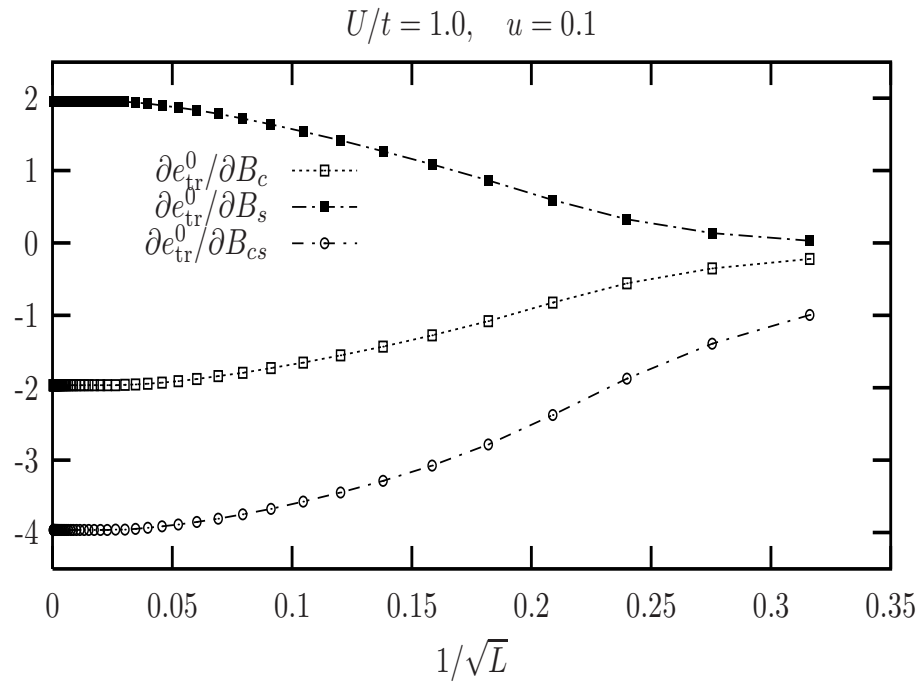


Figure 4.8: The derivative of  $e_{\text{tr}}^0$  with respect to the variational parameters  $B_c, B_s, B_{cs}$  needed to find the solution of equation (4.28), (4.29), for  $u \neq 0$ . With increasing  $L$  they converge to the values corresponding to the thermodynamic limit given in Table 4.1:  $\partial e_{\text{tr}}^0 / \partial B_c = 2$ ,  $\partial e_{\text{tr}}^0 / \partial B_s = -2$ ,  $\partial e_{\text{tr}}^0 / \partial B_{cs} = -4$ .

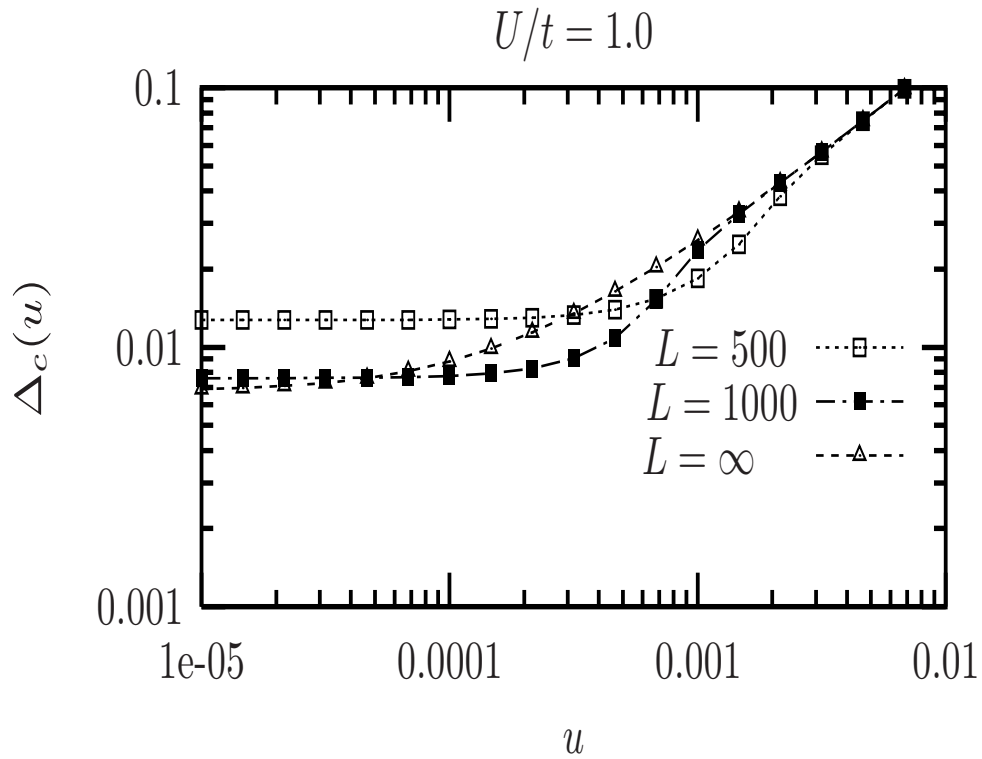


Figure 4.9: The gap parameter  $\Delta_c$  (in units of  $t$ ) as a function of the dimerization  $u$  for different system sizes compared with the thermodynamic limit.

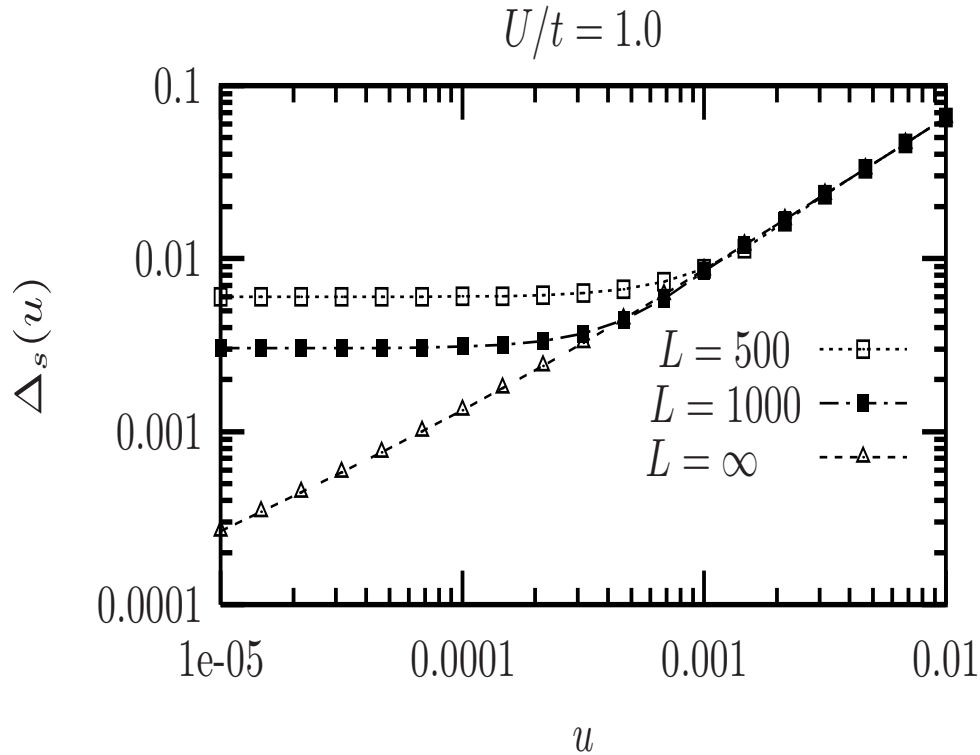


Figure 4.10: The gap parameter  $\Delta_s$  (in units of  $t$ ) as a function of the dimerization  $u$  for different systems sizes compared with the thermodynamic limit;  $\Delta_s$  has to be compared to the finite size energy  $v_F/L$ , which is e.g.  $v_F/L = 2 \cdot 10^{-3}t$  for  $L = 1000$ .

In Figs. 4.9 and 4.10 we show the dependence of the gap parameters  $\Delta_c$  and  $\Delta_s$  on the system size. Finite size effects are most pronounced in the small  $u$  region that corresponds to the Mott insulating phase. In particular the spin gap parameter  $\Delta_s$  approaches a finite value for all finite systems for  $u \rightarrow 0$ , while it goes to zero in the thermodynamic limit.

### 4.3 Ionic Hubbard model

The Hubbard model with an additional alternating on-site energy modulation has been used to study the organic mixed-stack charge transfer crystals with alternating donor and acceptor molecules [66, 65, 67, 68] or to understand the ferroelectric transition in perovskite materials such as  $\text{BaTiO}_3$  [69] or  $\text{KNbO}_3$ [70]. The model is described by the Hamiltonian

$$H = -t \sum_{j,\sigma} (c_{j\sigma}^+ c_{j+1\sigma} + \text{h.c.}) + U \sum_j n_{j\uparrow} n_{j\downarrow} + \Delta \sum_{j,\sigma} (-1)^j c_{j\sigma}^+ c_{j\sigma}, \quad (4.46)$$

where  $\Delta$  is the amplitude of the staggered potential. At  $U = 0$  and for  $\Delta > 0$ , the model corresponds to a conventional band insulator with a band gap  $2\Delta$ . The one-dimensional half-filled Hubbard model without an alternating potential ( $\Delta = 0$ ) and with  $U > 0$  describes a correlated insulator with vanishing spin gap.

In the atomic limit,  $t = 0$ , and for  $U < 2\Delta$ , every second site of the lattice with on-site energy  $-\Delta$  is occupied by two electrons while the sites with energy  $\Delta$  are empty. The energy difference between the ground state and the highly degenerate first excited state is  $2\Delta - U$ . For  $U > 2\Delta$ , each site is occupied by one electron and the energy gap is  $U - 2\Delta$ . Within this simplified picture one obtains a critical point  $U_c(\Delta) = 2\Delta$ , for which the excitation gap disappears. These considerations suggest that the system will be in two quantitatively different phases in the limits  $U \ll \Delta$  and  $U \gg \Delta$ , with a quantum phase transition from a band insulator to a correlated insulator in between.

The early numerical [71, 72] and analytical [73, 74] results reported that at  $T = 0$  and for fixed  $\Delta$  a single phase transition occurs if  $U$  is varied. Using bosonization Fabrizio et al. [75] predicted a *two – transition scenario* for the ground state phase diagram. For  $U < U_{c1}$  the system is a band insulator with finite charge and spin gaps. The first critical point  $U_{c1}$  is an Ising critical point, where the charge gap vanishes. The intermediate phase, for  $U_{c1} < U < U_{c2}$ , is a spontaneously dimerized insulator phase, in which the bosonic spin and charge gaps are finite. This phase is characterized by a non-zero expectation value of the dimerization operator

$$D = \sum_{i,\alpha} (-1)^i (c_{i\sigma}^+ c_{i+1\sigma} + \text{h.c.}). \quad (4.47)$$

The second transition, at  $U = U_{c2}$ , is of the Kosterlitz-Thouless type, and the system goes over into a correlated insulator phase with a finite charge gap and a vanishing spin gap. Various attempts based on numerical tools have been made to verify this scenario, without leading to a definite conclusion. In particular, exact diagonalization [76, 77], valence bond techniques [78], quantum Monte Carlo [79] and the DMRG [80, 81, 82] were used with different results in favor of one or two critical points.

In momentum space the Hamiltonian (4.46) reads

$$H = \sum_{k,\sigma} \epsilon_k c_{k\sigma}^+ c_{k\sigma} + \frac{U}{N} \sum_{k,p,q} c_{k+q\uparrow}^+ c_{p-q\downarrow}^+ c_{p\downarrow} c_{k\uparrow} + H_{\text{ionic}}, \quad (4.48)$$

where  $H_{\text{ionic}}$  is the contribution due to the alternating on-site energy modulation

$$H_{\text{ionic}} = \Delta \sum_{k\sigma} (c_{k\sigma}^+ c_{k+\pi\sigma} + \text{h.c.}), \quad (4.49)$$

which is referred to as the “ionic” term. In bosonized form it reads

$$H_{\text{ionic}} = \frac{\Delta}{2\pi a} \int_0^L dx F_{R\uparrow}^+ F_{L\uparrow} e^{-i\frac{\pi}{L}(N_c + N_s)x} e^{-i\sqrt{2}(\phi_c + \phi_s)}$$



$$+ \frac{\Delta}{2\pi a} \int_0^L dx F_{R\downarrow}^+ F_{L\downarrow} e^{-i\frac{\tilde{\Delta}}{L}(N_c - N_s)x} e^{-i\sqrt{2}(\phi_c - \phi_s)} + \text{h.c.}$$

At half filling,  $N_c = N_s = 0$ , the ionic contribution is

$$H_{\text{ionic}} = \tilde{\Delta} \int_0^L dx \{ F_{R\uparrow}^+ F_{L\uparrow} e^{-i\sqrt{2}(\phi_c + \phi_s)} + F_{R\downarrow}^+ F_{L\downarrow} e^{-i\sqrt{2}(\phi_c - \phi_s)} + \text{h.c.} \}, \quad (4.50)$$

where  $\tilde{\Delta} = \Delta/2\pi a$ . Similar to the case of the Peierls-Hubbard model, we express the Klein factors in terms of the operators  $A_\uparrow = F_{R\uparrow}^+ F_{L\uparrow}$  and  $A_\downarrow = F_{R\downarrow}^+ F_{L\downarrow}$ . We choose a basis in which these operators are diagonal, and using Eqs. (4.13) and (4.16), we replace the Klein factors in  $H_1$ ,  $H_2$  and  $H_{\text{ionic}}$  by their eigenvalues to obtain

$$H_1 = \tilde{U} \int_0^L dx \{ e^{i(k_\uparrow - k_\downarrow)} e^{-i2\sqrt{2}\phi_s} + \text{h.c.} \}, \quad (4.51)$$

$$H_2 = \tilde{U} \int_0^L dx \{ e^{i(k_\uparrow + k_\downarrow)} e^{-i2\sqrt{2}\phi_c} + \text{h.c.} \}, \quad (4.52)$$

$$H_{\text{ionic}} = \tilde{\Delta} \int_0^L dx \{ e^{ik_\uparrow} e^{-i\sqrt{2}(\phi_c + \phi_s)} + e^{ik_\downarrow} e^{-i\sqrt{2}(\phi_c - \phi_s)} + \text{h.c.} \}. \quad (4.53)$$

As in the case of the dimerized Hubbard model, the Hamiltonian of the ionic Hubbard model separates into different sectors of purely bosonic Hamiltonians, labeled by  $k_\uparrow$  and  $k_\downarrow$ . Using Majorana fermions [15] to represent the Klein factors, only one sector can be obtained and again the continuity is lost.

### 4.3.1 Self-consistent harmonic approximation

Since the nonlinear terms of the ionic Hubbard model cannot be treated exactly we again employ the SCHA as in the case of Peierls Hubbard model. In the thermodynamic limit we replace the Klein factors by their eigenvalues and introduce the trial Hamiltonian

$$H_{\text{tr}} = \sum_{\alpha=c,s} \int_0^L \frac{dx}{2\pi} \left\{ \frac{v_\alpha}{g_\alpha} (\partial_x \phi_\alpha)^2 + v_\alpha g_\alpha (\partial_x \theta_\alpha)^2 + \frac{\Delta_\alpha^2}{v_\alpha g_\alpha} \phi_\alpha^2 \right\}, \quad (4.54)$$

which provides us with a variational estimate for the ground state energy

$$\tilde{E} = \langle H_0 \rangle_{\text{tr}} + \langle H_1 \rangle_{\text{tr}} + \langle H_2 \rangle_{\text{tr}} + \langle H_{\text{ionic}} \rangle_{\text{tr}}, \quad (4.55)$$

$$\frac{\tilde{E}}{L} = \frac{E_{\text{tr}}}{L} - \sum_{\alpha=c,s} \frac{\Delta_\alpha^2}{2\pi v_\alpha g_\alpha} \langle \phi_\alpha^2 \rangle_{\text{tr}} + e(k_\uparrow, k_\downarrow), \quad (4.56)$$

$B_c > B_s$ , range	$k_\uparrow$	$k_\downarrow$	$e_0(B_c, B_s, B_{cs})$
$0 < B_{cs} < 2\sqrt{B_c B_s}$	0	$\pi$	$-2B_c - 2B_s$
$2\sqrt{B_c B_s} < B_{cs} < 2B_c$	$\arccos \frac{B_{cs}}{2B_c} + \pi$	$\arccos \frac{B_{cs}}{2B_c} - \pi$	$-2B_c + 2B_s - \frac{B_{cs}^2}{B_c}$
$2B_c < B_{cs}$	$\pi$	$\pi$	$2B_c + 2B_s - 4B_{cs}$

Table 4.2: Minimum  $e_0$  of  $e(k_\uparrow, k_\downarrow) = 2B_c \cos(k_\uparrow + k_\downarrow) + 2B_s \cos(k_\uparrow - k_\downarrow) + 2B_{cs}(\cos k_\uparrow + \cos k_\downarrow)$  which is used in the gap equations (4.61) and (4.62). The first line is only relevant for  $\Delta = 0$  (Hubbard model without on-site energy modulation), whereas the second and the third lines are relevant for  $\Delta > 0$ .

where  $E_{\text{tr}}$  is the ground state energy of  $H_{\text{tr}}$ , and

$$e(k_\uparrow, k_\downarrow) = 2B_c \cos(k_\uparrow + k_\downarrow) + 2B_s \cos(k_\uparrow - k_\downarrow) + 2B_{cs}(\cos k_\uparrow + \cos k_\downarrow), \quad (4.57)$$

with

$$B_c = \tilde{U} e^{-4\langle \phi_c^2 \rangle_{\text{tr}}}, \quad (4.58)$$

$$B_s = \tilde{U} e^{-4\langle \phi_s^2 \rangle_{\text{tr}}}, \quad (4.59)$$

$$B_{cs} = \tilde{\Delta} e^{-\langle \phi_c^2 \rangle_{\text{tr}}} e^{-\langle \phi_s^2 \rangle_{\text{tr}}}. \quad (4.60)$$

Minimizing the variational ground state energy with respect to  $\Delta_c$  and  $\Delta_s$  yields the gap equations

$$\frac{\Delta_c^2}{2\pi v_c g_c} = -4B_c \frac{\partial e_0}{\partial B_c} - B_{cs} \frac{\partial e_0}{\partial B_{cs}}, \quad (4.61)$$

$$\frac{\Delta_s^2}{2\pi v_s g_s} = -4B_s \frac{\partial e_0}{\partial B_s} - B_{cs} \frac{\partial e_0}{\partial B_{cs}}, \quad (4.62)$$

where  $e_0$  is the minimum of  $e(k_\uparrow, k_\downarrow)$  with respect to  $k_\uparrow$  and  $k_\downarrow$  (see Table 4.2). Depending on the values of  $B_c$ ,  $B_s$  and  $B_{cs}$ , different physical situations arise:

- 1) The solution  $e_0 = -2B_c - 2B_s$  corresponds to the Hubbard model without on-site energy modulation,  $\Delta = 0$ . The system is a Mott insulator with a vanishing spin gap, as in the Peierls-Hubbard model with  $u = 0$ , see Fig. 4.3 and Eqs. (4.30)-(4.35).

- 2) The solution  $e_0 = 2B_c + 2B_s - 4B_{cs}$  corresponds to a band insulator, where the charge and spin gap decrease with increasing  $U$ . In this case the gap equations (4.61)-(4.62) read

$$\frac{\Delta_c^2}{2\pi v_c g_c} = 4B_{cs} - 8B_c, \quad (4.63)$$

$$\frac{\Delta_s^2}{2\pi v_s g_s} = 4B_{cs} - 8B_s. \quad (4.64)$$

As shown in appendix F, this case corresponds to the limit  $\Delta/U \gg 1$ , and one obtains the following dependence of the gap parameters  $\Delta_c$  and  $\Delta_s$  on the ionic potential  $\Delta$ :

$$\Delta_c \propto \Delta^{2/(3-g_c)}, \quad (4.65)$$

$$\Delta_s \propto \Delta^{2/(3-g_s)}. \quad (4.66)$$

This is the same result as obtained for the Peierls-Hubbard model with  $u$  replaced by  $\Delta$ . For  $U = 0$ , i.e.  $g_c = 1$ , Eqs. (4.65)-(4.66) yield  $\Delta_{c,s} \propto \Delta$  in accordance with the known solution in the non-interacting limit.

- 3) The solution  $e_0 = -2B_c + 2B_s - B_{cs}^2/B_c$  corresponds to the spontaneously dimerized insulator phase where the dimerization operator has the expectation value

$$\langle D \rangle \sim \sin(k_\uparrow) + \sin(k_\downarrow) = -2\sqrt{1 - \left(\frac{B_{cs}}{2B_c}\right)^2}. \quad (4.67)$$

In this case the gap equations are

$$\frac{\Delta_c^2}{2\pi v_c g_c} = 8B_c - 2\frac{B_{cs}^2}{B_c}, \quad (4.68)$$

$$\frac{\Delta_s^2}{2\pi v_s g_s} = -8B_s + 2\frac{B_{cs}^2}{B_c}, \quad (4.69)$$

which are solved in appendix F. The result is

$$\Delta_c(\Delta) - \Delta_c(0) \propto \Delta^4, \quad (4.70)$$

$$\Delta_s(\Delta) \propto \Delta^2, \quad (4.71)$$

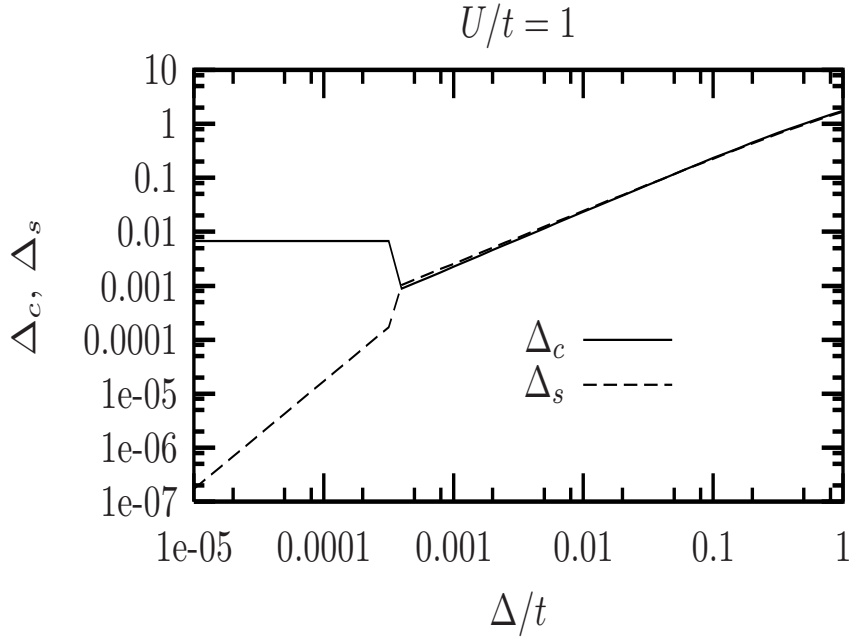


Figure 4.11: The mean field parameters  $\Delta_c$  and  $\Delta_s$  (in units of  $t$ ) as function of  $\Delta$ , the staggered potential, in the thermodynamic limit. At  $\Delta \sim 5 \cdot 10^{-4}t$  we find a discontinuous jump of the parameters.

which is similar to the behavior of the Peierls-Hubbard model, Eqs. (4.40)-(4.41), however with different exponents, 4 instead of  $4/3$  for the charge gap, and 2 instead of  $2/3$  for the spin gap. This different behavior can be understood in the strong coupling limit  $U \rightarrow \infty$  where in second order perturbation theory the Peierls term yields an alternating contribution to the Heisenberg exchange coupling  $J = 4t^2/U$ , while for the ionic Hubbard model the strong coupling limit is the antiferromagnetic Heisenberg model with uniform coupling. In this case the opening of the spin gap is associated with higher than second order processes in the strong coupling limit.

Fig. 4.11 shows the dependence of  $\Delta_c$  and  $\Delta_s$  on  $\Delta$  for fixed Hubbard interaction  $U/t = 1$ . Contrary to the case of the Peierls-Hubbard model there is no smooth crossover between the small and large  $\Delta$  region but a discontinuous transition at some intermediate value  $\Delta^*$ . In Fig. 4.12 the ionic parameter  $\Delta = 10^{-3}$  is kept fixed and  $\Delta_c$  and  $\Delta_s$  are plotted as functions of  $U$ . For small values of  $U$  spin and charge gaps are almost equal and decrease with increasing  $U$ , as highlighted in Fig. 4.13. At  $U/t \approx 1.05$  there is a discontinuous transition to a phase where  $\Delta_s$  goes to zero while  $\Delta_c$  increases strongly, as can be seen in Fig. 4.14.

Connecting the values of  $\Delta$  where the discontinuous transition occurs for different values of  $U$  one obtains the phase boundary between a Mott insulator ( $\Delta_s \rightarrow 0$ ) and a band insulator ( $\Delta_c \approx \Delta_s$ ) as shown in Fig. 4.15. We find only one phase transition, and

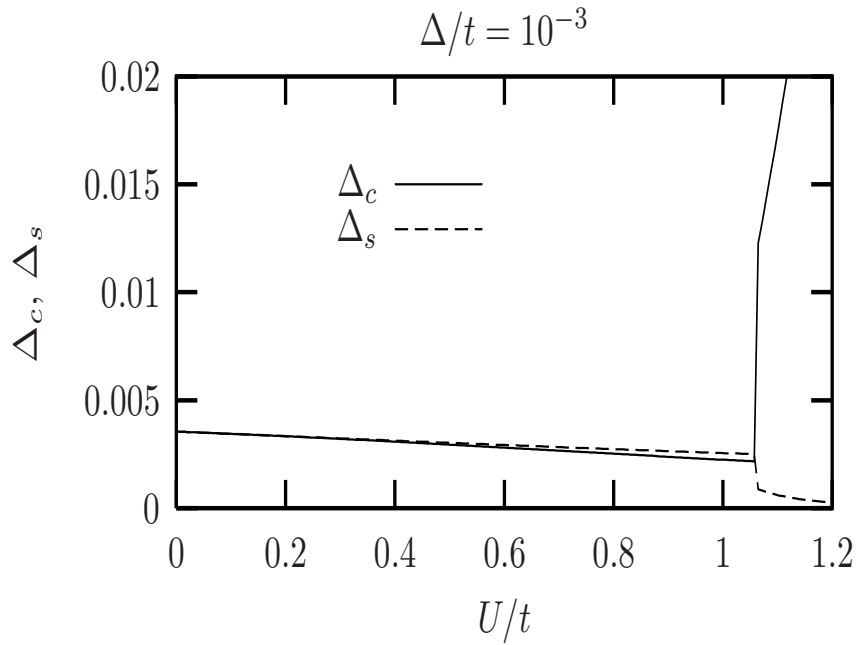


Figure 4.12: The mean field parameters  $\Delta_c$  and  $\Delta_s$  (in units of  $t$ ), as function of  $U$ , in the thermodynamic limit.

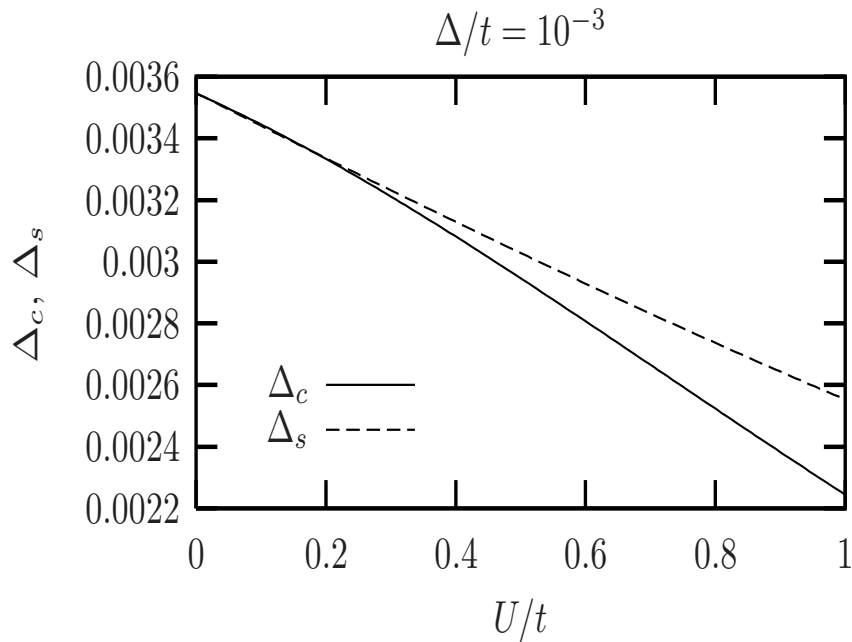


Figure 4.13: The mean field parameters  $\Delta_c$  and  $\Delta_s$  (in units of  $t$ ), as function of  $U$ , in the thermodynamic limit. Note the different scales compared to the previous figure.

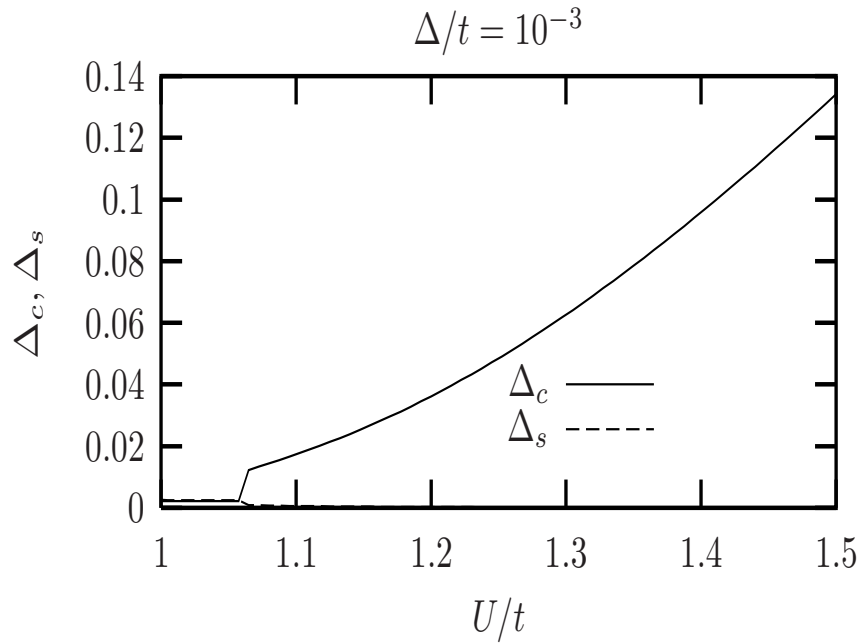


Figure 4.14: The mean field parameters  $\Delta_c$  and  $\Delta_s$  (in units of  $t$ ), as function of  $U$  in the thermodynamic limit. Note the different scales compared to the previous figures.

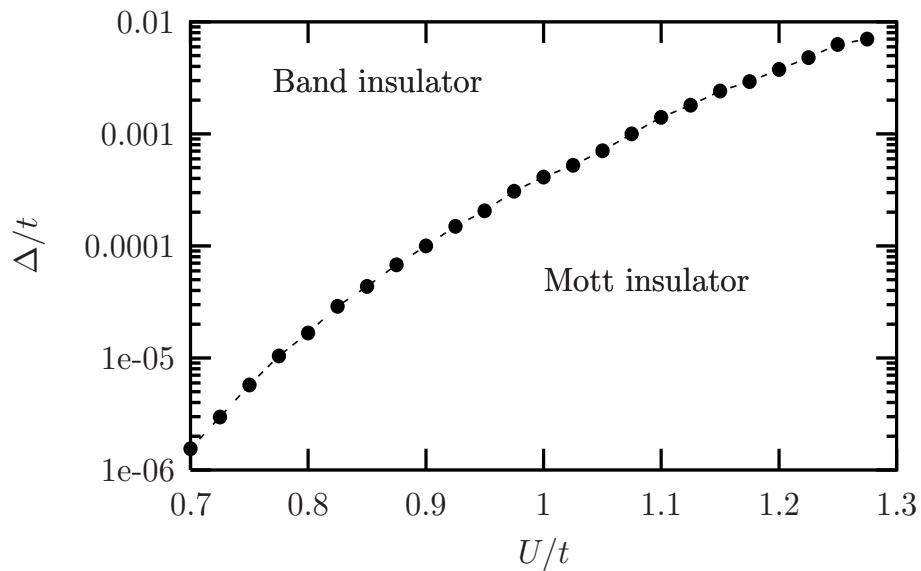


Figure 4.15: Phase diagram of the ionic Hubbard model. The dots correspond to the discontinuity of  $\Delta_c$  and  $\Delta_s$ , as for example shown in Fig. 4.11 for  $U/t = 1$ .

---

not two, in contrast to the phase diagram proposed by Fabrizio et al. [75]. However, in our bosonization approach, using SCHA to estimate the charge and the spin gap, we are limited to small values of  $U$  and  $\Delta$ .

### 4.3.2 Finite systems

To calculate the gaps of the ionic Hubbard model for a finite system we apply the same procedure as in the case of the Peierls-Hubbard model. We will find, unexpectedly, strong finite size effects near the phase transition. At present it is still not clear to us whether this behavior is an artefact of the SCHA or if it has physical reality.

We decouple the Klein factors from the bosonic fields introducing the Klein Hamiltonian

$$\begin{aligned}
H_{\text{tr}}^{B_{cs}B_cB_s} &= B_{cs}L(F_{R\uparrow}^+F_{L\uparrow} + F_{R\downarrow}^+F_{L\downarrow}) + B_cLF_{R\uparrow}^+F_{R\downarrow}^+F_{L\downarrow}F_{L\uparrow} \\
&+ B_sLF_{R\uparrow}^+F_{L\downarrow}^+F_{R\downarrow}F_{L\uparrow} + \text{h.c.} \\
&+ \frac{\pi}{4L}(v_c g_c J_c^2 + v_s g_s J_s^2),
\end{aligned} \tag{4.72}$$

where  $B_c$ ,  $B_s$  and  $B_{cs}$  are variational parameters.  $H_{\text{tr}}^{B_{cs}B_cB_s}$  is again of the form of a tight-binding Hamiltonian for a particle moving on a  $2d$  lattice in a harmonic potential. The explicit representation of this hopping Hamiltonian in the  $|J_c, J_s\rangle$  basis is given in appendix E for the Peierls-Hubbard model. For the ionic Hubbard model one has to replace  $\pm iB_{cs}$  by  $B_{cs}$  to obtain the corresponding matrix elements. As a result of the variational procedure, the Klein factors are replaced by their expectation values with respect to the ground state of the Klein Hamiltonian. Similar to the case of the Peierls-Hubbard model, in the framework of the SCHA, the quantity  $e_0$  which enters the gap equations (and which is explicitly given in Table 4.2) is replaced by  $e_{\text{tr}}^0$ , the ground state energy of  $H_{\text{tr}}^{B_{cs}B_cB_s}$  divided by  $L$ , which can be calculated only numerically. Fig. 4.16 shows the derivatives of  $e_{\text{tr}}^0$  with respect to  $B_c$ ,  $B_s$  and  $B_{cs}$  as function of the system size for fixed model parameters  $U/t = 1$  and  $\Delta/t = 0.1$ . For small  $L$  the derivatives are close to zero while with increasing  $L$  they converge to the values corresponding to the thermodynamic limit given in Table 4.2,  $\partial e_{\text{tr}}^0/\partial B_c = 2$ ,  $\partial e_{\text{tr}}^0/\partial B_s = 2$ ,  $\partial e_{\text{tr}}^0/\partial B_{cs} = -4$ . The scale  $1/\sqrt{L}$  is chosen in order to enlarge the crossover region.

In Fig. 4.17 we show the gap parameter  $\Delta_c$  as function of  $\Delta$  and fixed Hubbard interaction  $U/t = 1$  for different system sizes. While for large values of  $\Delta$ , corresponding to the band insulator phase, there are nearly no finite size effects, for small  $\Delta$ , corresponding to a Mott insulator phase, even for  $L = 5000$  the values have not yet converged to the thermodynamic limit. The transition between the Mott insulator and the band insulator phase appears continuous for small values of the system size  $L$  but becomes sharper with increasing  $L$  and finally turns over into a discontinuous one. The same observation holds for the spin gap parameter  $\Delta_s$ , which is displayed in Fig. 4.18 for the same set of parameters as before. In particular for  $\Delta \rightarrow 0$  the gap parameter  $\Delta_s$  approaches a constant for finite systems while in the thermodynamic limit it goes to zero according to  $\Delta_s \propto \Delta^2$ .

In order to show in more detail how the discontinuous transition emerges from the continuous one we plot the gap parameters  $\Delta_c$  and  $\Delta_s$  for several values of  $L$  in the



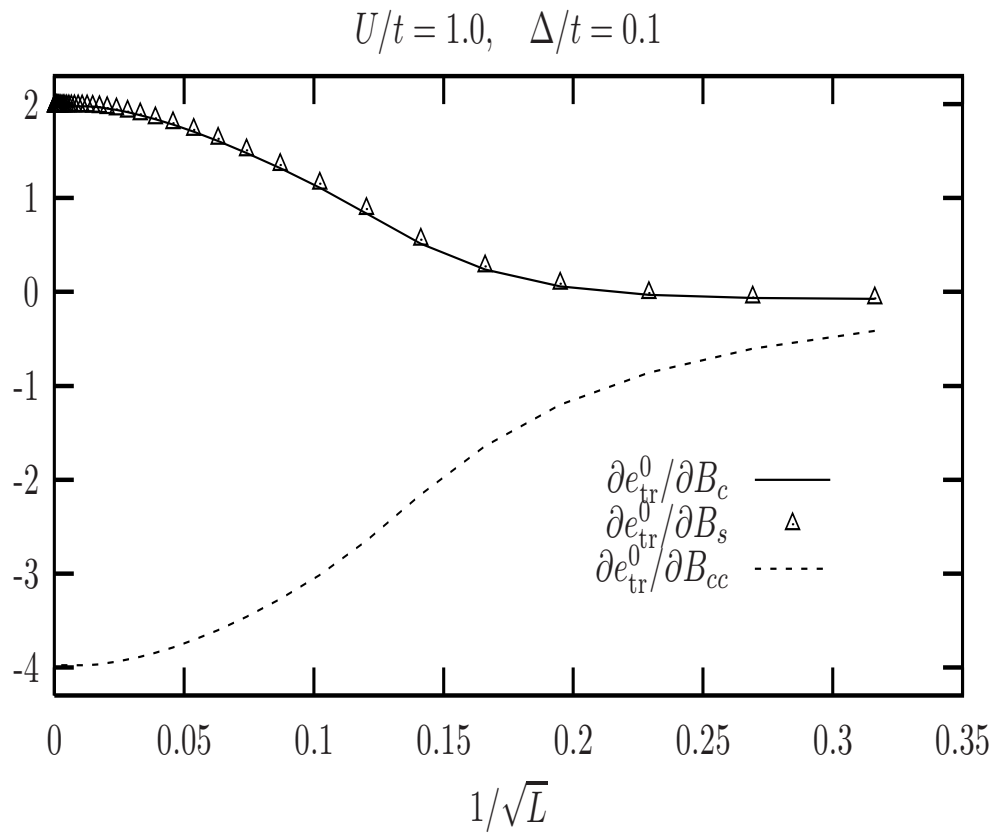


Figure 4.16: The derivative of  $e_{\text{tr}}^0$  with respect to the variational parameters  $B_c, B_s, B_{cs}$  needed in the equations (4.61) and (4.62).

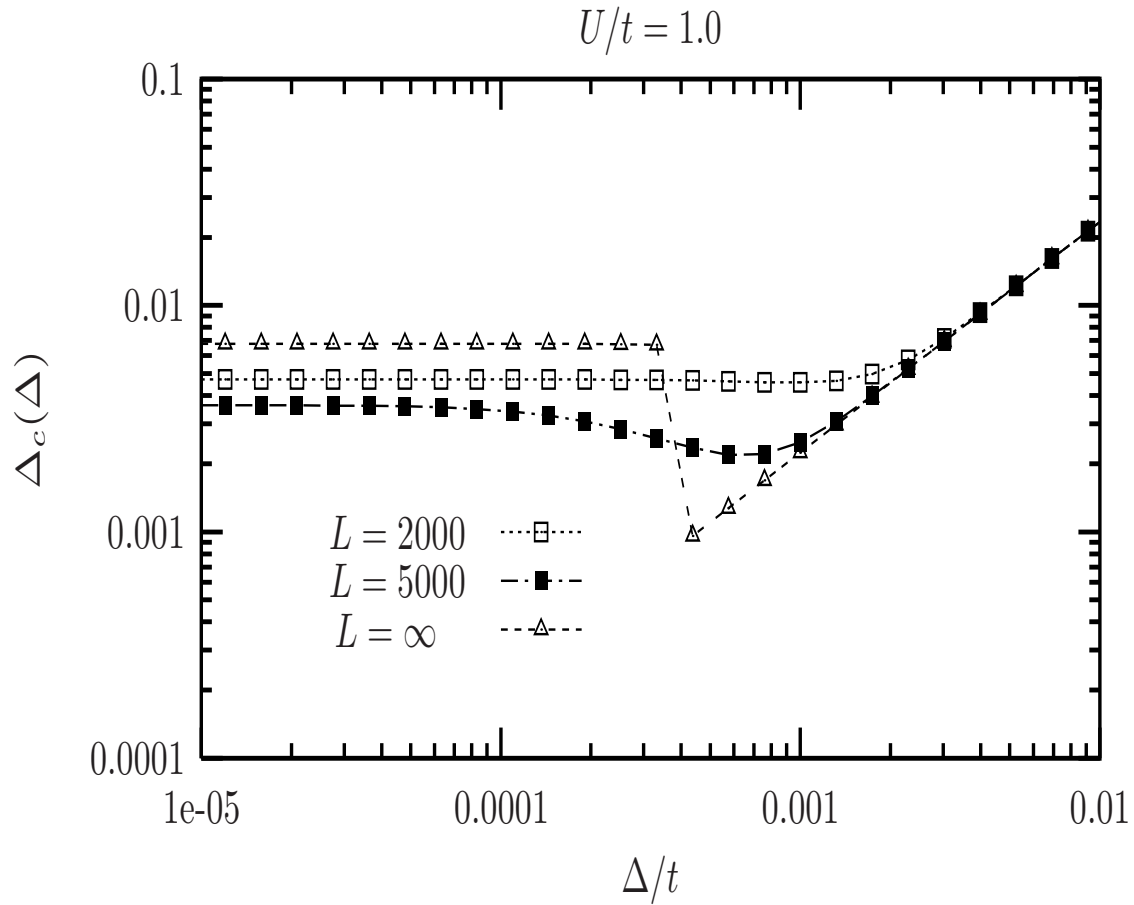


Figure 4.17: The charge gap parameter  $\Delta_c$  (in units of  $t$ ) as a function of  $\Delta$  for different values of the system size  $L$  compared with the thermodynamic limit.

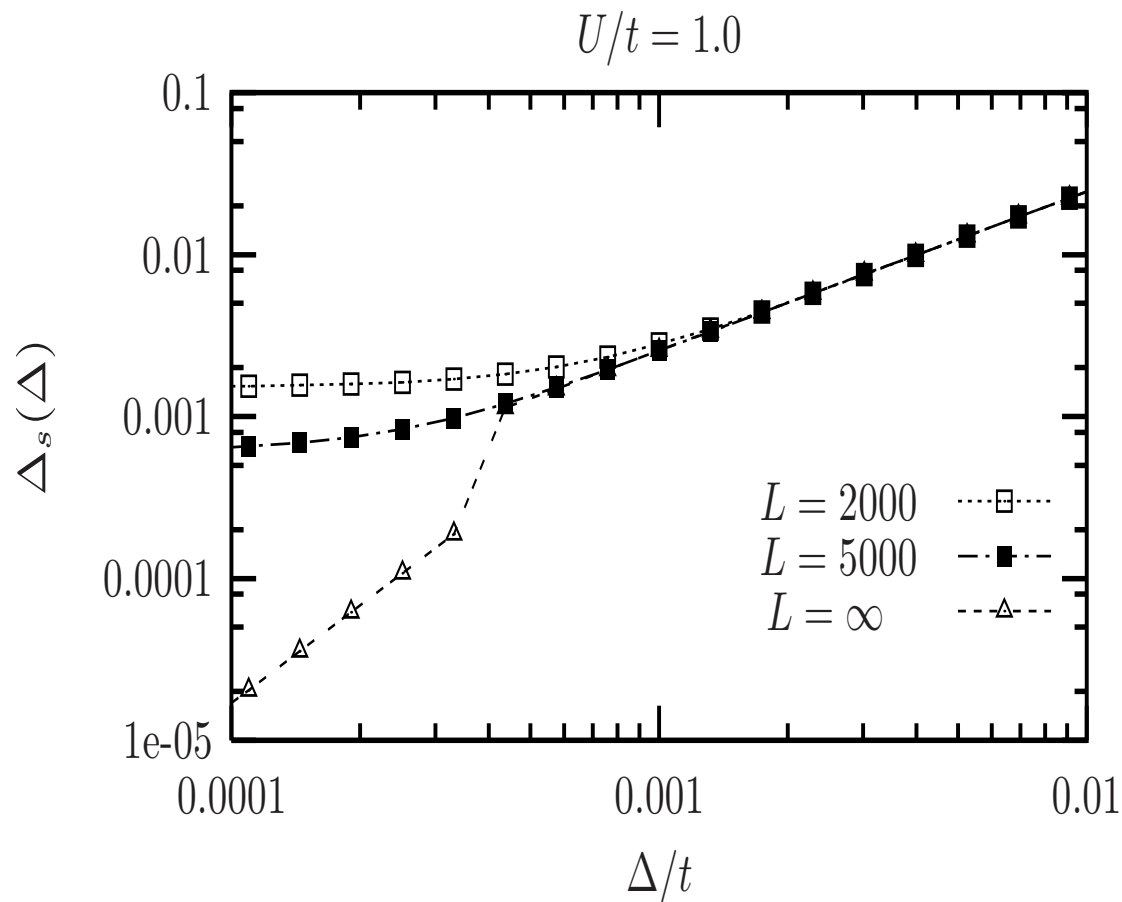


Figure 4.18: The spin parameter  $\Delta_s$  (in units of  $t$ ) as a function of  $\Delta$  for different values of the system size  $L$  compared with the thermodynamic limit.

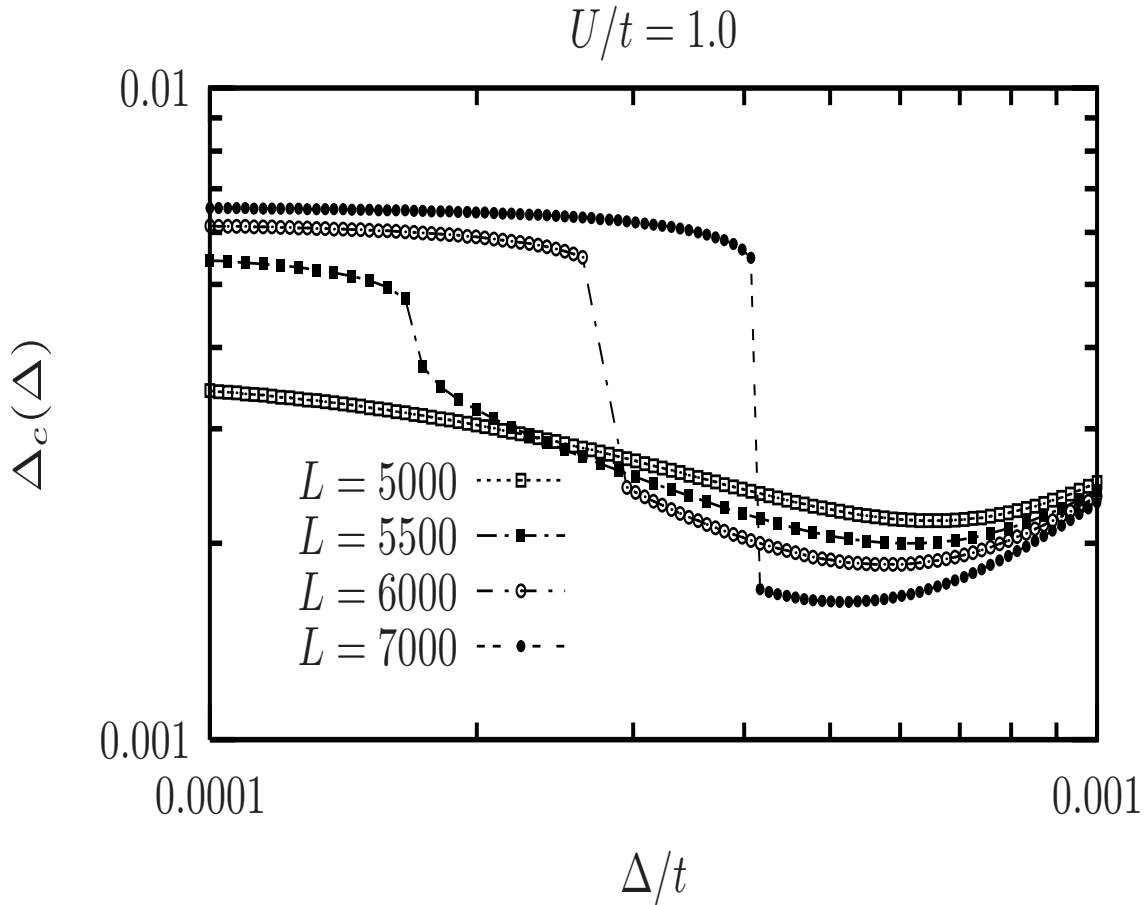


Figure 4.19: The charge parameter  $\Delta_c$  (in units of  $t$ ) as a function of  $\Delta$  for different values of the size system size  $L$  in the region where the transition from a band insulator to a Mott insulator appears.

region where the transition occurs in Figs. 4.19 and 4.20, respectively. For  $U/t = 1$ , the discontinuity appears somewhere between  $L = 5000$  and  $L = 5500$  and becomes more pronounced while  $L$  is increased further.

In Figs. 4.21 and 4.22 we show  $\Delta_c$  and  $\Delta_s$ , respectively, as function of the Hubbard interaction  $U/t$  for fixed value of the ionic parameter  $\Delta/t = 10^{-3}$  and different system sizes  $L$ . For this small value of  $\Delta/t$  there are still quite pronounced finite size effects for  $L = 1000$ . This indicates that numerical methods which are devised for finite systems like exact diagonalization or DMRG would probably fail in the small  $\Delta$  regime.



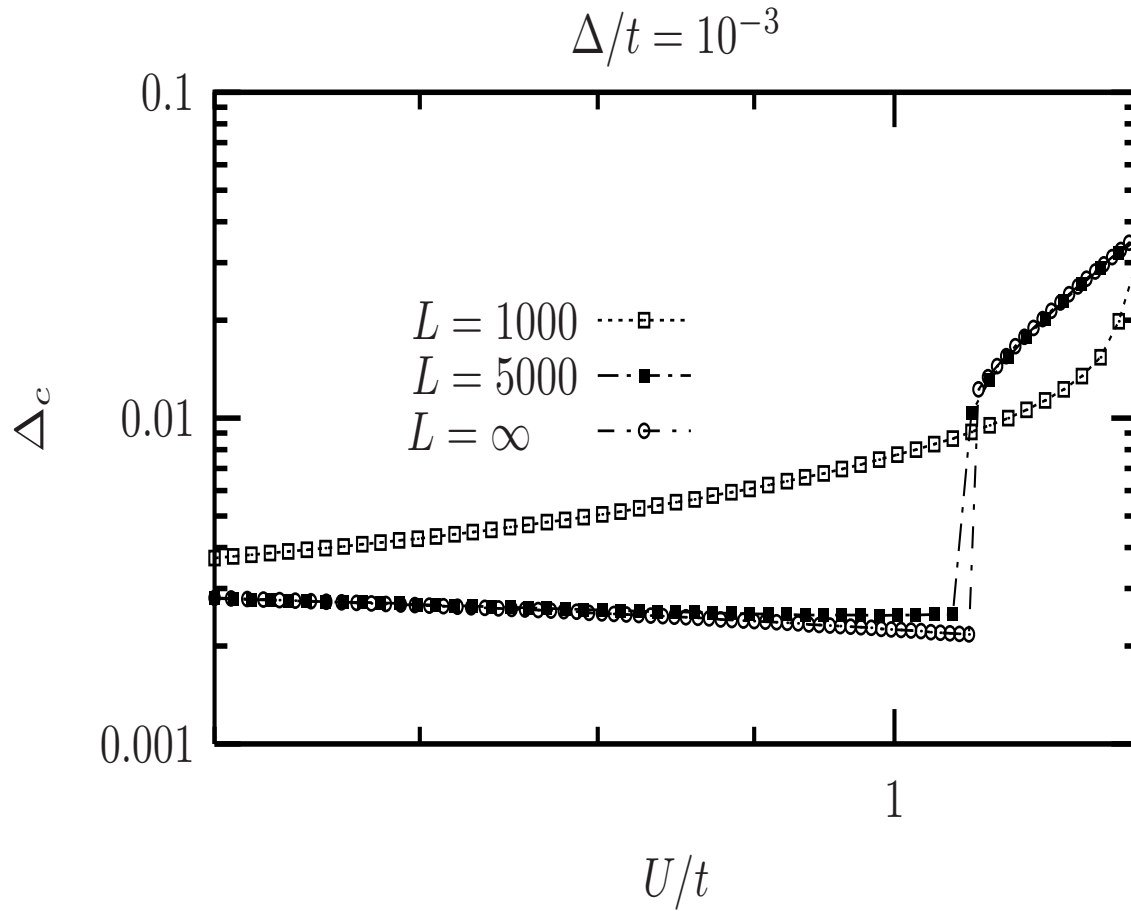


Figure 4.21: The charge parameter  $\Delta_c$  (in units of  $t$ ) as a function of the Hubbard interaction  $U/t$  for different system sizes compared with the thermodynamic limit.

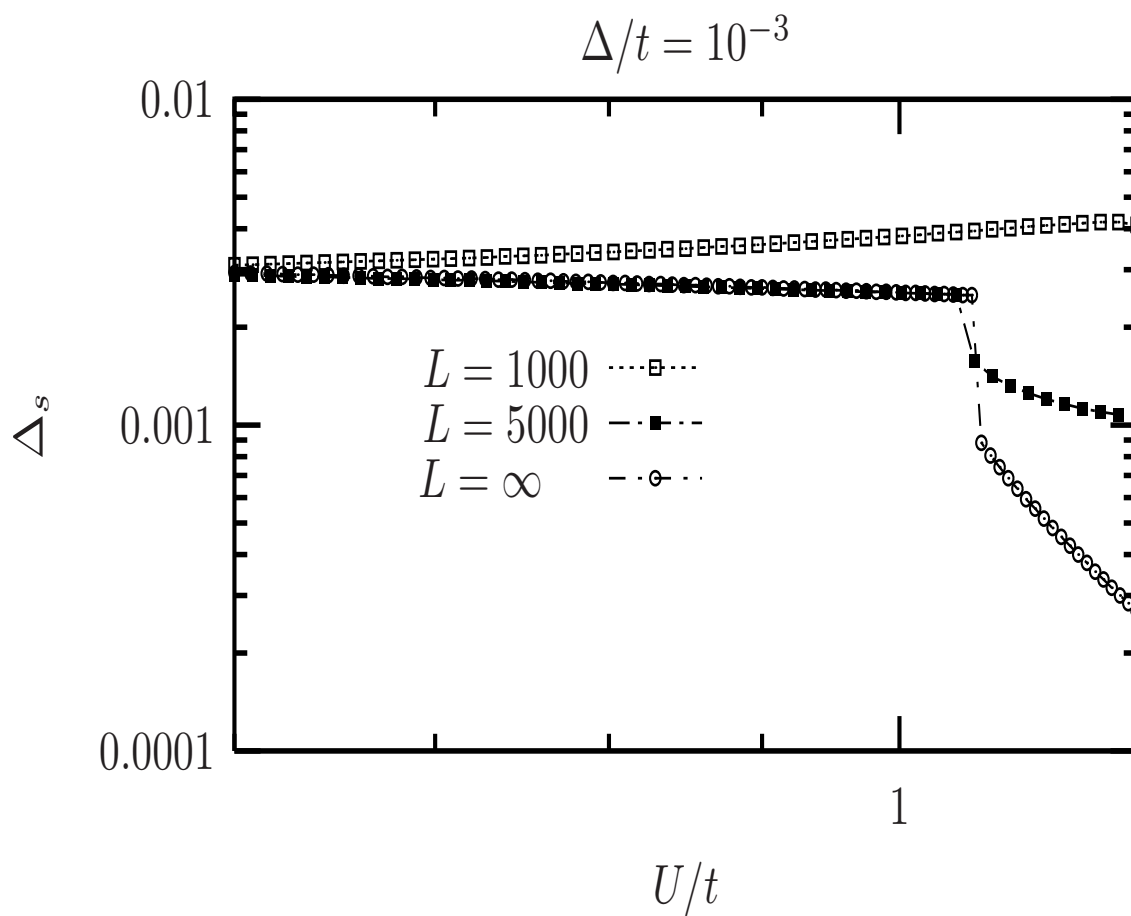


Figure 4.22: The spin parameter  $\Delta_s$  (in units of  $t$ ) as a function of the Hubbard interaction  $U/t$  for different system sizes compared with the thermodynamic limit

## 4.4 Conclusions

In this chapter we considered two different one-dimensional Hubbard models, the Peierls-Hubbard and the ionic Hubbard model. In the bosonized version of these models two kinds of bosonic fields have to be introduced which are associated with the spin and the charge degrees of freedom, respectively. The backward and the Umklapp scattering yield nonlinear terms in the spin and the charge sector, respectively, while the Peierls distortion and the ionic potential introduce a coupling between the spin and the charge sectors. These nonlinear terms lead to the opening of spin or charge gap, depending on the model parameters.

Our first goal was to stress the importance of Klein factors in bosonized Hamiltonians with nonlinear perturbations. In the study of such types of Hamiltonian, one has to keep in mind that the Klein factors which accompany the nonlinear terms do not commute with the total spin and charge currents,  $J_{c,s}$ , and therefore Klein factors and current operators cannot acquire a fixed value at the same time. In the thermodynamic limit the ground state of the gapped system is a superposition of many states with different  $J_c$  and  $J_s$ . In this situation it is possible to choose a fixed phase for the Klein operators. The bosonized Hamiltonian is then the conventional sine-Gordon Hamiltonian. For finite size systems the Klein factors can be replaced by their expectation values with respect to the ground state of a trial Hamiltonian, and the resulting bosonic Hamiltonian is also of a sine-Gordon type, however with size-dependent couplings.

Using a self-consistent variational scheme, we decoupled the bosonic Hamiltonian from the Klein Hamiltonian and we calculated the gap parameters  $\Delta_c$  and  $\Delta_s$  as a function of the strength of the perturbation (the dimerization  $u$  in the case of the Peierls-Hubbard model, and the ionic potential  $\Delta$  in the case of the ionic Hubbard model). In both cases we found a transition from a Mott insulator phase with vanishing or very small spin gap to a band insulator phase where spin and charge gaps are of the same order of magnitude. The main difference between the two models is that the transition between the Mott and the Peierls phase is continuous in the case of Peierls-Hubbard model and discontinuous for the ionic Hubbard model.



# Chapter 5

## Screening in low-dimensional electron systems

In order to extend the model calculations of the preceding sections towards a more realistic description of quasi one-dimensional systems we consider in the following a one-dimensional interacting system, characterized by a Luttinger model, coupled to a three-dimensional environment, and calculate the spin and the charge susceptibility. The motivation is an old discussion on the role of electronic correlations for the metal-insulator transition in  $\text{VO}_2$ .

### 5.1 Phase transition in $\text{VO}_2$

A detailed analysis of electronic structure of vanadium dioxide ( $\text{VO}_2$ ) is given in [83, 84]. In the following we recall some of the theoretical and experimental findings. Vanadium dioxide in the paramagnetic metallic phase above  $T_c = 340$  K has a rutile crystal structure, each vanadium atom being located at the center of an oxygen octahedron. The fivefold-degenerate  $d$  levels of the  $\text{V}^{4+}(3d^1)$  ion are split into doubly degenerate  $e_g$  levels and triply degenerate  $t_{2g}$  levels in the octahedral crystal field. The  $e_g$  orbitals are strongly hybridized with the O  $2p\sigma$  orbitals and have a large bandwidth, and are pushed far away from the Fermi surface. The  $t_{2g}$  levels are split into the  $d_{\parallel}$  and  $\pi^*$  levels by the orthorhombic component of the tetragonal crystal field. Thus the  $d_{\parallel}$  and  $\pi^*$  bands are situated at the lowest energies around the Fermi level. According to LDA calculations [83, 84] the  $d_{\parallel}$  bands show a strongly one-dimensional dispersion, whereas the  $\pi^*$  bands are three-dimensional. These bands play the crucial role in electronic (transport and magnetic) properties  $\text{VO}_2$ , and will be further studied in section 5.2.

In the insulating non-magnetic phase below  $T_c$ ,  $\text{VO}_2$  is distorted to a monoclinic crystal structure, involving a pairing of vanadium ions  $\text{V}^{4+}$  along the  $c_r$  axis. Because of the change in the V-O hybridization, the energy of the hybridized  $\pi^*$  band rises above the Fermi level and it becomes empty. Furthermore, the  $d_{\parallel}$  band is split into

two bands. A schematic energy diagram of the  $3d$  bands around the Fermi level for  $\text{VO}_2$  is shown in Fig. 5.1.

There is an old discussion concerning the driving mechanism for the metal-insulator transition in this material and the role of electronic correlations. Some authors argued that electronic correlation effects are in  $\text{VO}_2$  less pronounced than in the other vanadium oxides, like  $\text{V}_2\text{O}_3$ . Goodenough pointed out that the metal-insulator transition of  $\text{VO}_2$  may be explained by considering the change in crystal structure, which leads to the splitting of the  $d_{\parallel}$  band and the rising of the  $\pi^*$  bands [85]. Modern LDA [83, 84] and molecular dynamics [86] calculations support this point of view, although the splitting of the  $d_{\parallel}$  bands is underestimated, so that they predicted a metallic instead of an insulating state.

Further experimentals, however, demonstrated that electronic correlations play an important role also in  $\text{VO}_2$ . Pouget et al. [87, 88] performed nuclear magnetic resonance (NMR) measurements under uniaxial stress in  $\text{VO}_2$  and  $\text{V}_{1-x}\text{Cr}_x\text{O}_2$ . They found for  $\text{V}_{1-x}\text{Cr}_x\text{O}_2$  three different insulating phases ( $M_1$ ,  $M_2$  and  $T$ ). The  $M_1$  phase is identical to the insulating phase of pure  $\text{VO}_2$  at normal pressure, while in the  $M_2$  and  $T$  phases magnetic moments were observed. The appearance of the magnetic moments was considered as a clear sign for correlation effect in the insulating phase.

Zylbersztejn and Mott [93] emphasized the important role of the  $\pi^*$  electrons in the metal-insulator transition. They argued that, in the insulating phase, the hybridization between the the  $\pi^*$  and O  $2p\sigma$  orbitals increases due to the crystal distortion so that the  $\pi^*$  band rises in energy and becomes empty. Therefore the correlation energy of the  $d_{\parallel}$  electrons becomes enhanced leading to a splitting into the lower and the upper Hubbard bands. They argued that the metallic phase is adequately described within the framework of band theory, since the interaction of the  $d_{\parallel}$  electrons is screened by the  $\pi^*$  electrons. They estimated the effective intra atomic Coulomb repulsion in the metallic phase from the Stoner enhancement of the magnetic susceptibility as

$$\frac{\chi_{\parallel}}{\chi_{\parallel}^P} = \frac{1}{1 - U_{\text{eff}}\mathcal{N}_{d_{\parallel}}} = 3.2 \quad (5.1)$$

yielding  $U_{\text{eff}} = 0.13$  eV. Here  $\chi_{\parallel}^P$  is the Pauli spin susceptibility and  $\mathcal{N}_{d_{\parallel}} = 5.25$  states/eV is the density of states per spin at the Fermi surface in the  $d_{\parallel}$  band.

Shin et al. [89] measured the vacuum-ultraviolet reflectance and photoemission spectra of  $\text{VO}_2$  in order to investigate the  $3d$  bands and electron-correlation effects. The splitting energy between the two  $d_{\parallel}$  bands in the insulating phase was found to be about 2.5 eV, bigger than the value obtained from the cluster band calculation [90], namely 0.5 eV. They argued that in the insulating phase the band splitting of the  $\pi^* - d_{\parallel}$  and  $d_{\parallel} - d_{\parallel}$  bands cannot be explained by the crystal distortion alone, correlation effects playing an important role also. They estimated the correlation energy in the insulating phase of the  $d_{\parallel}$  band as about  $U(d_{\parallel}, d_{\parallel}) \approx 2.1$  eV. From the photoemission data they concluded that the correlation energy of the  $d_{\parallel}$  electrons must not be neglected even

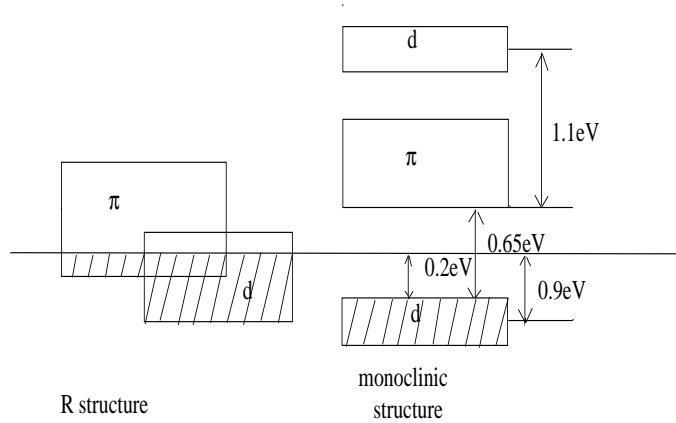


Figure 5.1: Schematic energy diagram of the  $3d$  bands around the Fermi level for  $\text{VO}_2$  [89]. The energy of 0.2 eV is obtained by the UPS spectra. The energies of 0.5 and 1.1 eV are obtained by ultraviolet reflectance spectra, while 0.65 eV is a value from the infrared absorption spectra [91]

in the metallic phase, and  $U(d_{\parallel}, d_{\parallel})$  was estimated to be not less than 1.3 eV.

## 5.2 The model

Following the ideas of Mott and Zylbersztein that in the metallic state of  $\text{VO}_2$  the electron-correlation effects in the one-dimensional  $d_{\parallel}$  bands are screened by the three-dimensional  $\pi^*$  electrons, we consider a one-dimensional, interacting Fermi system, which is coupled to a three-dimensional environment through a local interaction. The aim is to see how the presence of the three-dimensional system affects the one-dimensional system. We calculate the spin and charge susceptibility, with the result that the spin susceptibility is not changed due to the coupling to the environment, whereas the charge susceptibility shows screening.

We consider the Hamiltonian

$$H = H_{\text{Luttinger}} + H_{0\pi^*} + H_{d-\pi^*}, \quad (5.2)$$

where  $H_{\text{Luttinger}}$  is the Hamiltonian corresponding to the Luttinger model,

$$H_{0\pi^*} = \sum_{k,\sigma} \epsilon_{\pi}(\mathbf{k}) \pi_{\mathbf{k}\sigma}^{*+} \pi_{\mathbf{k}\sigma}^* \quad (5.3)$$

corresponds to a band of non-interacting  $\pi^*$  electrons with a three-dimensional dispersion  $\epsilon_{\pi}(k)$ , and

$$H_{d-\pi^*} = \frac{V}{N} \sum_{\mathbf{k}\mathbf{p}\mathbf{q},\sigma\sigma'} d_{\mathbf{k}\sigma}^+ d_{\mathbf{k}-\mathbf{q}\sigma} \pi_{\mathbf{p}\sigma'}^{*+} \pi_{\mathbf{p}+\mathbf{q}\sigma'}^* \quad (5.4)$$

describes coupling between  $\pi^*$  and  $d_{\parallel}$  electrons via an interaction of strength  $V$ ;  $N$  is the number of lattice points (in the three dimensional lattice). In order to make a connection between our calculation and the discussion on  $\text{VO}_2$ , we use the notation  $d^+$ ,  $d$  for the creation and annihilation operators of  $d_{\parallel}$  (one-dimensional) electrons, and the notation  $\pi^{*+}$ ,  $\pi^*$  for the creation and annihilation operators of  $\pi^*$  (three-dimensional) electrons. A similar Hamiltonian has been studied by Paquet and Leroux-Hugon [92]. In this work, electronic correlations in the one-dimensional  $d_{\parallel}$  band were taken into account in terms of a spatially inhomogenous mean field theory. In contrast, we describe the  $d_{\parallel}$  electrons as Luttinger liquid.

### 5.3 Charge and spin susceptibility

The dynamic susceptibility  $\chi$  is a measure of the system's response to an external field. Generally, the dynamic susceptibility is given by a retarded commutator of the form

$$\chi_{AA}(\mathbf{q}, t) = i\theta(t)\langle [A(\mathbf{q}, t), A(-\mathbf{q}, 0)] \rangle. \quad (5.5)$$

For the spin susceptibility  $A$  is the spin density operator,  $\sigma(\mathbf{q}) = \rho_{\uparrow}(\mathbf{q}) - \rho_{\downarrow}(\mathbf{q})$ , while for the charge susceptibility  $A$  is the charge density operator,  $\rho(\mathbf{q}) = \rho_{\uparrow}(\mathbf{q}) + \rho_{\downarrow}(\mathbf{q})$ . The density operators  $\rho_{\uparrow, \downarrow}$  are given by Eq. (2.8) where for the general case the one dimensional momenta have to be replaced by the three dimensional vectors.

#### 5.3.1 Luttinger model

For the calculation of the charge susceptibility in the Luttinger model we express the charge density in terms of left and right charge densities,

$$\rho(q) = \rho_R(q) + \rho_L(q).$$

Corresponding to this separation in left and right movers the correlator  $\chi_{\rho\rho}$  can be expressed as

$$\chi_{\rho\rho} = i\theta(t)\langle [\rho(q, t), \rho(-q, 0)] \rangle = \chi_{LL} + \chi_{LR} + \chi_{RL} + \chi_{RR}. \quad (5.6)$$

By taking the time derivative one finds for all four components  $\chi_{\eta\gamma}$  an equation of motion of the type

$$-i\partial_t \chi_{\eta\gamma} = \delta(t)\langle [\rho_{\eta}(q, 0), \rho_{\gamma}(-q, 0)] \rangle - i\theta(t)\langle [[\rho_{\eta}(q, t), H], \rho_{\gamma}(-q, 0)] \rangle. \quad (5.7)$$

For the ‘‘g-ology’’ Hamiltonian the commutators  $[\rho_{\eta}, H]$  are

$$[\rho_L, H] = qv_F(1 + \gamma_{4\parallel} + \gamma_{4\perp})\rho_L + qv_F(-\gamma_{1\parallel} + \gamma_{2\parallel} + \gamma_{2\perp})\rho_R, \quad (5.8)$$

$$[\rho_R, H] = -qv_F(1 + \gamma_{4\parallel} + \gamma_{4\perp})\rho_R - qv_F(-\gamma_{1\parallel} + \gamma_{2\parallel} + \gamma_{2\perp})\rho_L, \quad (5.9)$$

where  $\gamma_i = g_i/(2\pi v_F)$ . With this simple form of the commutators one can calculate the susceptibility explicitly, and the final result is

$$\chi_{\rho\rho}(q, \omega) = 2Na\mathcal{N}_{1d}(\epsilon_F) \frac{g_c v_F}{v_c} \frac{-(qv_c)^2}{\omega^2 - (qv_c)^2} = \chi_{\rho\rho}^{1d}, \quad (5.10)$$

where  $\mathcal{N}_{1d}(\epsilon_F) = (\pi v_F)^{-1}$  is the density of states per spin at the Fermi surface,  $a$  is the lattice constant, and  $v_c$  and  $g_c$  are the Luttinger parameters in the charge sector as given in Eqs. (2.52) and (2.54).

In a similar way, the spin density can be separated into left and right spin densities

$$\sigma(q) = \sigma_R(q) + \sigma_L(q). \quad (5.11)$$

Following the same steps as for the charge susceptibility one obtains for the spin susceptibility

$$\chi_{\sigma\sigma}(q, \omega) = 2Na\mathcal{N}_{1d}(\epsilon_F) \frac{g_s v_F}{v_s} \frac{-(qv_s)^2}{\omega^2 - (qv_s)^2}, \quad (5.12)$$

where  $v_s$  and  $g_s$  are the Luttinger parameters in the spin sector as given in Eqs. (2.51) and (2.53).

### 5.3.2 Luttinger model coupled to 3d electrons

Now we calculate the charge susceptibility of a one-dimensional electronic system which is coupled to a three-dimensional environment. The model is described by the Hamiltonian (5.2)

$$H = H_{\text{Luttinger}} + H_{0\pi^*} + H_{d-\pi^*}. \quad (5.13)$$

We consider in the following only interactions with small momentum transfer; in this case, in terms of density operators, the Hamilton  $H_{d-\pi^*}$  reads

$$H_{d-\pi^*} = \frac{V}{N} \sum_{\mathbf{q}} \rho_d(-\mathbf{q})\rho_{\pi^*}(\mathbf{q}), \quad (5.14)$$

where  $\mathbf{q}$  is the momentum transfer with  $\mathbf{q} = (q_{\parallel}, \mathbf{q}_{\perp})$ . Since the total charge (and spin) density is a sum of three contributions,  $\rho = \rho_L + \rho_R + \rho_{\pi^*}$ , then the correlator  $\chi_{\rho\rho}$  is

$$\chi_{\rho\rho} = \chi_{LL} + \chi_{RL} + \chi_{LR} + \chi_{RR} + \chi_{L\pi} + \chi_{R\pi} + \chi_{\pi\pi} + \chi_{\pi L} + \chi_{\pi R}. \quad (5.15)$$

To calculate the correlators  $\chi_{\eta\gamma}$ , we use again Eq. (5.7), this time for  $\eta, \gamma \in \{L, R, \pi^*\}$ . In addition we need the commutators

$$\langle[\rho_{\pi^*}(\mathbf{q}, 0), \rho_{\pi^*}(-\mathbf{q}, 0)]\rangle = \sum_{\mathbf{k}\sigma} (\langle n_{\pi^*\sigma}(\mathbf{k}+\mathbf{q}) \rangle - \langle n_{\pi^*\sigma}(\mathbf{k}) \rangle) \approx -2\mathcal{N}_{3d}(\epsilon_F) \mathcal{V} \mathbf{v}_F^{3d} \cdot \mathbf{q}, \quad (5.16)$$

$$\langle[[\rho_{\pi^*}(\mathbf{q}, t), H_{0\pi^*}], \rho_{\eta}(-\mathbf{q}, 0)]\rangle \approx -\mathbf{v}_F^{3d} \cdot \mathbf{q} \langle[\rho_{\pi^*}(\mathbf{q}, t), \rho_{\eta}(-\mathbf{q}, 0)]\rangle, \quad (5.17)$$

$$\begin{aligned} \langle[[\rho_{\pi^*}(\mathbf{q}, t), H_{d-\pi^*}], \rho_{\eta}(-\mathbf{q}, 0)]\rangle = \\ -2\mathcal{N}_{3d}(\epsilon_F) \mathbf{v}_F^{3d} \cdot \mathbf{q} \frac{V}{N} \mathcal{V} \langle[\rho_L(\mathbf{q}, t) + \rho_R(\mathbf{q}, t), \rho_{\eta}(-\mathbf{q}, 0)]\rangle, \end{aligned} \quad (5.18)$$

$$[\rho_L(\mathbf{q}, t), H_{d-\pi^*}] = -[\rho_R(\mathbf{q}, t), H_{d-\pi^*}] = \frac{V}{N} \frac{LN_{\perp}q_{\parallel}}{\pi} \rho_{\pi^*}(\mathbf{q}, t). \quad (5.19)$$

where  $N_{\perp}$  is the number of chains,  $\mathcal{N}_{3d}(\epsilon_F)$  is the density of states per spin and per volume at the Fermi surface, and  $\mathcal{V}$  is the volume. After some calculations we obtain the following expressions for the charge and spin susceptibility:

$$\chi_{\rho\rho} = \frac{\chi_{\rho\rho}^{1d} - 2\chi_{\rho\rho}^{1d}V\chi_{\pi^*}/N + \chi_{\pi^*}}{1 - \chi_{\rho\rho}^{1d}V\chi_{\pi^*}V/N^2}, \quad (5.20)$$

$$\chi_{\sigma\sigma} = \chi_{\sigma\sigma}^{1d} + \chi_{\pi^*}, \quad (5.21)$$

where  $\chi_{\rho\rho}^{1d}$  ( $\chi_{\sigma\sigma}^{1d}$ ) is the charge (spin) susceptibility of the Luttinger model given by Eq. (5.10) (Eq. (5.12)) with  $Na = LN_{\perp}$ , and  $\chi_{\pi^*}$  is the susceptibility corresponding to the free  $\pi^*$  electrons. The results (5.20) and (5.21) are equivalent to the RPA results obtained for a similar model with an electron-electron interaction characterized by a small momentum transfer, without applying the bosonization procedure.

### 5.3.3 Dispersion of the charge excitations

The charge excitation spectrum is given by equation

$$\frac{1}{\chi_{\rho\rho}(\mathbf{q}, \omega)} = 0, \quad (5.22)$$

which implicitly defines the dispersion relation  $\omega = \omega(\mathbf{q})$ . In the following we analyze the dispersion of the charge excitations: We want to see how the linearized dispersion of

a clean one-dimensional system is modified due to the presence of the three-dimensional electrons. In this case Eq. (5.22) leads to

$$1 - \chi_{\rho\rho}^{1d}(\omega, q_{\parallel})V\chi_{\pi^*}(\omega, \mathbf{q})V/N^2 = 0, \quad (5.23)$$

where  $\chi_{\rho\rho}^{1d}(\omega, q_{\parallel})$  is the dynamical susceptibility of the Luttinger model, compare Eq. (5.10),

$$\chi_{\rho\rho}^{1d}(\omega, q_{\parallel}) = 2Na\mathcal{N}_{1d}\frac{g_c v_F}{v_c} \frac{-(q_{\parallel}v_c)^2}{\omega^2 - (q_{\parallel}v_c)^2}, \quad (5.24)$$

and  $\chi_{\pi^*}^0(\omega, \mathbf{q})$  is the dynamical susceptibility of the free three-dimensional fermionic system,

$$\chi_{\pi^*}(\omega, \mathbf{q}) = 2\mathcal{N}_{3d}\mathcal{V} \left\langle \frac{\mathbf{v}_F^{3d} \cdot \mathbf{q}}{\omega + \mathbf{v}_F^{3d} \cdot \mathbf{q}} \right\rangle_{FS}, \quad (5.25)$$

where  $\mathcal{N}_{3d}$ ,  $\mathbf{v}_F^{3d}$  are the density of states per spin and per volume and the velocity of the  $\pi^*$  electrons at the Fermi surface and  $\langle \dots \rangle_{FS}$  is a Fermi surface average. We separate the three-dimensional momentum  $\mathbf{q}$  in two components, one parallel to the one-dimensional chain,  $q_{\parallel}$ , and the other perpendicular to it,  $\mathbf{q}_{\perp}$ . If we insert Eqs. (5.24) and (5.25) into Eq. (5.23), the dispersion is found as the solution of the following equation:

$$\omega^2 - (q_{\parallel}v_c)^2 \left[ 1 - 4V^2\mathcal{N}_{1d}\mathcal{N}_{3d}\frac{a\mathcal{V}}{N}\frac{g_c v_F}{v_c} \left\langle \frac{\mathbf{v}_F^{3d} \cdot \mathbf{q}}{\omega + \mathbf{v}_F^{3d} \cdot \mathbf{q}} \right\rangle_{FS} \right] = 0. \quad (5.26)$$

In the limit  $\omega \ll \mathbf{v}_F^{3d} \cdot \mathbf{q}$  the three dimensional charge susceptibility can be approximated by its static value

$$\chi_{\pi^*}(\omega, \mathbf{q}) \approx \chi_{\pi^*}(0, \mathbf{q}) = 2\mathcal{N}_{3d}\mathcal{V}$$

and the dispersion of the one-dimensional charge excitations is given by

$$\omega = \pm q_{\parallel}v_c \sqrt{1 - 4V^2\mathcal{N}_{1d}\mathcal{N}_{3d}\frac{a\mathcal{V}}{N}\frac{g_c v_F}{v_c}}. \quad (5.27)$$

In this case the dispersion maintains its one-dimensional linear characteristic. The only effect of the coupling to the three-dimensional environment is a renormalization of the Luttinger parameters

$$v_c \longrightarrow \tilde{v}_c = v_c \sqrt{1 - 4V^2\mathcal{N}_{1d}\mathcal{N}_{3d}\frac{a\mathcal{V}}{N}\frac{g_c v_F}{v_c}}, \quad (5.28)$$

$$g_c \longrightarrow \tilde{g}_c = g_c \left( \sqrt{1 - 4V^2\mathcal{N}_{1d}\mathcal{N}_{3d}\frac{a\mathcal{V}}{N}\frac{g_c v_F}{v_c}} \right)^{-1}, \quad (5.29)$$

which is equivalent to a decrease of the interaction strength in the charge channel. In the opposite limit,  $\omega \gg \mathbf{v}_F^{3d} \cdot \mathbf{q}$  we can expand in powers of  $\mathbf{v}_F^{3d} \cdot \mathbf{q}/\omega$ , and obtain

$$\left\langle \frac{\mathbf{v}_F^{3d} \cdot \mathbf{q}}{\omega + \mathbf{v}_F^{3d} \cdot \mathbf{q}} \right\rangle_{FS} \approx \frac{1}{3} \frac{(v_F^{3d})^2 (q_{\parallel}^2 + \mathbf{q}_{\perp}^2)}{\omega^2}. \quad (5.30)$$

In this situation the dispersion is given by the equation

$$\omega^4 - \omega^2 (q_{\parallel} v_c)^2 + (q_{\parallel} v_c)^2 V^2 \mathcal{N}_{1d} \mathcal{N}_{3d} \frac{a\mathcal{V}}{N} \frac{4g_c v_F}{3v_c} (v_F^{3d})^2 (q_{\parallel}^2 + \mathbf{q}_{\perp}^2) = 0, \quad (5.31)$$

with the following solutions:

$$\omega_+^2 = (q_{\parallel} v_c)^2 \left[ 1 - V^2 \mathcal{N}_{1d} \mathcal{N}_{3d} \frac{a\mathcal{V}}{N} \frac{4g_c v_F}{3v_c} \frac{(v_F^{3d})^2 (q_{\parallel}^2 + \mathbf{q}_{\perp}^2)}{(q_{\parallel} v_c)^2} \right], \quad (5.32)$$

$$\omega_-^2 = V^2 \mathcal{N}_{1d} \mathcal{N}_{3d} \frac{a\mathcal{V}}{N} \frac{4g_c v_F}{3v_c} (v_F^{3d})^2 (q_{\parallel}^2 + \mathbf{q}_{\perp}^2). \quad (5.33)$$

In the weak coupling limit the solution  $\omega_-^2$  is not compatible with the assumption  $\omega \gg \mathbf{v}_F^{3d} \cdot \mathbf{q}$ . To analyze the solution  $\omega_+^2$  we must distinguish between two limiting cases. If the parallel component of the momentum is much larger than the perpendicular component  $q_{\parallel} \gg q_{\perp}$ , then again the effect of the tree-dimensional electrons is only to renormalize the Luttinger parameters and the dispersion remains approximately, linear

$$\omega_+ \approx \pm q_{\parallel} v_c \sqrt{1 - \left( \frac{v_{F\parallel}^{3d}}{v_c} \right)^2 \frac{4g_c v_F}{3v_c} \frac{a\mathcal{V}}{N} V^2 \mathcal{N}_{1d} \mathcal{N}_{3d}}. \quad (5.34)$$

A more interesting situation arises in the opposite limit,  $q_{\parallel} \ll q_{\perp}$ , when the charge dispersion loses its linearized characteristic and the one dimensional modes are mixed with the three-dimensional modes through the  $q_{\perp}$  component, i.e.

$$\omega_+ \approx \pm q_{\parallel} v_c \sqrt{1 - \frac{(v_{F\perp}^{3d} q_{\perp})^2}{(q_{\parallel} v_c)^2} \frac{4g_c v_F}{3v_c} \frac{a\mathcal{V}}{N} V^2 \mathcal{N}_{1d} \mathcal{N}_{3d}} = \pm v_c \sqrt{q_{\parallel}^2 - \alpha q_{\perp}^2}, \quad (5.35)$$

with

$$\alpha = \frac{(v_{F\perp}^{3d})^2}{v_c^2} \frac{4g_c v_F}{3v_c} \frac{a\mathcal{V}}{N} V^2 \mathcal{N}_{1d} \mathcal{N}_{3d} \approx \frac{V^2}{\epsilon_F^{1d} \epsilon_F^{3d}} \approx 10^{-2} \dots 10^{-1}$$

where we have assumed that  $V$  is roughly one order of magnitude smaller than the Fermi energies.



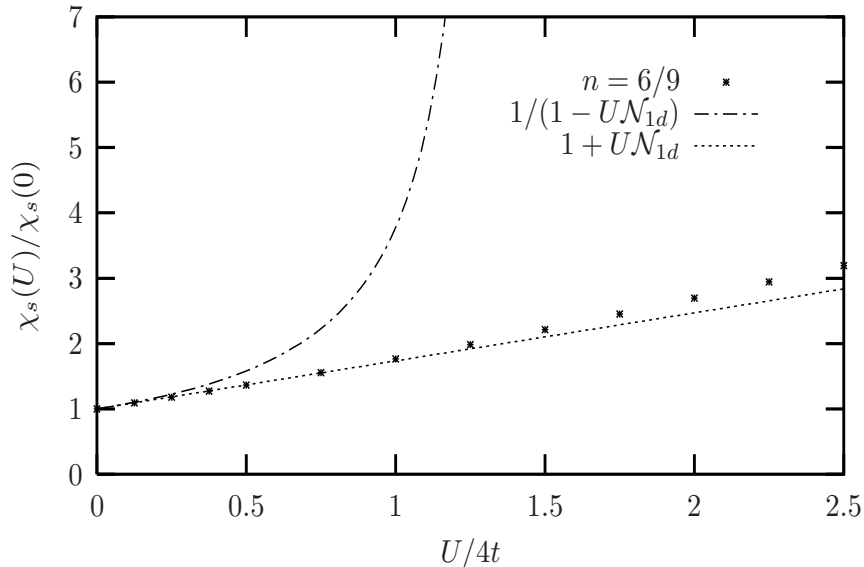


Figure 5.2: The spin susceptibility of the one-dimensional Hubbard model. Within RPA one finds  $\chi_s(U) = \chi_s(0)/(1 - UN_{1d})$ , where  $\mathcal{N}_{1d} = (\pi v_F)^{-1}$ . The data points are numerical results [95] obtained with exact diagonalization of a Hubbard chain with 6 electrons on 9 lattice sites ( $n$  is the electron density).

## 5.4 Discussion

In order to see how the three-dimensional electrons affect the electrons in the one-dimensional  $d_{\parallel}$  band, we have calculated the charge and the spin susceptibility of the system; the coupling is introduced as a local Coulomb interaction of strength  $V$ . We found that the spin susceptibility of the  $d_{\parallel}$  electrons remains unchanged in the presence of the  $\pi^*$  electrons. This seems to contradict [93], where from the spin susceptibility in the metallic phase a smaller  $U_{\text{eff}} \approx 0.13$  eV has been estimated. The apparent contradiction is easily solved, however, when calculating the spin susceptibility in a  $1d$  Hubbard model numerically, and comparing with the RPA estimate. Fig. 5.4 clearly demonstrates that for a Stoner enhancement of about  $\chi/\chi_0 \approx 3$  the RPA drastically underestimates the interaction strength which is necessary to obtain such an enhancement.

Concerning the charge susceptibility, we found that it is changed in the presence of the  $\pi^*$  electrons. To make the effect more visible, we analyzed the dispersion of the collective charge excitations. When the dynamics of the  $\pi^*$  electrons is fast compared to the  $d_{\parallel}$  electrons, we found that the major effect of the  $\pi^*$  electrons is to renormalize the charge velocity. When the Fermi velocity of the  $d_{\parallel}$  and  $\pi^*$  electrons are comparable in size, the dynamics of the  $\pi^*$  electrons is on comparable time scales. In this limit collective modes can mix, so that the  $d_{\parallel}$  electrons lose their one-dimensional character.



# Chapter 6

## Summary and outlook

In this work we have investigated the low energy properties of different one-dimensional fermionic lattice models using the bosonization technique. We have attached much importance to a proper consideration of the Klein factors which are neglected or inaccurately treated in the majority of the literature.

In order to deal with the nonlinear terms, arising from the dimerization or similar scattering processes, we used the self-consistent harmonic approximation (SCHA), a variational method where the nonlinearities are replaced by a quadratic potential. We have constructed an extension of the SCHA in order to account for the existence of Klein factors in bosonized Hamiltonians.

As a first application, we have investigated a model of spinless fermions with nearest-neighbor interaction and a modulated hopping. For the infinite system, both, the value of the Luttinger parameter  $g_c = 2$  where the transition from a gapless to a gapped phase takes places, and the exponent  $1/(2 - g)$  that characterizes the opening of the gap for small dimerization, are correctly obtained within the SCHA. In the thermodynamic limit replacing the Klein operators by a c-number is justified. When considering a finite system a more careful treatment is necessary. In this case the Klein Hamiltonian can be mapped onto a Mathieu equation which can be solved analytically in certain limits. Within our approach it turns out that the effect of the Klein factors is negligible as long as the dimerization gap is larger than the finite-size gap,  $v_F/L$ .

In addition, the finite-size formalism allows calculation of the size-dependence of the Drude weight. The Drude weight reflects the sensitivity of the system with respect to a change of boundary conditions and is related to the properties of the current operator  $J$  in the bosonized version of the Hamiltonian. In a finite system with an energy gap  $\Delta$  the Drude weight is expected to be nonzero but exponentially small,  $D \sim \exp(-\text{const} \cdot L\Delta)$ . In our extended version of the SCHA we confirm the exponential behavior.

As an application to fermions with spin, we studied the role of Klein factors for the Peierls-Hubbard and the ionic Hubbard model. In the bosonized version of these models two kinds of bosonic fields have to be introduced which are associated with the spin and the charge degrees of freedom, respectively. Nonlinear terms arising from backward and

Umklapp scattering lead to the opening of spin or charge gaps depending on the model parameters. Using the SCHA we have calculated the corresponding gap parameters  $\Delta_c$  and  $\Delta_s$  as a function of the strength of the perturbation (the dimerization  $u$  in the case of the Peierls-Hubbard model, and the ionic potential  $\Delta$  in the case of the ionic Hubbard model). In both cases we found a transition from a Mott insulator phase with vanishing or very small spin gap to a band insulator phase with almost equal spin and charge gaps. The opening of the spin gap with increasing perturbation strength occurs according to a power law with universal exponents,  $2/3$  in the case of the Peierls-Hubbard model, and  $2$  in the case of the ionic Hubbard model. The main difference between the two models, however, is that in the Peierls-Hubbard model the transition between the Mott and the Peierls phase is continuous, while for the ionic Hubbard model a first order transition is observed, with a jump in  $\Delta_c$  and  $\Delta_s$ . As to the ionic Hubbard model we could not confirm the scenario proposed by Fabrizio et al. [75] who argued in favor of two phase transitions. However, in our bosonization approach we are strictly limited to weak coupling with regard to the Hubbard interaction  $U$  and to the ionic potential  $\Delta$ , while Fabrizio et al. [75] used a strong coupling approach in order to obtain the second transition. While there is some evidence for the two phase transitions scenario from DMRG calculations in the case of a strong ionic potential ( $\Delta/t = 0.5$  in Ref. [82] and  $\Delta/t = 20$  in Ref. [81]), it is not clear whether this scenario persists to small values of  $\Delta$ , e.g.  $\Delta/t = 0.1$  that we have used in our calculations.

Concerning the role of Klein factors one has to recall that they do not commute with the total spin and charge currents,  $J_{c,s}$ , and therefore Klein factors and current operators cannot acquire a fixed value at the same time. In the thermodynamic limit the ground state of the gapped systems is a superposition of many states with different  $J_c$  and  $J_s$ . In this situation it is possible to choose a fixed phase for the Klein operators. The bosonized Hamiltonian is then the conventional sine-Gordon-like Hamiltonian. In the framework of our variational scheme we decoupled the bosonic Hamiltonian from the Klein Hamiltonian. For finite size systems the eigenvalues of the Klein factors are replaced by their expectation values with respect to the ground state of the trial Hamiltonian, and the resulting bosonic Hamiltonian is also of a sine-Gordon type. The Klein Hamiltonian is of the form of a tight-binding Hamiltonian for a particle moving on a  $2d$  lattice in a harmonic potential. The strength of the potential is inversely proportional to the length of the systems, i.e. for small systems the potential contribution to the ground state energy is relevant. On the other hand, when the size of the system approaches the thermodynamic limit, the confining potential becomes irrelevant.

In an attempt to describe more realistic systems we considered a model where one-dimensional electrons are coupled to a three-dimensional conduction band via a local interaction, having in mind an application to embedded Peierls systems like vanadium dioxide,  $\text{VO}_2$ . In order to see how the one-dimensional electron system is modified in the presence of the three-dimensional environment, we calculated the charge and the

spin susceptibility, and analyzed the collective excitations within RPA. We found that the spin excitations remain unaffected. In the charge channel, the collective modes of the  $1d$  and  $3d$  subsystems are coupled. If the Fermi velocity of the  $3d$  system is much larger than in the  $1d$  system, the  $3d$  electrons react practically instantaneously to changes in the  $1d$  chains. In this case the  $3d$  electrons simply renormalize or “screen” the Luttinger parameters in the chains. When  $v_F^{3d} \approx v_F^{1d}$  the situation becomes more complex, since the dynamics of screening becomes relevant. In this case the charge excitations lose their one-dimensional character and become three-dimensional.

The next step beyond the current work would be to derive an effective model of one-dimensional chains coupled via the  $3d$  environment, and to use the methods developed and tested in the first chapters to calculate the phase diagram. A major difficulty to overcome is the fact that dynamic screening leads to retarded interactions which in general cannot be cast into a Hamiltonian formalism, such as the one used in the simple model calculations, but rather requires a path integral formulation for the bosonized systems. While it is more or less standard to represent a bosonic theory in the path integral language, it is not clear how the Klein factors in this formulation can be incorporated.



# Appendix A

## Derivation of the gap equations

In this appendix we derive the SCHA equations for the Peierls-Hubbard model. The derivation for the ionic Hubbard model is similar. For a finite system the Klein factors cannot be replaced by their eigenvalues, but we can choose a trial Hamiltonian where the bosonic fields are decoupled from the Klein factors as follows

$$H_{\text{tr}} = H_{\text{tr}}^{\Delta_c} + H_{\text{tr}}^{\Delta_s} + H_{\text{tr}}^{B_{cs}B_cB_s}, \quad (\text{A.1})$$

with the usual bosonic part, in which the nonlinear terms are replaced by a quadratic form

$$H_{\text{tr}}^{\Delta_c} + H_{\text{tr}}^{\Delta_s} = \sum_{\alpha=c,s} \int_0^L \frac{dx}{2\pi} \left\{ \frac{v_\alpha}{g_\alpha} (\partial_x \phi_\alpha)^2 + v_\alpha g_\alpha (\partial_x \theta_\alpha)^2 + \frac{\Delta_\alpha^2}{v_\alpha g_\alpha} \phi_\alpha^2 \right\} \quad (\text{A.2})$$

and a Hamiltonian containing the Klein factors

$$\begin{aligned} H_{\text{tr}}^{B_{cs}B_cB_s} &= iB_{cs}L(F_{R\uparrow}^+ F_{L\uparrow} + F_{R\downarrow}^+ F_{L\downarrow}) + B_c L F_{R\uparrow}^+ F_{R\downarrow}^+ F_{L\downarrow} F_{L\uparrow} \\ &\quad + B_s L F_{R\uparrow}^+ F_{L\downarrow}^+ F_{R\downarrow} F_{L\uparrow} + \text{h.c.} \\ &\quad + \frac{\pi}{4L} (v_c g_c J_c^2 + v_s g_s J_s^2). \end{aligned} \quad (\text{A.3})$$

Taking the ground state of  $H_{\text{tr}}$  as a variational state for the full Hamiltonian we obtain an upper bound  $\tilde{E}$  for the ground state

$$\begin{aligned} \tilde{E} &= \langle H_0 \rangle_{\text{tr}} + \langle H_1 \rangle_{\text{tr}} + \langle H_2 \rangle_{\text{tr}} + \langle H_{\text{Peierls}} \rangle_{\text{tr}}, \\ \frac{\tilde{E}}{L} &= \frac{E_{\text{tr}}}{L} - \sum_{\alpha=c,s} \frac{\Delta_\alpha^2}{2\pi v_\alpha g_\alpha} \langle \phi_\alpha^2 \rangle_{\text{tr}} - B_c \frac{\partial e_{\text{tr}}^0}{\partial B_c} - L \frac{\partial e_{\text{tr}}^0}{\partial B_s} - B_{cs} \frac{\partial e_{\text{tr}}^0}{\partial B_{cs}} \\ &\quad + \tilde{U} e^{-4\langle \phi_c^2 \rangle_{\text{tr}}} \frac{\partial e_{\text{tr}}^0}{\partial B_c} + \tilde{U} e^{-4\langle \phi_s^2 \rangle_{\text{tr}}} \frac{\partial e_{\text{tr}}^0}{\partial B_s} + \tilde{u} e^{-\langle \phi_c^2 \rangle_{\text{tr}} - \langle \phi_s^2 \rangle_{\text{tr}}} \frac{\partial e_{\text{tr}}^0}{\partial B_{cs}}. \end{aligned} \quad (\text{A.4})$$

Here  $E_{\text{tr}}$  is the ground state energy of  $H_{\text{tr}}$  given by Eq. (A.1), and  $e_{\text{tr}}^0 = E_{\text{tr}}^0(B_{cs}, B_c, B_s)/L$ , where  $E_{\text{tr}}^0(B_{cs}, B_c, B_s)$  is the ground state energy of the Klein Hamiltonian  $H_{\text{tr}}^{B_{cs}B_cB_s}$

given by Eq. (A.3). In addition,  $\tilde{u} = tu/\pi a$ , and  $\tilde{U} = UL/[(2\pi a)^2 N]$ . We have used the Feynmann-Hellmann theorem [37, 38] to express the expectation values of the Klein factors in terms of the derivatives of  $e_{\text{tr}}^0$ , the ground state energy  $E_{\text{tr}}^0$  divided by system length, with respect to the  $B$ 's:

$$\frac{\partial e_{\text{tr}}^0}{\partial B_c} = \langle F_{R\uparrow}^+ F_{R\downarrow}^+ F_{L\downarrow} F_{L\uparrow} + \text{h.c.} \rangle, \quad (\text{A.5})$$

$$\frac{\partial e_{\text{tr}}^0}{\partial B_s} = \langle F_{R\uparrow}^+ F_{L\downarrow}^+ F_{R\downarrow} F_{L\uparrow} + \text{h.c.} \rangle, \quad (\text{A.6})$$

$$\frac{\partial e_{\text{tr}}^0}{\partial B_{cs}} = i \langle F_{R\uparrow}^+ F_{L\uparrow} + F_{R\downarrow}^+ F_{L\downarrow} \rangle + \text{h.c.} \quad (\text{A.7})$$

The parameters  $\Delta_c$ ,  $\Delta_s$ ,  $B_c$ ,  $B_s$  and  $B_{cs}$  are obtained from the condition that  $\tilde{E}$  should be minimized. For the parameters  $B_c$ ,  $B_s$  and  $B_{cs}$  the minimum condition for  $\tilde{E}$  yields the following equations:

$$\begin{aligned} & \left[ \tilde{u} e^{-\langle \phi_c^2 \rangle - \langle \phi_s^2 \rangle} - B_{cs} \right] \frac{\partial^2 e_{\text{tr}}^0}{\partial B_{cs}^2} + \left[ \tilde{U} e^{-4\langle \phi_c^2 \rangle} - B_c \right] \frac{\partial^2 e_{\text{tr}}^0}{\partial B_{cs} \partial B_c} \\ & + \left[ \tilde{U} e^{-4\langle \phi_s^2 \rangle} - B_s \right] \frac{\partial^2 e_{\text{tr}}^0}{\partial B_{cs} \partial B_s} = 0, \end{aligned} \quad (\text{A.8})$$

$$\begin{aligned} & \left[ \tilde{u} e^{-\langle \phi_c^2 \rangle - \langle \phi_s^2 \rangle} - B_{cs} \right] \frac{\partial^2 e_{\text{tr}}^0}{\partial B_c \partial B_{cs}} + \left[ \tilde{U} e^{-4\langle \phi_c^2 \rangle} - B_c \right] \frac{\partial^2 e_{\text{tr}}^0}{\partial B_c^2} \\ & + \left[ \tilde{U} e^{-4\langle \phi_s^2 \rangle} - B_s \right] \frac{\partial^2 e_{\text{tr}}^0}{\partial B_s \partial B_c} = 0, \end{aligned} \quad (\text{A.9})$$

$$\begin{aligned} & \left[ \tilde{u} e^{-\langle \phi_c^2 \rangle - \langle \phi_s^2 \rangle} - B_{cs} \right] \frac{\partial^2 e_{\text{tr}}^0}{\partial B_s \partial B_{cs}} + \left[ \tilde{U} e^{-4\langle \phi_c^2 \rangle} - B_c \right] \frac{\partial^2 e_{\text{tr}}^0}{\partial B_s \partial B_c} \\ & + \left[ \tilde{U} e^{-4\langle \phi_s^2 \rangle} - B_s \right] \frac{\partial^2 e_{\text{tr}}^0}{\partial B_s^2} = 0, \end{aligned} \quad (\text{A.10})$$

with the solutions

$$B_{cs} = \tilde{u} e^{-\langle \phi_c^2 \rangle - \langle \phi_s^2 \rangle}, \quad (\text{A.11})$$

$$B_c = \tilde{U} e^{-4\langle \phi_c^2 \rangle}, \quad (\text{A.12})$$

$$B_s = \tilde{U} e^{-4\langle \phi_s^2 \rangle}. \quad (\text{A.13})$$

Minimizing  $\tilde{E}$  with respect to  $\Delta_c$  and  $\Delta_s$  yields

$$\frac{\Delta_c^2}{2\pi v_c g_c} = -4B_c \frac{\partial e_{\text{tr}}^0}{\partial B_c} - B_{cs} \frac{\partial e_{\text{tr}}^0}{\partial B_{cs}}, \quad (\text{A.14})$$

$$\frac{\Delta_s^2}{2\pi v_s g_s} = -4B_s \frac{\partial e_{\text{tr}}^0}{\partial B_s} - B_{cs} \frac{\partial e_{\text{tr}}^0}{\partial B_{cs}}, \quad (\text{A.15})$$



where we have used that

$$\frac{\partial e_{\text{tr}}^0}{\partial(\Delta_\alpha^2)} = \frac{\langle \phi_\alpha^2 \rangle_{\text{tr}}}{2\pi v_\alpha g_\alpha}. \quad (\text{A.16})$$

These equations are identical to the equations obtained in the thermodynamic limit, see Eqs. (4.28)-(4.29), if the minimum of  $e(k_\uparrow, k_\downarrow)$ , given by Eq. (4.24), is replaced with  $e_{\text{tr}}^0$ , the ground state energy  $E_{\text{tr}}^0$  of the Klein Hamiltonian divided by system length.



# Appendix B

## The trial Hamiltonian in terms of bosonic operators

The bosonic part of the trial Hamiltonian for spinless fermions with static dimerization in the thermodynamic limit reads

$$H_{\text{tr}}^{\Delta} = \int_0^L \frac{dx}{2\pi} \left\{ \frac{v}{g} (\partial_x \phi)^2 + vg (\partial_x \theta)^2 + \frac{\Delta^2}{vg} \phi^2(x) \right\}. \quad (\text{B.1})$$

After Fourier transformation

$$\phi(x) = \frac{1}{\sqrt{L}} \sum_{q \neq 0} e^{iqx} \phi(q), \quad \theta(x) = \frac{1}{\sqrt{L}} \sum_{q \neq 0} e^{iqx} \theta(q),$$

it can be rewritten as

$$H_{\text{tr}}^{\Delta} = \frac{1}{2\pi} \sum_{q>0} \left[ \left( \frac{v}{g} q^2 + \frac{1}{vg} \Delta^2 \right) \phi(q) \phi(-q) + vg q^2 \theta(q) \theta(-q) \right]. \quad (\text{B.2})$$

If we express  $\phi(\pm q)$  and  $\theta(\pm q)$  in terms of the boson operators

$$\phi(q) = \sqrt{\frac{\pi}{2q}} (b_{Lq}^+ - b_{Rq}) e^{-aq/2}, \quad (\text{B.3})$$

$$\theta(q) = \sqrt{\frac{\pi}{2q}} (b_{Lq}^+ + b_{Rq}) e^{-aq/2}, \quad (\text{B.4})$$

$$\phi(-q) = \sqrt{\frac{\pi}{2q}} (b_{Lq} - b_{Rq}^+) e^{-aq/2}, \quad (\text{B.5})$$

$$\theta(-q) = \sqrt{\frac{\pi}{2q}} (b_{Lq} + b_{Rq}^+) e^{-aq/2}, \quad (\text{B.6})$$

where  $q > 0$ , the trial Hamiltonian becomes

$$H_{\text{tr}}^{\Delta} = \sum_{q>0} \left[ \left( v_F + \frac{g_4}{2\pi} \right) q + \frac{1}{2q} \Delta^2 \right] [b_{Lq}^+ b_{Lq} + b_{Rq}^+ b_{Rq}] e^{-aq} - \sum_{q>0} \left[ \frac{g_2}{2\pi} q + \frac{1}{2q} \Delta^2 \right] [b_{Lq}^+ b_{Lq}^+ + b_{Rq}^+ b_{Rq}^+] e^{-aq} + \sum_{q>0} \left[ \frac{e^{-aq}}{2q} \Delta^2 \right]. \quad (\text{B.7})$$

This Hamiltonian can be diagonalized with a Bogoliubov transformation of the following form:

$$B_1(q) = \alpha b_{Rq} + \beta b_{Lq}^+, \quad (\text{B.8})$$

$$B_2(q) = \beta b_{Rq} + \alpha b_{Lq}^+, \quad (\text{B.9})$$

with  $\alpha$  and  $\beta$  parameters to be determined. The operators  $B_1$  and  $B_2$  are also bosonic operators, i.e.

$$[B_1, B_1^+] = [B_2, B_2^+] = 1 \quad \Rightarrow \quad \alpha^2 - \beta^2 = 1.$$

The  $b_{\eta,q}$  operators in the Hamiltonian (B.7) are replaced by the new operators  $B_1$  and  $B_2$ . The restriction that the Hamiltonian in terms of  $B_1$  and  $B_2$  has to be diagonal yields the second equation for the parameters  $\alpha$  and  $\beta$

$$2\alpha\beta(\gamma_4 q^2 + \Delta^2/2) + (\gamma_2 q^2 + \Delta^2/2)(\alpha^2 + \beta^2) = 1,$$

with  $\gamma_4 = v_F + g_4/2\pi v_F$  and  $\gamma_2 = g_2/2\pi v_F$ . The diagonalized Hamiltonian is

$$H_{\text{tr}}^{\Delta} = \sum_{q>0} \sqrt{v^2 q^2 + \Delta^2} (B_1^+ B_1 + B_2^+ B_2) e^{-aq} + \sum_{q>0} \left[ \frac{e^{-aq}}{q} \Delta^2 (1 + \beta^2) + 2\beta(\beta\gamma_4 + \alpha\gamma_2)q \right] \quad (\text{B.10})$$

The last sum gives a infinite constant which is removed by the normal ordering operation. At the end we obtain in the limit  $a \rightarrow 0$

$$: H_{\text{tr}}^{\Delta} : = \sum_{q>0} \epsilon(q) (B_1^+ B_1 + B_2^+ B_2) \quad \text{with} \quad \epsilon(q) = \sqrt{v^2 q^2 + \Delta^2}. \quad (\text{B.11})$$

# Appendix C

## Quantum theory of Josephson junctions

Here we wish to point out that the study of the Klein factors within the SCHA, for the spinless-fermions model, leads to a trial Hamiltonian which is well known from the quantum theory of Josephson junctions in the zero-damping limit [39]. Considering again Eq. (3.31) and putting  $2p_J \rightarrow x$ , we have

$$H_{\text{tr}}^B \rightarrow -\frac{2\pi v g}{L} \frac{d^2}{dx^2} + 2B \cos x \quad (\text{C.1})$$

with periodic boundary conditions for the wave function,  $\Psi(x + 2\pi) = \Psi(x)$ . On the other hand, the Josephson junction Hamiltonian in standard notation [39] reads

$$H^{JJ} = -4E_c \frac{d^2}{d\varphi^2} - E_J \cos \varphi, \quad (\text{C.2})$$

$$\Psi(\varphi + 2\pi) = \Psi(\varphi), \quad (\text{C.3})$$

where  $\varphi$  is the order parameter phase difference across the junction,  $E_J$  the Josephson coupling energy, and  $E_c = e^2/2C$  ( $C$  is the capacitance) the charging energy. The correspondence is obvious.

Note that the “kinetic energy” in (C.2) corresponds to  $Q^2/2C$ , where  $Q = 2eN$  is the  $2e$  times the Cooper pair number, such that  $N$  and  $\varphi$  are conjugate variables,  $[N, \varphi] = -i$ . For large junctions,  $E_c \ll E_J$  (corresponding to large  $L$ ), the variable  $\varphi$  can be treated classically. On the other hand, for small junctions,  $E_c \gg E_J$  (corresponding to small  $L$ ), the appropriate eigenstates are particle, i.e. Cooper pair, number eigenstates. These two limits correspond to two representations of the BCS wave functions, namely with a definite phase and with a definite number of Cooper pairs, respectively [39].



# Appendix D

## Mathieu equation

The Mathieu equation in its canonical form [40] reads

$$\frac{d^2y}{dx^2} + (a - 2q \cos(2x))y = 0. \quad (\text{D.1})$$

This is exactly equation (3.31) if we identify

$$y(x) \longrightarrow \Psi(p_J), \quad (\text{D.2})$$

$$a \longrightarrow \frac{2LE}{\pi v g}, \quad (\text{D.3})$$

$$q \longrightarrow \frac{2LB}{\pi v g}. \quad (\text{D.4})$$

It can be shown that there exists a set of *characteristic values*  $a_r(q)$  which yield even periodic solutions and a set of *characteristic values*  $b_r(q)$  which yield odd periodic solutions, where  $r = 0, 1, 2, \dots$ . If  $q$  is real then the sets of *characteristic values*  $a_r$  and  $b_r$  have the following properties:

- a) The characteristic values  $a_r$  and  $b_r$  are real and distinct, if  $q \neq 0$ ;  $a_0 < b_1 < a_1 < b_2 < \dots$ ,  $q > 0$ , and  $a_r(q)$ ,  $b_r(q)$  approaches  $r^2$  as  $q$  approaches zero.
- b) A solution of the Mathieu equation associated with  $a_r$  or  $b_r$  has  $r$  zeros in the interval  $0 \leq x < \pi$ .

In Ref. [94] the asymptotic behavior of the characteristic values  $a_r$  and  $b_r$  is derived. In particular for  $q \gg 1$

$$b_{r+1}(q) - a_r(q) \approx 2^{4r+5} \sqrt{\frac{2}{\pi}} q^{r/2+3/4} e^{-4\sqrt{q}} \frac{1}{r!} \quad (\text{D.5})$$

If we consider the case  $r = 0$ , we can estimate the difference  $E(\pi) - E(0)$  needed in Eq. (3.45). We identify  $E(\pi) = b_1(q)q/B$  and  $E(0) = a_0(q)q/B$  to obtain Eq. (3.40).

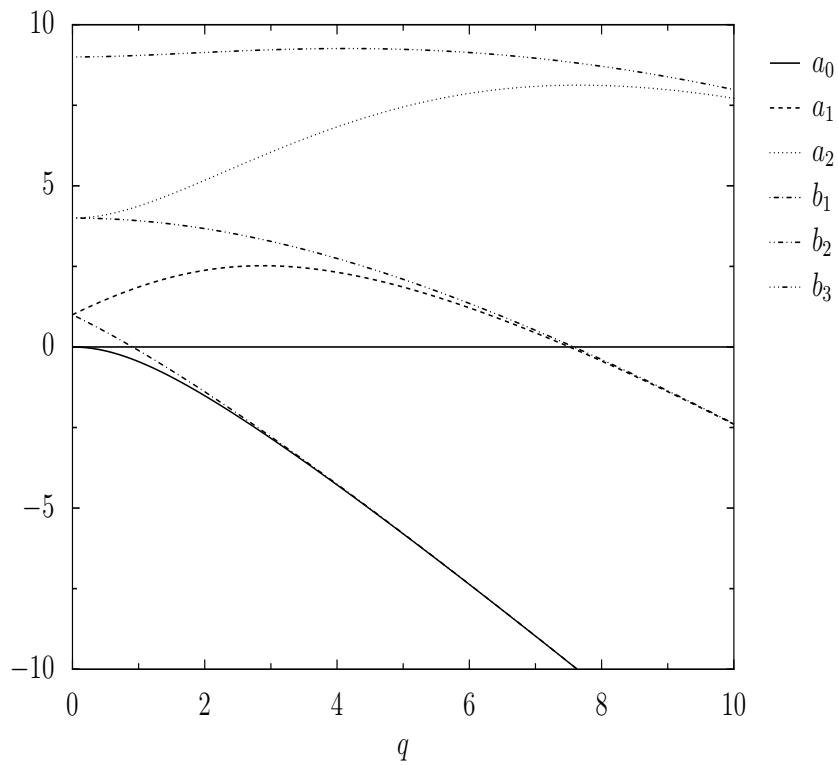


Figure D.1: The lowest eigenvalues of the Mathieu equation as function of  $q$ . The  $a$ 's correspond to periodic and the  $b$ 's to anti-periodic solutions. With increasing  $q$  the difference  $b_r - a_{r-1}$  goes to zero.



# Appendix E

## The Klein Hamiltonian as a $2d$ tight binding model

In the following we represent the Klein Hamiltonian of the Peierls-Hubbard model,

$$\begin{aligned}
H_{\text{tr}}^{B_{cs}B_cB_s} &= iB_{cs}L(F_{R\uparrow}^+F_{L\uparrow} + F_{R\downarrow}^+F_{L\downarrow}) + B_cLF_{R\uparrow}^+F_{R\downarrow}^+F_{L\downarrow}F_{L\uparrow} \\
&\quad + B_sLF_{R\uparrow}^+F_{L\downarrow}^+F_{R\downarrow}F_{L\uparrow} + \text{h.c.} \\
&\quad + \frac{\pi}{4L}(v_c g_c J_c^2 + v_s g_s J_s^2), \tag{E.1}
\end{aligned}$$

in the basis of  $J_c$  and  $J_s$  in order to show explicitly that it has the form of a  $2d$  tight binding model for a particle in a harmonic potential. Using the sign convention for the Klein factors that we have chosen in section 2.2 one obtains

$$\begin{aligned}
H_{\text{tr}}^{B_{cs}B_cB_s} &= iB_{cs}L \sum_{J_c, J_s} (-1)^{\frac{J_c}{2}} |J_c, J_s\rangle \langle J_c + 2, J_s + 2| \\
&\quad + iB_{cs}L \sum_{J_c, J_s} (-1)^{\frac{J_s}{2}} |J_c + 2, J_s\rangle \langle J_c, J_s + 2| \\
&\quad + B_sL \sum_{J_c, J_s} |J_c, J_s\rangle \langle J_c, J_s + 4| + B_cL \sum_{J_c, J_s} |J_c, J_s\rangle \langle J_c + 4, J_s| + \text{h.c.} \\
&\quad + \frac{\pi v_c g_c}{4L} \sum_{J_c, J_s} J_c^2 |J_c, J_s\rangle \langle J_c, J_s| + \frac{\pi v_s g_s}{4L} \sum_{J_c, J_s} J_s^2 |J_c, J_s\rangle \langle J_c, J_s|. \tag{E.2}
\end{aligned}$$

For  $N_c = 0$  and  $N_s = 0$ , according to Eqs. (2.56) and (2.58) the quantum numbers  $J_c$  and  $J_s$  are even and  $J_c \pm J_s$  are multiples of 4. In Fig. E.1 the allowed hoppings are displayed schematically.

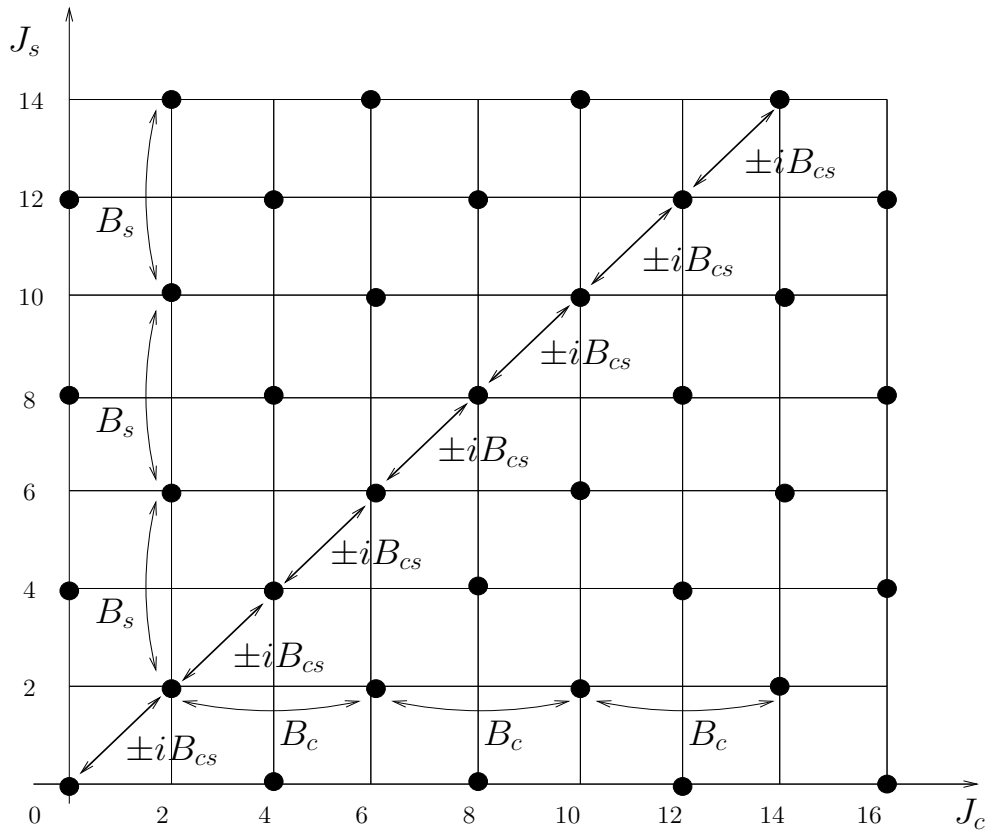


Figure E.1: Pictorial representation of the hopping Hamiltonian (E.2).

# Appendix F

## Analytical solution of the gap equations

In this appendix we present the solutions of the gap equations, both for the Peierls-Hubbard model, Eqs. (4.28)-(4.29), and for the ionic Hubbard model, Eqs. (4.61)-(4.62).

### Peierls-Hubbard model

In the case of the Peierls-Hubbard model, for non-zero dimerization the charge and spin mean field parameters are given by

$$\frac{\Delta_c^2}{2\pi v_c g_c} = 4B_{cs} + 8B_c = \frac{4tu}{\pi} e^{-\langle\phi_c^2\rangle_{\text{tr}}} + \frac{2U}{\pi^2} e^{-4\langle\phi_c^2\rangle_{\text{tr}}}, \quad (\text{F.1})$$

$$\frac{\Delta_s^2}{2\pi v_s g_s} = 4B_{cs} - 8B_s = \frac{4tu}{\pi} e^{-\langle\phi_c^2\rangle_{\text{tr}}} - \frac{2U}{\pi^2} e^{-4\langle\phi_s^2\rangle_{\text{tr}}}, \quad (\text{F.2})$$

where we set  $a$  equal to one. If we insert the analytical values for  $\langle\phi_c^2\rangle_{\text{tr}}$  and  $\langle\phi_s^2\rangle_{\text{tr}}$ , given by Eqs. (4.32)-(4.32), we obtain the following set of equations:

$$\frac{\Delta_c^2}{2\pi v_c g_c} = \frac{4tu}{\pi} \left(\frac{\Delta_c}{\Delta_{0c}}\right)^{g_c/2} \left(\frac{\Delta_s}{\Delta_{0s}}\right)^{1/2} + \frac{2U}{\pi^2} \left(\frac{\Delta_c}{\Delta_{0c}}\right)^{2g_c}, \quad (\text{F.3})$$

$$\frac{\Delta_c^2}{2\pi v_c g_c} = \frac{4tu}{\pi} \left(\frac{\Delta_s}{\Delta_{0s}}\right)^{1/2} \left(\frac{\Delta_c}{\Delta_{0c}}\right)^{g_c/2} - \frac{2U}{\pi^2} \left(\frac{\Delta_s}{\Delta_{0s}}\right)^2. \quad (\text{F.4})$$

Introducing the following notation:  $\Delta_c/\Delta_{0c} = x$ ,  $\Delta_s/\Delta_{0s} = y$ ,  $\Delta_{0c}/2\pi v_c g_c = A_c$ ,  $\Delta_{0s}/2\pi v_s g_s = A_s$ ,  $4tu/\pi = \tilde{u}$  and  $2U/\pi^2 = \tilde{U}$  yields

$$A_c x^2 = \tilde{u} x^{g_c/2} y^{1/2} + \tilde{U} x^{2g_c}, \quad (\text{F.5})$$

$$A_s y^2 = \tilde{u} x^{g_c/2} y^{1/2} - \tilde{U} y^2. \quad (\text{F.6})$$

Using Eq. (F.6), we may express  $y$  as a function of  $x$

$$y = \tilde{u}^{2/3} x^{g_c/3} \left( \frac{1}{A_s + \tilde{U}} \right)^{2/3}, \quad (\text{F.7})$$

which we insert in (F.5) to obtain

$$A_c x^2 = \tilde{u}^{4/3} x^{2g_c/3} \left( \frac{1}{A_s + \tilde{U}} \right)^{1/3} + \tilde{U} x^{2g_c}. \quad (\text{F.8})$$

We solve this equation in two limits. For  $\tilde{u} \rightarrow 0$  the solution of Eq. (F.8) yields a constant

$$x_0 = \left( \frac{\tilde{U}}{A_c} \right)^{1/(2-2g_c)}. \quad (\text{F.9})$$

For  $\tilde{u}/\tilde{U} \ll 1$  we make the ansatz

$$x = x_0 + C\tilde{u}^\alpha, \quad (\text{F.10})$$

with  $C$  and  $\alpha$  to be determined. Since  $C\tilde{u}^\alpha$  is only a small correction we keep it only in linear order in the following and obtain

$$\begin{aligned} A_c x_0^2 (1 - \tilde{U} x_0^{2g_c-2}) + 2C\tilde{u}^\alpha (A_c x_0 - \tilde{U} g_c x_0^{2g_c-1}) \\ = \tilde{u}^{4/3} x_0^{2g_c/3} \left[ 1 + \frac{2Cg_c\tilde{u}^\alpha}{x_0} \right] \left( \frac{1}{A_s + \tilde{U}} \right)^{1/3}. \end{aligned} \quad (\text{F.11})$$

We consider this equation as a polynomial equation in  $\tilde{u}$  which has to be fulfilled for every  $\tilde{u}$ . Neglecting the term  $2Cg_c\tilde{u}^\alpha/x_0 \ll 1$  in the square brackets we obtain the following expressions:

$$\alpha = \frac{4}{3}, \quad (\text{F.12})$$

$$C = \frac{x_0^{(3-4g_c)/3}}{2\tilde{U}(1-g_c)(A_s + \tilde{U})^{1/3}}, \quad (\text{F.13})$$

Finally we reinsert the solution for  $x$  into equation (F.7) and obtain the result

$$\begin{aligned} \frac{\Delta_c(u) - \Delta_c(0)}{\Delta_{0c}} &\approx \left( \frac{4u}{\pi} \right)^{4/3} \left( \frac{\Delta_c(0)}{\Delta_{0c}} \right)^{(3-4g_c)/3} \\ &\quad \times \frac{\pi^2}{4(1-g_c)U} \left( \frac{\Delta_{0s}^2}{2\pi v_s g_s} + \frac{2U}{\pi^2} \right)^{-1/3}, \end{aligned} \quad (\text{F.14})$$

$$\frac{\Delta_s(u)}{\Delta_{0s}} \approx \left( \frac{4u}{\pi} \right)^{2/3} \left( \frac{\Delta_c(0)}{\Delta_{0c}} \right)^{g_c/3} \left( \frac{\Delta_{0s}^2}{2\pi v_s g_s} + \frac{2U}{\pi^2} \right)^{-2/3}. \quad (\text{F.15})$$

In the other limit,  $\tilde{u}/\tilde{U} \gg 1$  we take the logarithm of Eq. (F.8),

$$\ln(A_c x^{2-2g_c}) = \ln \left[ \tilde{U} \left( 1 + \frac{\tilde{u}^{4/3} x^{-4g_c/3}}{(A_s + \tilde{U})^{1/3} \tilde{U}} \right) \right] \quad (\text{F.16})$$

and make the ansatz

$$x = B \tilde{u}^\beta. \quad (\text{F.17})$$

In the limit  $\tilde{u} \gg \tilde{U}$  we may neglect the 1 in the logarithm of (F.16) compared to the second term and obtain

$$B = \frac{1}{A_c (A_s + \tilde{U})^{1/3}}^{3/(6-2g_c)}, \quad (\text{F.18})$$

$$\beta = \frac{2}{3 - g_c}. \quad (\text{F.19})$$

Finally the charge and the spin gap are

$$\frac{\Delta_c(u)}{\Delta_{0c}} \approx \left( \frac{4u}{\pi} \right)^{2/(3-g_c)} \left( \frac{2\pi v_c g_c}{\Delta_{0c}^2} \right)^{3/(6-2g_c)} \left( \frac{\Delta_{0s}^2}{2\pi v_s g_s} + \frac{2U}{\pi^2} \right)^{-1/(6-2g_c)}, \quad (\text{F.20})$$

$$\frac{\Delta_s(u)}{\Delta_{0s}} \approx \left( \frac{4u}{\pi} \right)^{2/(3-g_c)} \left( \frac{2\pi v_c g_c}{\Delta_{0c}^2} \right)^{g_c/2(3-g_c)} \left( \frac{\Delta_{0s}^2}{2\pi v_s g_s} + \frac{2U}{\pi^2} \right)^{(4-g_c)/(6-2g_c)}. \quad (\text{F.21})$$

## Ionic Hubbard model

For the ionic Hubbard model in the case  $2B_c < B_{cs}$  the mean field parameters are given by the equations

$$\frac{\Delta_c^2}{2\pi v_c g_c} = 4B_{cs} - 8B_c = \frac{2\Delta}{\pi} e^{-\langle \phi_c^2 \rangle - \langle \phi_s^2 \rangle} + \frac{2U}{\pi^2} e^{-4\langle \phi_c^2 \rangle}, \quad (\text{F.22})$$

$$\frac{\Delta_s^2}{2\pi v_s g_s} = 4B_{cs} - 8B_s = \frac{2\Delta}{\pi} e^{-\langle \phi_c^2 \rangle - \langle \phi_s^2 \rangle} + \frac{2U}{\pi^2} e^{-4\langle \phi_s^2 \rangle}. \quad (\text{F.23})$$

As in the previous case we insert the analytical values of  $\langle \phi_c^2 \rangle$  and  $\langle \phi_s^2 \rangle$  and introduce the notation  $\Delta_c/\Delta_{0c} = x$ ,  $\Delta_s/\Delta_{0s} = y$ ,  $\Delta_{0c}/2\pi v_c g_c = A_c$ ,  $\Delta_{0s}/2\pi v_s g_s = A_s$ ,  $2\Delta/\pi = \tilde{u}$  and  $2U/\pi^2 = \tilde{U}$ . We obtain

$$A_c x^2 = \tilde{\Delta} x^{g_c/2} y^{1/2} + \tilde{U} x^{2g_c}, \quad (\text{F.24})$$

$$A_s y^2 = \tilde{\Delta} x^{g_c/2} y^{1/2} + \tilde{U} y^2. \quad (\text{F.25})$$

Eqs. (F.24)-(F.25) are identical to Eqs. (F.5)-(F.6), if  $\tilde{u}$  is replaced with  $\tilde{\Delta}$  and  $A_s + \tilde{U}$  with  $A_s - \tilde{U}$ . In the limit  $\tilde{\Delta}/\tilde{U} \gg 1$  we can use the results given by Eqs. (F.16)-(F.21) and obtain

$$\frac{\Delta_c(\Delta)}{\Delta_{0c}} \approx \left(\frac{2\Delta}{\pi}\right)^{2/(3-g_c)} \left(\frac{2\pi v_c g_c}{\Delta_{0c}^2}\right)^{3/(6-2g_c)} \left(\frac{\Delta_{0s}^2}{2\pi v_s g_s} - \frac{2U}{\pi^2}\right)^{-1/(6-2g_c)}, \quad (\text{F.26})$$

$$\frac{\Delta_s(\Delta)}{\Delta_{0s}} \approx \left(\frac{2\Delta}{\pi}\right)^{2/(3-g_c)} \left(\frac{2\pi v_c g_c}{\Delta_{0c}^2}\right)^{g_c/2(3-g_c)} \left(\frac{\Delta_{0s}^2}{2\pi v_s g_s} - \frac{2U}{\pi^2}\right)^{(4-g_c)/(6-2g_c)} \quad (\text{F.27})$$

For  $2B_c > B_{cs}$  the gap equations read

$$\frac{\Delta_c^2}{2\pi v_c g_c} = 8B_c - 2\frac{B_{cs}^2}{B_c}, \quad (\text{F.28})$$

$$\frac{\Delta_s^2}{2\pi v_s g_s} = -8B_s + 2\frac{B_{cs}^2}{B_c}, \quad (\text{F.29})$$

which is equivalent to

$$A_c x^2 = -\frac{2\Delta^2}{U} x^{-g_c} y + \frac{2U}{\pi^2} x^{2g_c}, \quad (\text{F.30})$$

$$A_s y^2 = \frac{2\Delta^2}{U} x^{-g_c} y - \frac{2U}{\pi^2} y^2. \quad (\text{F.31})$$

We assume for  $x$  a dependence on  $\Delta$  of the form

$$x(\Delta) = x_0 + B\Delta^\beta, \quad (\text{F.32})$$

with  $x_0/B\tilde{\Delta}^\beta \gg 1$ . If we insert Eqs. (F.31) and (F.32) in Eq. (F.30) and compare the prefactors of same powers of  $\Delta$  we obtain for  $x_0$ ,  $\beta$  and  $B$  the following expressions:

$$x_0 = \left(\frac{2U}{A_c \pi^2}\right)^{1/(2-2g_c)}, \quad (\text{F.33})$$

$$\beta = 4, \quad (\text{F.34})$$

$$B = -\frac{2}{A_c(1-g_c)U^2(A_s + 2U/\pi^2)} x_0^{-2g_c-1}. \quad (\text{F.35})$$

Finally the charge and spin parameter are given by

$$\begin{aligned} \frac{\Delta_c(\Delta) - \Delta_c(0)}{\Delta_{0c}} &\approx -\Delta^4 \left( \frac{\Delta_{0s}^2}{2\pi v_s g_s} + \frac{2U}{\pi^2} \right)^{-1} \\ &\quad \times \frac{2\pi v_c g_c}{(1-g_c)U^2 \Delta_{0c}} \left( \frac{\Delta_c(0)}{\Delta_{0c}} \right)^{(-1-2g_c)}, \end{aligned} \quad (\text{F.36})$$

$$\frac{\Delta_s(\Delta)}{\Delta_{0s}} \approx \Delta^2 \left( \frac{\Delta_{0s}^2}{2\pi v_s g_s} + \frac{2U}{\pi^2} \right)^{-1} \frac{2}{U} \left( \frac{\Delta_c(0)}{\Delta_{0c}} \right)^{-g_c}. \quad (\text{F.37})$$





# Bibliography

- [1] S. Tomonaga, *Prog. Theor. Phys.* **5**, 544 (1950).
- [2] J. M. Luttinger, *J. Math. Phys. (N. Y.)* **4**, 1154 (1963).
- [3] A. Luther and V. J. Emery, *Phys. Rev. Lett.* **33**, 589 (1974).
- [4] A. J. Heeger, in *Chemistry and Physics of One-Dimensional Metals*, edited by H. J. Keller (Plenum Press, New York, 1977), pp. 87-135.
- [5] D. Jerome and H. J. Schulz, *Adv. Phys.* **31**, 299 (1982).
- [6] A. J. Heeger, S. Kivelson, J. R. Schrieffer, and W. P. Su, *Rev. Mod. Phys.* **60**, 781 (1988).
- [7] H. G. Keiss, *Conjugated Conducting Polymers* (Springer-Verlag, Berlin, 1992).
- [8] M. Hase, I. Terasaki, and K. Uchinokura, *Phys. Rev. Lett.* **70**, 3651 (1993).
- [9] M. Isobe and Y. Ueda, *J. Phys. Soc. Jpn.* **65**, 1178 (1996).
- [10] S. Tarucha, T. Honda, and T. Saku, *Solid State Commun.* **94**, 413 (1995).
- [11] M. Bockrath, D. H. Cobden, J. Lu, A. G. Rinzler, R. E. Smalley, T. Balents, and P. L. McEuen, *Nature (London)* **397**, 598 (1999).
- [12] F. D. M. Haldane, *Phys. Rev. Lett.* **47**, 1840 (1981).
- [13] H. J. Schulz, in *Proceeding of Les Houches Summer School LXI* edited by E. Akkermans, G. Montambaux, J. Pichard, and J. Zinn-Justin (Elsevier, Amsterdam, 1995), p. 533.
- [14] J. von Delft and H. Schoeller, *Ann. Phys. (Leipzig)* **7**, 225 (1998).
- [15] H. J. Schulz, G. Cuniberti, and P. Pieri, in *Field Theories for Low-Dimensional Condensed Matter Systems: Spin Systems and Strongly Correlated Electrons*, edited by G. Morandi et al. (Springer, New York, 2000) (cond-mat/9807366).

- 
- [16] R. J. Baxter, *Exactly Solved Models in Statistical Mechanics* (Academic Press, New York, 1982).
- [17] J. Solyom, *Adv. in Physics* **28**, 201 (1979).
- [18] S. Coleman, *Phys. Rev. D* **11**, 2088 (1975).
- [19] T. Nakano and H. Fukuyama, *J. Phys. Soc. Jpn.* **50**, 2489 (1981).
- [20] H. Fukuyama and H. Takayama, in *Electronic properties of Inorganic One-Dimensional Compounds*, edited by P. Monceau (D. Reidel, Dordrecht, Holland, 1985), Part I, pp. 41-104.
- [21] A. Gogolin, *Phys. Rev. Lett.* **71**, 2995 (1993).
- [22] C. Rojas and J. V. José, *Phys. Rev. B* **54**, 12361 (1996).
- [23] C. Schuster and U. Eckern, *Eur. Phys. J. B* **5**, 395 (1998).
- [24] M. E. Gouvea, G. M. Wysin, S. A. Leonel, A. S. T. Pires, T. Kampeter, and F. G. Mertens, *Phys. Rev. B* **59**, 6229 (1999).
- [25] G. Kotliar and Q. Si, *Phys. Rev. B* **53**, 12373 (1996).
- [26] K. Schönhammer, *Phys. Rev. B* **63**, 245102 (2001).
- [27] K. Schönhammer, *Phys. Rev. A* **66**, 014101 (2002).
- [28] J. O. Fjærestad and J. B. Marston, *Phys. Rev. B* **65**, 125106 (2002).
- [29] D. C. Mattis and E. H. Lieb, *J. Math. Phys.* **6**, 304 (1965).
- [30] Y. A. Bychkov, L. P. Gorkov, and I. E. Dzyaloshinskii, *Sov. Phys. JETP* **23**, 498 (1966).
- [31] C. M. Varma, Z. Nussinov, and Wim van Saarloos, *Phys. Rep.* **361**, 267 (2002).
- [32] C. Mocanu, M. Dzierzawa, P. Schwab, and U. Eckern, *J. Phys.: Condens. Matter* **16**, 6445 (2004).
- [33] P. Jordan and E. Wigner, *Z. Phys.* **47**, 631 (1928).
- [34] M. Kohmoto, M. den Nijs, and L. P. Kadanoff, *Phys. Rev. B* **24**, 5229 (1981).
- [35] J. Zang, A. R. Bishop, and D. Schmeltzer, *Phys. Rev. B* **52**, 6723 (1995).
- [36] G. S. Uhrig and H. J. Schulz, *Phys. Rev. B* **54**, R9624 (1996).

- [37] R. P. Feynman, Phys. Rev. **56**, 340 (1939).
- [38] H. Hellmann, Acta Physicochim. URSS I, **6**, 913 (1935).
- [39] M. Tinkham, *Introduction to superconductivity*, second edition (McGraw-Hill, New York, 1996), chap. 7.3.
- [40] M. Abramowitz and I. Stegun, *Handbook of Mathematical Functions* (Dover Publications, 1965).
- [41] W. Kohn, Phys. Rev. **133**, A171 (1964).
- [42] U. Eckern and P. Schwab, Adv. Phys. **44**, 387 (1996).
- [43] U. Eckern and P. Schwab, J. Low Temp. Phys. **126**, 1291 (2002).
- [44] D. Loss, Phys. Rev. Lett. **69**, 343 (1992).
- [45] B. Nathanson, O. Entin-Wohlman, and B. Mühlischlegel, Phys. Rev. B **45**, 3499 (1992).
- [46] M. C. Cross and D. S. Fisher, Phys. Rev. B **19**, 402 (1979).
- [47] H. Otsuka, Phys. Rev. B **56**, 15609 (1997).
- [48] E. H. Lieb and F. Y. Wu, Phys. Rev. Lett. **20**, 1445 (1968).
- [49] D. J. Klein and W. A. Seitz, Phys. Rev. B **10**, 3217 (1974).
- [50] R. E. Peierls, *Quantum Theory of Solids* (Oxford University Press, Oxford, 1955).
- [51] T. Ishiguro and K. Yamaji, *Organic Superconductors* (Springer-Verlag, Berlin, 1990).
- [52] W. P. Su, J. R. Schrieffer, and A. J. Heeger, Phys. Rev. Lett. **42**, 1698 (1979); Phys. Rev. B **22**, 2099 (1980).
- [53] P. Horsch, Phys. Rev. B **24**, 7351 (1981).
- [54] D. Baeriswyl and K. Maki, Phys. Rev. B **48**, 913 (1987).
- [55] S. Kivelson and D. E. Heim, Phys. Rev. B **26**, 4278 (1987).
- [56] J. E. Hirsch, Phys. Rev. Lett. **51**, 296 (1983).
- [57] S. Mazumdar and S. N. Dixit, Phys. Rev. Lett. **51**, 292 (1983).
- [58] G. W. Hayden and Z. G. Soos, Phys. Rev. B **38**, 6075 (1988).

- [59] V. Waas, H. Büttner, and J. Voit, Phys. Rev. B **41**, 9366 (1990).
- [60] M. Sugiura and Y. Suzumura, J. Phys. Soc. Jpn. **71**, 697 (2002).
- [61] C. Mocanu, M. Dzierzawa, P. Schwab, and U. Eckern, *physica status solidi b*, in print: DOI 10.1002/pssb.200460041 (cond-mat/0411315).
- [62] J. Malek, K. Kladko, and S. Flash, JETP Lett. **67**, 1052 (1998).
- [63] J. Malek, S.-L. Drechsler, S. Flash, E. Jeckelmann, and K. Kladko, J. Phys. Soc. Jpn. **72**, 2277 (2003).
- [64] C. Schuster, *Random and periodic lattice distortions in one-dimensional Fermi and spin systems* (Shaker, Aachen, 1999) [PhD Thesis, Universität Augsburg (1999)].
- [65] N. Nagaosa and J. Takimoto, J. Phys. Soc. Jpn. **55**, 2735 (1986).
- [66] J. Hubbard and J. B. Torrance, Phys. Rev. Lett. **47**, 1750 (1981).
- [67] M. Le Cointe et al., Phys. Rev. B **51**, 3374 (1995).
- [68] S. Caprara, M. Avignon, and O. Navarro, Phys. Rev. B **61**, 15667 (2000).
- [69] T. Egami, S. Ishihara, and M. Tachiki, Science **261**, 1307 (1993); S. Ishihara, T. Egami, and M. Tachiki, Phys. Rev. B **49**, 8944 (1994).
- [70] T. Neumann, T. Neumann, G. Borstel, C. Scharfschwerdt, and M. Neumann, Phys. Rev. B **46**, 10623 (1992).
- [71] Z. G. Soos and S. Mazumdar, Phys. Rev. B **18**, 1991 (1978).
- [72] R. Resta and S. Sorella, Phys. Rev. Lett. **74**, 4738 (1995); Phys. Rev. Lett. **82**, 370 (1999).
- [73] P. J. Strebler and Z. G. Soos, J. Chem. Phys. **53**, 4077 (1970).
- [74] G. Ortiz, P. Ordejón, R. M. Martin, and G. Chiappe, Phys. Rev. B **54**, 13515 (1996).
- [75] M. Fabrizio, A. O. Gogolin, and A. A. Nersesyan, Phys. Rev. Lett. **83**, 2014 (1999); Nucl. Phys. B **580**, 647 (2000).
- [76] N. Gidopoulos, S. Sorella, and E. Tosatti, Eur. Phys. J. B **14**, 217 (2000).
- [77] M. E. Torio, A. A. Aliaga, and H. A. Ceccatto, Phys. Rev. B **64**, 121105 (2001).
- [78] Y. Anusooya-Pati, Z. G. Soos, and A. Painelli, Phys. Rev. B **63**, 205118 (2001).

- [79] T. Wilkens and R. Martin, Phys. Rev. B **63**, 235108 (2001).
- [80] Y. Takanada and M. Kido, J. Phys. Soc. Jpn. **70**, 21 (2001).
- [81] S. R. Manmana, V. Meden, R. M. Noack, and K. Schönhammer, Phys. Rev. B **70**, 155115 (2004).
- [82] A. P. Kampf, M. Sekania, G. I. Japaridze, and P. Brune, J. Phys.: Condens. Matter **15**, 5895 (2003).
- [83] V. Eyert, *Octahedral Deformations and Metal-Insulator Transition in Transition Metal Calcogenides*, Habilitation thesis (Universität Augsburg, 1998).
- [84] V. Eyert, Ann. Phys. (Leipzig) **11**, 648 (2002).
- [85] J. B. Goodenough, J. Solid State Chem. **3**, 490 (1971).
- [86] R. M. Wentzcovitch, W. W. Schulz, and P. B. Allen, Phys. Rev. Lett. **72**, 3389 (1994).
- [87] J. P. Pouget, H. Launois, T. M. Rice, P. Dernier, A. Gossard, G. Villeneuve, and P. Hagenmuller, Phys. Rev. B **10**, 1801 (1974).
- [88] J. P. Pouget, H. Launois, J. P. D'Haenens, P. Merenda, and T. M. Rice, Phys. Rev. Lett **35**, 873 (1971).
- [89] S. Shin et al., Phys. Rev. B **41**, 4993 (1990).
- [90] C. Sommers, R. de Groot, D. Kaplan, and A. Zylbersztejn, Phys. Lett. **36**, L157 (1975).
- [91] L. Ladd and W. Paul, Solid State Commun. **7**, 425 (1969).
- [92] D. Paquet and P. Leroux-Hugon, Phys. Rev. B **22**, 5284 (1980).
- [93] A. Zylbersztejn and N. F. Mott, Phys. Rev. B **11**, 4383 (1975).
- [94] J. Meixner and F. W. Schärfke, *Mathieusche Funktionen und Sphäroidfunktionen* (Springer-Verlag, Berlin, 1954).
- [95] C. Schuster, private communication.